Tesi di Dottorato

Monte Carlo Study of Electron Spin Relaxation in n-type GaAs Bulk

Analisi Monte Carlo della dinamica di rilassamento dello spin elettronico in campioni di GaAs drogati di tipo n

Tutor:
Prof.ssa Dominique Persano Adorno

Dottorando:
Dott. Ing. Stefano Spezia

Coordinatore:
Prof. Bernardo Spagnolo

SSD: Fis03

Università degli Studi di Palermo - Dipartimento di Fisica

Corso di DOTTORATO DI RICERCA INTERNAZIONALE in FISICA APPLICATA
XXIII CICLO - 2012

To the love
of my life,
Maria

Acknowledgements

First and foremost, I would like to thank my advisor, Prof. Dr. Dominique Persano Adorno, for giving me the opportunity to work on this fascinating project. I thank Dominique for giving me the freedom to explore, sharing her critical insights and mentoring me throughout this years of research. Moreover, I thank her for encouragements and inspirations, unyielding support and vision that drives this research program forward. Without her organizational and scientific skills, I would not have had the opportunity to venture as researcher in the amazing field of the *Semiconductor Spintronics*.

By continuing ever in the *Department of Physics* (DIFI) of the *University of Palermo*, my second thanking goes to Prof. Bernardo Spagnolo which has discovered my abilities as physicist, when I had just received my Master Degree in Electronic Engineering. Without his initial support, probably I would not have begun to enjoy the taste of scientific research. Soon after, I would like to thank Dr. Nicola Pizzolato, for his endless willingness to support me from a point of view technical and scientific. Thanks to him I could become able to develop and to extend the numerical codes used in this thesis. Then, I thank Prof. Dr. Davide Valenti, for his useful suggestions during my study for course exams, expecially in Advanced Quantum Mechanics. Further thanking to Professors of my qualification courses for the obtained skills through their seminars: Diego Molteni (Computational Physics), Giuseppe Raso (Semiconductor Detectors), Francesco Fauci (Image Processing Theory and Techniques), Salvatore Basile (Theoretical Physics), Giacomo D'Alì Staiti (Experimental Physics) and, last but not least, Giuseppe Falci (Information and Decoherence in Nanodevices) at the *University of Catania* (Italy).

I also wish to thank Prof. Dr. Ming-Wei Wu at *University of Science and Technology of China* in Hefei (China) for valuable scientific discussions on some topics of this thesis and for the kind hospitality in his research laboratories. His knowledge of condensed matter physics, of spin physics, and frank opinions are always appreciated. Again in Hefei, I would to thank the collegue PhD student Ka Shen for useful discussions and tecnical support during my visit in China. Following in same Hefei's group: Peng Zhang, Yang Zhou, Lin Wang, Hua Tong, Bo-Ye Sun and Min Wang were always welcoming and helpful.

I would need to thank Prof. Dr. Alia Tadjer and members of the *Laboratory*

of Quantum and Computational Chemistry at *Sofia University St. Kliment Ohridski* (Bulgaria) for giving me the opportunity to attempt as invited lecturer at the *Fourth workshop on Advanced Computing Techniques in the Microworld* organized within the Framework of the project IRC-CoSiM (Integrated Research Center on Computational Sciences in the Microworld) by Bulgarian National Science Fund.

Then I would like remind my collegues whom have lived this PhD experience before me and with whom I spent two years in the same laboratory. Beginning with Dr. Angelo La Cognata, he has been the colleague with whom I have spent the most hours of work in the laboratory. With him, I could discuss about many topics about physics, mathematics and also about our personal lifes. With great enthusiasm, also I remember Dr. Pasquale Caldara, who continues to be a big mate of fork in our lunch pauses. I can not forget Giovanni Denaro, actually first year PhD student, who has been mate of laboratory in last months of my PhD. I would like to mention the collegues of the my PhD cycle, Maria Francesca Alberghina, Marius Iacomi, Anna Longo and Benedetto Schiavo. I would like to extend my thanks to all DIFI's colleagues, and in particular to Dr. Davide Gurrera, Dr. Fabio Vizzini and Dr. Rosario Grammauta. Furthermore, special thanking goes to Luciano Curcio with who I started my research experience with a fellowship in the research topic: *Noise induced phenomena in complex biological systems with threshold*, and another thanking to Prof. Dr. Alessandro Fiasconaro at *University of Zaragoza* (Spain) for his useful suggestions. Another special thanking goes to Maria Antonietta Lodato with my wish to get a long chain of successes in the research line of semiconductor spintronics, as novel and next PhD student of my advisor.

Before the last, I would need to express my profound gratitude for my family: dad, mom, Francesca, Giuseppe, Federica and the little Miriam, for their love and unwavering support throughout these years.

Finally, I would like to cuddle the love of my life, for every kind of support to the research activity of my PhD, and I would like to wish us to continue our life together, by keeping the same immense passion that we have had for the sciences in our years of PhD.

Commonly Used Abbreviations

Elliott-Yafet: EY
D'yakonov-Perel: DP
Bir-Aronov-Pikus: BAP
Spin-orbit coupling: SOC
Bulk inversion asymmetry: BIA
Structure inversion asymmetry: SIA
Tight binding: TB
Linear combination of atomic orbitals: LCAO
Boltzmann Transport Equation: BTE
Random phase approximation: RPA
Inhomogeneous broadening: IB
Longitudinal optical: LO
Monte Carlo: MC
Simple-Particle Monte Carlo: SMC
Ensemble Monte Carlo: EMC
Kinetic Spin Bloch Equations: KSBEs
Electron-electron: e-e
electron-Longitudinal optical: e-LO
Ornstein-Uhlenbeck: OU
High Performing Computing: HPC
Density Functional Theory: DFT

Contents

Introduction

The capabilities of many digital electronic devices are strongly linked to *Moore's law*. Processing speed, memory capacity, sensors and even number and size of pixels in digital cameras are growing at roughly exponential rates. This exponential improvement has so dramatically enhanced the impact of digital electronics in nearly every segment of the world economy, that *Moore's law* is seem as a driving force of technological and social change in the late 20^{th} and early 21^{st} centuries. Moore's law describes a long-term trend in the rising of computing hardware: the number of transistors that can be inexpensively placed inside an integrated circuit approximately doubles every two years. This trend has been observed for more than half a century. However, the 2010 update to the *International Technology Roadmap for Semiconductors* shows a growth slowing up the end of 2013 and after that time transistor counts and densities can double only every 3 years[1].

Because of the limits imposed by the increasing miniaturization of integrated circuits, there has been a strong push to seek a new paradigm on which to build a radically new technology that allows to satisfy the world market continuing demand of processors small in size, but faster and with more capacious memories. In addition, due to the miniaturization, even when the applied voltage is very low, the system is typically subject to intense electric fields and it can exhibit a strongly non-linear behavior.

Currently on the world market, the new processors are implemented with *Field-Effect Transistors* (FETs) having channel lengths of a few tens of nanometers, the MISFETs. The MISFETs (Metal Insulator Semiconductor FETs) are very similar to the MOSFETs (Metal Oxide Semiconductor FETs) with the difference that the dielectric gate is not silicon oxide, but plastic material or polymers.

[1] http://www.itrs.net/

At present, the processing of high volume of information and world wide communication are based on semiconductor technology, whereas information storage devices rely on multilayers of magnetic metals and insulators. The semiconductor devices exploit the charge of the electron, while the magnetic systems take advantage of the electron spin and the associated magnetic moment. The new field of *semiconductor spintronics* represents a possible direction towards the development of hybrid devices that could perform logic operations, communication and storage, within the same material technology. In fact, the electron spin can be used, in addition to the electronic charge, to store information, which could be transferred, as attached, to mobile carriers and finally detected [1]-[13].

Spin dynamics is one of the central focuses of semiconductor spintronics. The possibility of obtaining long spin relaxation times or spin diffusion lengths in electronic materials makes spintronics a viable prospective technology. Nevertheless, the designers of spin-based devices have to worry about the loss of spin polarization (spin coherence) before, during and after the necessary manipulations. In particular, efficient injection, transport, control and detection of spin polarization must be carefully treated [3, 12, 13]. Electron-spin states depolarize by scattering with imperfections or elementary excitations such as phonons. Furthermore, miniaturization process brings the system to experience very intense electric fields. Hence, for the operability of potential spintronic devices, the features of spin relaxation at relatively high temperature jointly with the influence of transport conditions should be firstly understood [2, 14].

From the pioneering works of Lampel [15] and Parsons [16], and the following extensive experimental and theoretical works at Ioffe Institute in St. Petersburg and Ecole Polytechnique in Paris in 1970s and early 1980s, a great understanding of spin dynamics in semiconductors has been achieved. Starting from the late 1990s, there was a big revival of research interest in the spin dynamics of semiconductors, after some experimental works of Kikkawa and Awschalom [17, 18].

Despite decades of studies, spin relaxation is still not fully understood. Thanks to the fast development of experimental techniques, including the sample preparations and ultrafast optical techniques, experimental findings have gone far beyond the previous theoretical understandings. Moreover, much progress has been achieved on the spin injection from ferromagnetic materials into semiconductors. Neverthe-

less, a satisfactory realization of spin transistor, which is crucial for the application of semiconductor spintronics, is yet to come.

In recent years there was a proliferation of experimental works in which the influence of transport conditions on relaxation of spins in semiconductors has been investigated [17]-[25]. However, all these works are focused on the study of coherent spin transport at low temperatures ($T_L < 30$ K) and under the influence of weak electric fields ($F < 0.1$ kV/cm), except for few works [19, 20] in which spin depolarization has been investigated with driving fields up to 6 kV/cm. Very little is known about the effects of stronger electric fields or lattice temperatures higher than 30 K.

Many theoretical approaches can be used to describe spin dynamics and spin-polarized electron transport. Between them, the simplest is the two-component drift-diffusion model [26]-[29]. However, the temporal evolution of the spin and the evolution of the momentum of an electron can not be separated. The spin depolarization rates are functionals of the electron distribution function in momentum space which continuously evolves with time. Thus, the dephasing rate is a dynamical variable that needs to be treated self-consistently in step with the dynamical evolution of the electron momentum [30].

A way to solve this problem is to describe the transport of spin polarization by making use of Boltzmann-like kinetic equations. This can be done within the density matrix approach [31], methods of nonequilibrium Green's functions, as the microscopic kinetic spin Bloch equation approach [13],[32]-[36], or Wigner functions [37, 38], where spin property is accounted for starting from quantum mechanics equations. All methods allow to include the relevant spin relaxation phenomena for electron systems and take into account the details of electron scattering mechanisms. Their predictions have been demonstrated to be in good agreement with experiments.

Another way to solve the Boltzmann equation is the use of a semiclassical Monte Carlo approach, by taking into account the spin polarization dynamics with the inclusion of the precession mechanism of the spin polarization vector. Monte Carlo approaches have been widely adopted by groups of scientists to study spin polarized transport in 2D channels, heterostructures, quantum wells, quantum wires [14],[39]-[45].

However, till today, to the best of our knowledge, in semiconductor bulk struc-

tures a Monte Carlo theoretical investigation of the influence of transport conditions on the spin depolarization in the presence of electric fields, comprehensive of the effects of both lattice temperature and impurity density, is still lacking.

The detailed knowledge of spin relaxation times and lengths in semiconductor materials is important for several reasons: (i) from a theoretical point of view, the knowledge of the electron spin dynamics gives information about microscopic features of spin dephasing mechanism, that is about the electron interaction processes with the phonons, ionized impurities and defects; (ii) in technological applications, it allows to get the best working conditions for a spintronic device. In fact, in physics of devices, the spin depolarization process is a disturbance to eliminate, because it limits the functionality of the device for the storage of the information and it affects the sensibility of its detection.

The core of this thesis is, hence, dedicated to the complete analysis of the electron spin relaxation of n-doped GaAs crystals in the presence of an electric field. Spin lifetimes and spin depolarization lengths are obtained by means of a Monte Carlo method, which is a complete microscopic model of the transport properties taking into account details of the energy band structure, scattering mechanisms, material properties and specific device design. The spin dephasing is analyzed by varying several parameters of interest, as the lattice temperature, the doping density and the electric field amplitude. Moreover, the role played of fluctuations of the static electric field has been investigated for different values of the noise amplitude.

Many of the results of this thesis have been obtained by taking into account the electron-electron Coulomb scattering mechanism, which has been proved to be essential to simulate spin dynamics in semiconductors [13]. The inclusion of this kind of interaction in our Monte Carlo procedure and the obtained results have been discussed during my two-months visiting as reseacher student at the laboratories of Prof. Dr. Ming-Wei Wu in *Hefei's National Laboratory for Physical Sciences at Microscale* and in *Department of Physics* of the *University of Science and Technology of China*.

The study of noise-induced effects on spin relaxation process has been possible thank to an one-year HPC 2010 Grant received from *CASPUR Consortium (Interuniversity Consortium for Supercomputing Applications for Universities and Research)*. The demand for computing resources has been justified by the necessity

to perform a number sufficient of different realizations with the aim to evaluate both average values and error bars of the extracted spin depolarization times and lengths.

The plan of this thesis is as follows. In chapter 1 we give a very short introduction of both the semiconductor spin dynamics and the main spin relaxation mechanisms. In chapter 2, we describe the models adopted and some peculiar features of the developed Monte Carlo procedure. In chapter 3, we report the main obtained results for the electron spin relaxation in the presence of electric field less intense than the Gunn field (low-field conditions), the necessary static field that allows the electrons to move towards the upper energy valleys. We have analyzed a n-type lightly doped GaAs bulk for values of the electric field ($0.1 - 2$ kV/cm) and lattice temperatures in wide range $10 < T_L < 300$ K. In the last part of the chapter, we also show the impurity density effect on the fast process of spin relaxation at different lattice temperatures T_L. In chapter 4, we show the results of the investigation of the electron spin relaxation under high-field conditions, focusing on the effects due to the inclusion of the upper valleys of the semiconductor. In chapter 5 we investigate the role of the fluctuations added to the electric field on electron spin relaxation. Finally, conclusions and some future prospects are discussed.

Chapter 1

Spin relaxation and spin dynamics in semiconductors

In the first part of the chapter, after a brief description of both spin orientation and spin detection procedures, we introduce a simple classical model that contains the relevant physics of spin relaxation without explicitly resorting to quantum mechanics: *the electron spin in a randomly fluctuating magnetic field* [6].

The spin of conduction electrons in semiconductors decays due to the combined effect of spin-orbit coupling and momentum scattering. The spin-orbit coupling couples the spin to the electron momentum, which is randomized by momentum scattering with impurities and other carriers, as like, phonons and electrons. Seen from the perspective of the electron spin, the spin-orbit coupling gives rise to a spin precession, while momentum scattering makes this precession randomly fluctuating, both in magnitude and orientation.

We widely discuss only the mechanism of D'yakonov and Perel, which is the dominant spin relaxation mechanism in non-centrosymmetric semiconductors, as GaAs [13, 36].

The last part of the chapter covers the description of both the spin dynamics model for GaAs bulk and the spin-orbit coupling parameters.

1.1 Introduction: spin orientation and spin detection

New devices, now generally referred as spintronic devices, exploit the ability of conduction electrons in metals and semiconductors to carry spin-polarized current. Three factors make spin of conduction electrons attractive for future technology: (i) electron spin can store information, (ii) the spin information can be transferred as it is attached to mobile carriers, and (iii) the spin information can be detected. In addition, the possibility of having long spin relaxation time or spin diffusion length leads spintronics a workable technology.

Currently used methods of polarizing electron spins include magnetic field, optical orientation, and spin injection. Polarization by magnetic field is the traditional method that works for both metals and semiconductors. Spin dynamics in semiconductors, however, is best studied by optical orientation where spin-polarized electrons and holes are created by a circularly polarized light. Finally, in the spin injection technique a spin-polarized current is driven, by an interface from a ferromagnet into the semiconductor material.

The ability of information transfer by electron spins, relies on two facts. First, electrons are mobile and second, electrons have a relatively large spin memory. Indeed, the spin states of conduction electrons have lifetime much longer than those of the momentum states.

Finally, after the spin is transferred, it has to be detected. In many experiments, the spin polarization is optically read: photoexcited spin-polarized electrons and holes in a semiconductor recombine by emitting circularly polarized light; or the electron spins interact with light and cause a rotation of the light polarization plane. It was discovered, however, that spin can be also electronically measured, through charge-spin coupling. When electrons spin accumulates at the interface between a conductor and a ferromagnet, a voltage (or a current) appears. By measuring the polarity of the voltage (or the current), one can detect the spin orientation in the conductor. Differently from spin injection yet proved in semiconductors [11], spin-charge coupling has been experimentally confirmed only in metals [2].

In an optical spin orientation experiment a semiconductor is excited by circularly polarized light with $\hbar\omega > E_g$, where ω is the optical frequency of light and E_g the

band gap of the semiconductor. In particular, in cubic semiconductors, like GaAs, the conduction band originates from an atomic s-state, while the valence band originates from a p-state. Because of the spin-orbit interaction the valence band is splitted into bands having different angular momentum J, namely, light and heavy holes, and split-off band. When a circularly polarized photon is absorbed during an interband transition, its angular momentum is distributed between the photo-excited electron and hole according to the selection rules determined by the band structure of the semiconductor. This means that absorption produces an average electron spin (projection on the direction of excitation) equal to the angular momentum of the absorbed photon. Thus, in a p-type semiconductor the degree of spin polarization of the photo-excited electrons will be -50%. The minus sign indicates that the spin orientation is opposite to the angular momentum of incident photons. If our electron immediately recombines with its partner hole, a 100% circularly polarized photon will be emitted. Finally, the analysis of the circular polarization of the luminescence gives a direct measure of the electron spin polarization [9].

1.2 Spin relaxation of conduction electrons

In semiconductor structures, spin relaxation may be caused by interactions with local magnetic fields originating from nuclei and spin-orbit interactions or magnetic impurities. The most relevant spin relaxation mechanisms for an electron system under nondegenerate regime are:

1. The Elliott-Yafet (EY) mechanism, in which an electron has a small chance to flip its spin at each scattering, due to the mixing between the spin-up and spin-down states in the conduction band[1]. This mechanism works in systems with and without a center of inversion. The spin-flip amplitudes are due to spin-orbit coupling induced by lattice ions, while the momentum scattering is due to the presence of impurities (that also contribute to the spin-orbit coupling), phonons, rough boundaries, and everything capable of randomizing the electron momentum [46, 47].

[1]The Elliott-Yafet mechanism is based on the fact that in real crystals Bloch states are not spin eigenstates.

2. The D'yakonov-Perel (DP) mechanism, based on the spin-orbit splitting of the conduction band in non-centrosymmetric semiconductors, in which the electron spins decay because of their precession around the **k**-dependent spin-orbit fields [48, 49, 9].

3. The Bir-Aronov-Pikus (BAP) mechanism, in which electrons exchange their spins with holes in the electron-hole exchange interaction. This interaction depends on the spins of interacting electrons and holes and acts on electron spins as an effective magnetic field. The spin relaxation takes place as electron spins precess along this field. In many cases, however, hole spins change with a rate which is much faster than the precession frequency. When that happens, the effective field generated by the hole spins, fluctuates and the precession angle about a fixed axis diffuses as in the case of the D'yakonov-Perel process. This mechanism only dominates in p-doped semiconductors [50].

4. The hyperfine interaction, where the electron spin interacts with the spins of the lattice nuclei, which are normally in a disordered state and provide a random effective magnetic field, acting on the electron spin. The corresponding relaxation rate is rather weak, but may become important for localized electrons, when other mechanisms, associated with electron motion, do not work. For electrons confined on impurity levels or in quantum dots, the electron wave function will spread over a region containing many nuclear spins, whose interaction with the electron will lead to a spin flip and, more significantly, spin dephasing. While for free electrons, fast moving through nuclei with random spins, the action of nuclear spin is averaged [51, 52].

5. The anisotropic exchange interaction is an efficient spin relaxation mechanism in the insulating phase of doped semiconductors, and exists in semiconductor structures that are not symmetric with respect to spatial inversion, for example in bulk zinc-blende semiconductors. It is important for spin relaxation of localized electrons, but ineffective in metallic regime where most of the carriers are in extended states. The spins of two localized electrons are known to be coupled by exchange interactions. Isotropic interactions conserve the total spin of the two electrons, and for this reason they do not cause spin relaxation. Differently, anisotropic exchange interactions resulting from the spin-orbit in-

teraction, produce spin relaxation. In fact, in the exchange interaction, when two electrons interact, their spins turn around the direction of the spin-orbit field [53, 54].

Previous theoretical [13, 36] and experimental [55] investigations indicate that the EY mechanism is totally irrelevant on electron spin relaxation in n-doped III-V semiconductors.

1.3 Electron spin dynamics in a fluctuating magnetic field [6]

Consider an electron spin $\vec{S}$ (or the corresponding magnetic moment $\vec{\mu}_S$) in the presence of an external time-independent magnetic field $\vec{B}_0 = B_0\hat{z}$ giving rise to the Larmor precession frequency $\vec{\omega}_0 = \omega_0\hat{z}$, and a fluctuating time-dependent field $\vec{B}(t)$ giving the Larmor frequency $\vec{\omega}(t)$; see Fig. 1.1. It is assumed that the field $\vec{B}(t)$ fluctuates about zero and correlated on the time scale of τ_c:

$$\overline{\omega(t)} = 0, \quad \overline{\omega_\alpha(t)\omega_\beta(t')} = \delta_{\alpha\beta}\overline{\omega_\alpha^2}e^{-|t-t'|/\tau_c}. \tag{1.1}$$

Here α and β denote the cartesian coordinates and the overline denotes averaging over different random realizations of $\vec{B}(t)$.

Writing out the torque equation, $\frac{d\vec{S}}{dt} = \vec{\omega} \times \vec{S}$, we get the following equations of motion:

$$\dot{S}_x = -\omega_0 S_y + \omega_y(t)S_z - \omega_z(t)S_y, \tag{1.2}$$

$$\dot{S}_y = \omega_0 S_x - \omega_x(t)S_z + \omega_z(t)S_x, \tag{1.3}$$

$$\dot{S}_z = \omega_x(t)S_y - \omega_y(t)S_x. \tag{1.4}$$

These equations are valid for one specific realization of $\vec{\omega}(t)$. Our goal is to find effective equations for the time evolution of the average spin $< \vec{S}(t) >$, given the ensemble of Larmor frequencies $\vec{\omega}(t)$.

It is convenient to introduce the complex "rotating" spins $S_\pm$ and the Larmor frequencies $\omega_\pm$ in the (x, y) plane:

$$S_+ = S_x + iS_y, \quad S_- = S_x - iS_y, \tag{1.5}$$

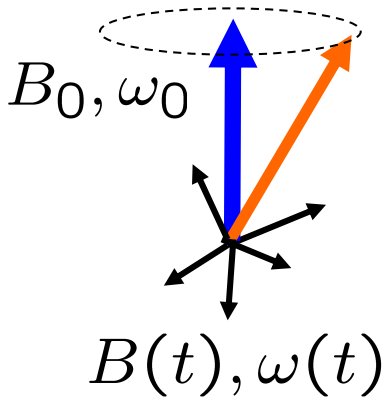

Figure 1.1: Electron spin precesses about the static B_0 field along $\hat{z}$. The randomly fluctuating magnetic field $\vec{B}(t)$ causes spin relaxation and spin dephasing [6].

$$\omega_+ = \omega_x + i\omega_y, \quad \omega_- = \omega_x - i\omega_y. \tag{1.6}$$

The inverse relations are

$$S_x = \frac{1}{2}\left(S_+ + S_-\right), \quad S_y = \frac{1}{2i}\left(S_+ - S_-\right), \tag{1.7}$$

$$\omega_x = \frac{1}{2}\left(\omega_+ + \omega_-\right), \quad \omega_y = \frac{1}{2i}\left(\omega_+ - \omega_-\right). \tag{1.8}$$

The equations of motion for the spin set (S_+, S_-, S_z) are,

$$\dot{S}_+ = i\omega_0 S_+ + i\omega_z S_+ - i\omega_+ S_z, \tag{1.9}$$

$$\dot{S}_- = -i\omega_0 S_- - i\omega_z S_- + i\omega_- S_z, \tag{1.10}$$

$$\dot{S}_z = -(1/2i)\left(\omega_+ S_- - \omega_- S_+\right). \tag{1.11}$$

In the absence of the fluctuating fields the spin S_+ rotates in the complex plane anticlockwise (for $\omega_0 > 0$), while S_- clockwise.

In analogous way, the precession about B_0 can be factored out by applying the ansatz:

$$S_\pm = s_\pm(t) e^{\pm i\omega_0 t}. \tag{1.12}$$

Indeed, it is straightforward to find the time evolution of the set $(s_+, s_-, s_z \equiv S_z)$:

$$\dot{s}_+ = i\omega_z s_+ - i\omega_+ s_z e^{-i\omega_0 t}, \tag{1.13}$$

$$\dot{s}_- = -i\omega_z s_- + i\omega_- s_z e^{i\omega_0 t}, \tag{1.14}$$

$$\dot{s}_z = -(1/2i)\left(\omega_+ s_- e^{-i\omega_0 t} - \omega_- s_+ e^{i\omega_0 t}\right). \tag{1.15}$$

The disadvantage for transforming into this *rotating frame* is the appearance of the phase factors $\exp(\pm i\omega_0 t)$.

The solutions of Eqs. (1.13)-(1.15), can be written in terms of the integral equations,

$$s_+(t) = s_+(0) + i\int_0^t dt'\omega_z(t')s_+(t') - i\int_0^t dt'\omega_+(t')s_z(t')e^{-i\omega_0 t'}, \quad (1.16)$$

$$s_-(t) = s_-(0) - i\int_0^t dt'\omega_z(t')s_-(t') + i\int_0^t dt'\omega_-(t')s_z(t')e^{i\omega_0 t'}, \quad (1.17)$$

$$s_z(t) = s_z(0) - \frac{1}{2i}\int_0^t dt'\left[\omega_+(t')s_-(t')e^{-i\omega_0 t'} - \omega_-(t')s_+(t')e^{i\omega_0 t'}\right]. \quad (1.18)$$

Now, by substituting the above solutions back into Eqs. (1.13)-(1.15), we get

$$\begin{aligned}\dot{s}_+(t) = \quad & i\omega_z(t)s_+(0) - \omega_z(t)\int_0^t dt'\omega_z(t')s_+(t') \\ & +\omega_z(t)\int_0^t dt'\omega_+(t')s_z(t')e^{-i\omega_0 t'} - i\omega_+(t)e^{-i\omega_0 t}s_z(0) \\ & +\frac{1}{2}e^{-i\omega_0 t}\omega_+(t)\int_0^t dt'\left[\omega_+(t')s_-(t')e^{-i\omega_0 t'} - \omega_-(t')s_+(t')e^{i\omega_0 t'}\right].\end{aligned} \quad (1.19)$$

$$\begin{aligned}\dot{s}_-(t) = \quad & -i\omega_z(t)s_-(0) - \omega_z(t)\int_0^t dt'\omega_z(t')s_-(t') \\ & +\omega_z(t)\int_0^t dt'\omega_-(t')s_z(t')e^{i\omega_0 t'} + i\omega_-(t)e^{i\omega_0 t}s_z(0) \\ & -\frac{1}{2}e^{i\omega_0 t}\omega_-(t)\int_0^t dt'\left[\omega_+(t')s_-(t')e^{-i\omega_0 t'} - \omega_-(t')s_+(t')e^{i\omega_0 t'}\right].\end{aligned} \quad (1.20)$$

$$\begin{aligned}\dot{s}_z(t) = \quad & -\frac{1}{2i}\omega_+(t)s_-(0)e^{-i\omega_0 t} + \frac{1}{2}\omega_+(t)e^{-i\omega_0 t}\int_0^t dt'\omega_z(t')s_-(t') \\ & -\frac{1}{2}\omega_+(t)e^{-i\omega_0 t}\int_0^t dt'\omega_-(t')s_z(t')e^{i\omega_0 t'} + \frac{1}{2i}\omega_-(t)s_+(0)e^{i\omega_0 t} \\ & +\frac{1}{2}\omega_-(t)e^{i\omega_0 t}\int_0^t dt'\omega_z(t')s_+(t') - \frac{1}{2}\omega_-(t)e^{i\omega_0 t}\int_0^t dt'\omega_+(t')s_z(t')e^{-i\omega_0 t'}.\end{aligned} \quad (1.21)$$

In order to solve these equations two approximations will be made. First, the assumption that the fluctuating field is rather weak such that $|\omega(t)|\tau_c \ll 1$, so that the spin does not fully precess about the fluctuating field before the field makes a random change (strong scattering regime). This assumption, called *Born approximation* allows to factorize the averaging over the statistical realizations of the field,

$$\overline{\omega(t)\omega(t')s(t')} \approx \overline{\omega(t)\omega(t')}\ \overline{s(t')} \quad (1.22)$$

as the spin changes only weakly over the time scale (τ_c) of the changes of the fluctuating fields.

As second assumption, we do the following approximation,

$$\int_0^{t\gg\tau_c} dt' \overline{\omega(t)\omega(t')}\ \overline{s(t')} \approx \int_0^{t\gg\tau_c} dt' \overline{\omega(t)\omega(t')}\ \overline{s(t)}, \tag{1.23}$$

because the correlation function $\overline{\omega(t)\omega(t')}$ is only significant in the time interval of $|t-t'| \approx \tau_c$. The Eq. (1.23) is a realization of the *Markov approximation*. The physical meaning is that the spin s varies only slowly on the time scale of τ_c over which the correlation of the fluctuating fields is significant.

Applying these two approximations to Eq. (1.20) it is possible to obtain for the average spin $\overline{s}_+$ the following time evolution equation:[2]

$$\begin{aligned}\dot{\overline{s}}_+ = \quad & i\overline{\omega_z(t)}s_+(0) - \int_0^t dt' \overline{\omega_z(t)\omega_z(t')}\ \overline{s_+(t)} \\ & + \int_0^t dt' \overline{\omega_z(t)\omega_+(t')} e^{-i\omega_0 t'} \overline{s_z(t)} - i\overline{\omega_+(t)} e^{-i\omega_0 t} s_z(0) \\ & + \frac{1}{2} e^{-i\omega_0 t} \int_0^t dt' \left[\overline{\omega_+(t)\omega_+(t')} e^{-i\omega_0 t'} \overline{s_-(t)} - \overline{\omega_+(t)\omega_-(t')} e^{i\omega_0 t'} \overline{s_+(t)} \right].\end{aligned} \tag{1.24}$$

Using the rules of Eqs. (1.1) the above simplifies to

$$\begin{aligned}\dot{\overline{s}}_+ = \quad & -\overline{\omega_z^2} \int_0^t dt' e^{-(t-t')/\tau_c} \overline{s_+(t)} \\ & + \frac{1}{2} e^{-i\omega_0 t} \int_0^t dt' \left[(\overline{\omega_x^2} - \overline{\omega_y^2}) e^{-i\omega_0 t'} \overline{s_-(t)} - (\overline{\omega_x^2} + \overline{\omega_y^2}) e^{i\omega_0 t'} \overline{s_+(t)} \right] e^{-(t-t')/\tau_c}.\end{aligned} \tag{1.25}$$

Since $t \gg \tau_c$, we can approximate

$$\int_0^t dt' e^{-(t-t')/\tau_c} \approx \int_{-\infty}^t dt' e^{-(t-t')/\tau_c} = \tau_c. \tag{1.26}$$

Similarly,

$$\int_0^t dt' e^{-(t-t')/\tau_c} e^{-i\omega_0(t\pm t')} \approx \int_{-\infty}^t dt' e^{-(t-t')/\tau_c} e^{-i\omega_0(t\pm t')} = \tau_c \frac{1 \mp i\omega_0\tau_c}{1+\omega_0^2\tau_c^2}. \tag{1.27}$$

The imaginary parts induce the precession of $s_\pm$, which is equivalent to shifting (renormalizing) the Larmor frequency ω_0. The relative change of the frequency is $(\omega\tau_c)^2$ which in the Born approximation is assumed much smaller than one. Thus it sufficient to only consider the real parts obtaining

$$\dot{\overline{s}}_+ = -\overline{\omega_z^2}\tau_c \overline{s_+} + \frac{1}{2}\frac{\tau_c}{1+\omega_0^2\tau_c^2} \left[(\overline{\omega_x^2} - \overline{\omega_y^2}) \overline{s_-} e^{-2i\omega_0 t} - (\overline{\omega_x^2} + \overline{\omega_y^2}) \overline{s_+} \right]. \tag{1.28}$$

[2]The initial values of the spin $s(0)$ are fixed and not affected by averaging.

By using the same procedure (or simply using $s_- = s_+^*$) the analogous equation for s_- can be written:

$$\dot{\overline{s}}_- = -\overline{\omega_z^2}\tau_c\overline{s_-} + \frac{1}{2}\frac{\tau_c}{1+\omega_0^2\tau_c^2}\left[(\overline{\omega_x^2}-\overline{\omega_y^2})\overline{s_+}e^{2i\omega_0 t} - (\overline{\omega_x^2}+\overline{\omega_y^2})\overline{s_-}\right]. \tag{1.29}$$

Similarly,

$$\dot{\overline{s}}_z = -(\overline{\omega_x^2}+\overline{\omega_y^2})\frac{\tau_c}{1+\omega_0^2\tau_c^2}\overline{s_z} \tag{1.30}$$

For sake of simplicity, in the rest of this section, the overline on the symbols for the spins will be omitted, so that S will label the average spin. Returning back to the rest frame of the spins rotating with frequency ω_0,

$$\dot{S}_+ = i\omega_0 S_+ - \overline{\omega_z^2}\tau_c\frac{1}{2}\frac{\tau_c}{1+\omega_0^2\tau_c^2}\left[(\overline{\omega_x^2}-\overline{\omega_y^2})S_- - (\overline{\omega_x^2}+\overline{\omega_y^2})S_+\right], \tag{1.31}$$

$$\dot{S}_- = i\omega_0 S_- - \overline{\omega_z^2} - \frac{1}{2}\frac{\tau_c}{1+\omega_0^2\tau_c^2}\left[(\overline{\omega_x^2}-\overline{\omega_y^2})S_+ - (\overline{\omega_x^2}+\overline{\omega_y^2})S_-\right], \tag{1.32}$$

$$\dot{S}_z = -(\overline{\omega_x^2}+\overline{\omega_y^2})\frac{\tau_c}{1+\omega_0^2\tau_c^2}S_z. \tag{1.33}$$

Finally, going back to S_x and S_y:

$$\dot{S}_x = -\omega_0 S_y - \overline{\omega_z^2}\tau_c S_x - \frac{\tau_c}{1+\omega_0^2\tau_c^2}\overline{\omega_y^2}S_x, \tag{1.34}$$

$$\dot{S}_y = \omega_0 S_x - \overline{\omega_z^2}\tau_c S_y - \frac{\tau_c}{1+\omega_0^2\tau_c^2}\overline{\omega_x^2}S_y, \tag{1.35}$$

$$\dot{S}_z = -(\overline{\omega_x^2}+\overline{\omega_y^2})\frac{\tau_c}{1+\omega_0^2\tau_c^2}S_z. \tag{1.36}$$

A more conventional form of the above equation is given by introducing two spin decay times. Firstly, the *spin relaxation time* T_1, given by

$$\frac{1}{T_1} = \left(\overline{\omega_x^2}+\overline{\omega_y^2}\right)\frac{\tau_c}{1+\omega_0^2\tau_c^2}, \tag{1.37}$$

and secondly the *spin dephasing times* T_2, given by

$$\frac{1}{T_{2x}} = \overline{\omega_z^2}\tau_c + \frac{\overline{\omega_y^2}\tau_c}{1+\omega_0^2\tau_c^2}, \tag{1.38}$$

$$\frac{1}{T_{2y}} = \overline{\omega_z^2}\tau_c + \frac{\overline{\omega_x^2}\tau_c}{1+\omega_0^2\tau_c^2}. \tag{1.39}$$

So, it is possible to write the equations (1.34)-(1.36) as follows:

$$\dot{S}_x = -\omega_0 S_y - \frac{S_x}{T_{2x}}, \tag{1.40}$$

$$\dot{S}_y = \omega_0 S_x - \frac{S_y}{T_{2y}}, \tag{1.41}$$

$$\dot{S}_z = -\frac{S_z}{T_1}. \tag{1.42}$$

The considered fluctuating field is valid at infinite temperature, for which the average value of the spin in a magnetic field is zero. A more general spin dynamics is described by

$$\dot{S}_x = -\omega_0 S_y - \frac{S_x}{T_{2x}}, \tag{1.43}$$

$$\dot{S}_y = \omega_0 S_x - \frac{S_y}{T_{2y}}, \tag{1.44}$$

$$\dot{S}_z = -\frac{S_z - S_{0z}}{T_1}. \tag{1.45}$$

where S_{0z} is the equilibrium value of the spin in the presence of the static magnetic field $\vec{B}_0$ at the temperature of the environment. The above equations are called *Bloch equations*.

The spin components S_x and S_y, which are perpendicular to the applied static field $\vec{B}_0$, decay exponentially on the time scales of T_{2x} and T_{2y}, respectively. These times are termed spin *dephasing* times, as they describe the loss of the *phase* of the spin components perpendicular to the static field $\vec{B}_0$. For that reason, they are also often called *transverse* times. The time T_1 is termed spin *relaxation* time, as it describes the (thermal) relaxation of the spin to the equilibrium. During the spin relaxation in a static magnetic field the energy is exchanged with the environment.

Consider now an isotropic system in which

$$\overline{\omega_x^2} = \overline{\omega_y^2} = \overline{\omega_z^2} = \overline{\omega^2}. \tag{1.46}$$

If the static magnetic field is weak, $\omega_0 \tau_c \ll 1$ (strong scattering regime), and the three times are equal:

$$T_{1\cdot} = T_{2x} = T_{2y} = \frac{1}{\overline{\omega^2}\tau_c}. \tag{1.47}$$

The above equation is called *D'yakonov-Perel formula*. In this case, there is no difference between spin relaxation and spin dephasing. Spin relaxation time is inversely proportional to the correlation time: more random the external field appears, and less the spin decays.

In the opposite limit, i.e. for large Larmor frequency, $\omega_0\tau_c \gg 1$ (weak scattering regime), spin relaxation rate vanishes,

$$\frac{1}{T_1} \approx \frac{\overline{\omega^2}}{\omega_0^2}\frac{1}{\tau_c} \to 0, \tag{1.48}$$

while spin dephasing time is given by the *secular broadening*,

$$T_2 \approx \frac{1}{\overline{\omega_z^2}\tau_c}. \tag{1.49}$$

If secular broadening is absent, the leading term in the dephasing rate will be, as in the relaxation,

$$\frac{1}{T_2} \approx \frac{\overline{\omega^2}}{\omega_0^2}\frac{1}{\tau_c}. \tag{1.50}$$

In this limit, spin dephasing rate is proportional to the correlation rate, that is inversely proportional to the correlation time.

In the case in which there is no distinction between T_1 and T_2, we use the symbol

$$\tau = \tau_s = T_1 = T_2, \tag{1.51}$$

to describe the *generic spin relaxation* and we will call them: *spin relaxation time*, *spin depolarization time*, *spin dephasing time*, *spin decoherence time* or *spin lifetime*.

Motional narrowing

The surprising fact that, for low amplitude of the magnetic field, spin relaxation rate is proportional to the correlation time of the fluctuating field, is explained by the *motional narrowing* phenomenum.

Consider the spin perpendicular to an applied magnetic field and assume that the field has a single magnitude, but can randomly switch between up and down, leading to a random precession of the spin (clock and anticlockwise). The spin phase executes a random walk, in which a single step takes the time τ_c, the correlation time of the fluctuating field. After n steps, that is, after the time $t = n\tau_c$, the standard deviation of the phase will be $\delta\phi = (\omega\tau_c)\sqrt{n}$, the well known result for a random walk. We call spin dephasing time the time needed to have $\delta\phi \approx 1$. This happens after the time $\tau_s = \tau_c/(\omega\tau_c)^2$, or $\tau_s = 1/(\omega^2\tau_c)$, which is the result that has been derived earlier by using the described two approximations (see Eq. (1.47)).

1.3.1 Spin ensemble in spatially random magnetic field

Previous calculation was carried out for a single spin in a fluctuating magnetic field, and the decay times of the spin components have been derived. After the decay of the spin components, the information contained in the original spin polarization is irreversibly lost. Such irreversible loss of spin polarization is often termed spin *decoherence* process.

An important example of spin ensemble in a spatially random magnetic field is represented by the conduction electrons in non-centrosymmetric crystals, such as GaAs, in which the spin-orbit coupling acts as a magnetic field dependent on momentum. The spins of electrons having different momenta precess with different frequencies. We are interested in the total spin as the sum of individual spins.

Consider the external field along the z direction, and the fluctuating frequencies described by the Gaussian distribution:

$$P(\omega_1) = \frac{1}{\sqrt{2\pi\delta\omega^2}} e^{-\omega_1^2/2\delta\omega^2}, \tag{1.52}$$

with zero mean and $\delta\omega_1^2$ variance. Denote the in-plane components of the spin of the electron a by S_x^a and S_y^a. This spin precesses with the frequency $\omega_0 + \omega_1^a$, leading to the time evolution for the rotating spins

$$S_\pm^a(t) = S_x^a(t) \pm iS_y^a(t) = S_\pm^a(0) e^{\pm i\omega_0 t} e^{\pm i\omega_1^a t}. \tag{1.53}$$

At $t = 0$ suppose that all the spins are lined up, that is, $\sum_a S_\pm^a(0) = S_\pm(0)$. The total spin $S_\pm(t)$ is the sum,

$$S_\pm(t) = \sum_a S_\pm^a(t) = S_\pm(0) e^{\pm i\omega_0 t} \int_{-\infty}^{\infty} d\omega_1 P(\omega_1) e^{\pm i\omega_1 t}. \tag{1.54}$$

Evaluating the Gaussian integral follows

$$S_\pm(t) = S_\pm(0) e^{\pm i\omega_0 t} e^{-\delta\omega_1^2 t^2/2}. \tag{1.55}$$

In this case, the disappearance of the spin is purely due to the statistical averaging over an ensemble in which the individual spins have, after certain time, random phases. This spin decay is not a simple exponential, but rather Gaussian.

1.4 Spin transport in nonmagnetic semiconductor using drift-diffusion model

Assuming that the charge density in nonmagnetic semiconductor is uniform and that electronic transport coefficients are not affected by the spin polarization, one can write the transport equation for the magnetic momentum $\mathbf{S}$ in a uniform electric field $\mathbf{E}$ and a magnetic field $\mathbf{B}$ as [9],

$$\frac{\partial \mathbf{S}}{\partial t} = D_s \nabla^2 \mathbf{S} - \mathbf{e}\mu \mathbf{F} \cdot \nabla \mathbf{S} + \mathbf{g}\mu_{\mathbf{B}} \mathbf{B} \times \mathbf{S} - \frac{\mathbf{S}}{\tau_{\mathbf{s}}}, \tag{1.56}$$

with μ, D_s, and τ_s being the charge mobility, the diffusion coefficient and the spin relaxation time, respectively. Here, the drift-diffusion equation has been modified to include the Larmor precession of the spin around the applied magnetic field $\mathbf{B}$.

When a semiconductor is in contact with a spin polarization source at $x = 0$, in absence of magnetic field ($\mathbf{B} = \mathbf{0}$) and with a static electric field ($\mathbf{F} = F\hat{\mathbf{x}}$) directed along the $\hat{\mathbf{x}}$-direction, the $\hat{\mathbf{x}}$-component of the Eq. (1.56) leads to a spin accumulation with an exponential decay where the shape of a spin polarized carrier packet changes with time due to drift and diffusion.

The temporal evolution of a δ-polarized spin packet of height S_0 at $x = 0$ is

$$S(x,t) = \frac{S_0}{2\sqrt{\pi D_s t}} \exp\left[-\frac{t}{\tau_s} - \frac{(x - v_d t)^2}{4 D_s t}\right], \tag{1.57}$$

which has the form of a Gaussian function whose center is determined by the drifting, $v_d t$, while the width is determined by the diffusion, $\sqrt{D_s t}$.
Within this model, at a fixed time t the total spin as, i.e. as the sum over the whole electron ensemble, is given by the integral

$$S(t) = \int_{-\infty}^{\infty} S(x,t) dx. \tag{1.58}$$

By replacing the Eq. (1.57) in (1.58), we obtain

$$S(t) = S_0 \exp\left(-\frac{t}{\tau_s}\right). \tag{1.59}$$

Moreover, by substituting $x = v_d t$ in Eq. (1.59) and defining the spin depolarization length as $L = v_d \tau_s$, the spin relaxation on distance is also described by an exponential decay as

$$S(x) = S_0 \exp\left(-\frac{x}{L}\right). \tag{1.60}$$

Hence, in presence of a drifting electric field, the assumption of a simple exponential decay is valid.

1.5 The D'yakonov-Perel mechanism

D'yakonov and Perel [9, 48, 49] have considered solids without a center of inversion symmetry, such as GaAs or InAs. In such crystals the spin-orbit coupling is manifested as an effective magnetic field, *the spin-orbit field*, dependent on the electron momentum. Electrons in different momentum states feel different spin-orbit fields; for this reason, spin precesses with a given Larmor frequency until the electron is scattered into another momentum state (see Fig. 1.2). As the electron momentum changes on the time scale of the momentum scattering time interval, the net effect of the momentum scattering on the spin is to produce random fluctuations of the Larmor frequencies; that is the motional narrowing. Since these frequencies are correlated by τ_c, the D'yakonov-Perel formula for spin relaxation time becomes

$$\frac{1}{\tau} = <| \, \mathbf{\Omega}(\mathbf{k}) \, |^2> \tau_c, \tag{1.61}$$

where the average squared precession frequency $<| \, \mathbf{\Omega}(\mathbf{k}) \, |^2>$ is a measure of the strength of the spin-orbit coupling. The spin relaxation rate is directly proportional to the momentum scattering time interval: more the electron scatters and less its spin dephases.

Spin-orbit field

Spin-orbit coupling splits the electron energies:

$$\varepsilon_{\mathbf{k},\uparrow} \neq \varepsilon_{\mathbf{k},\downarrow}. \tag{1.62}$$

Due to time reversal symmetry, only the Kramers degeneracy is left [56]:

$$\varepsilon_{\mathbf{k},\uparrow} = \varepsilon_{-\mathbf{k},\downarrow}. \tag{1.63}$$

The energy splitting at a given momentum $\mathbf{k}$ is conveniently described by the spin-orbit field $\mathbf{\Omega}$, giving a Zeeman-like (but momentum dependent) energy contribution to the electronic states, described by the additional Hamiltonian H_{SO}.

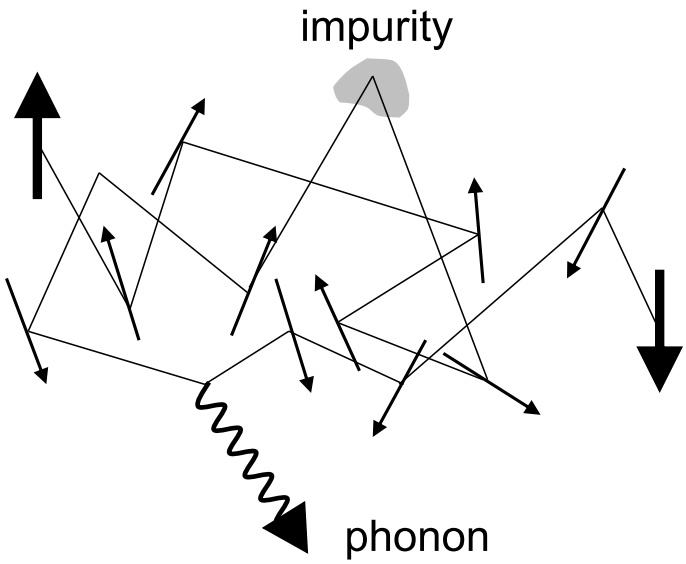

Figure 1.2: *D'yakonov-Perel mechanism.* The electron starts with the spin up. As it moves, its spin precesses about the axis corresponding to the electron velocity. Phonons and impurities change the electron velocity, making the spin to precess about a different axis (and with different speed).

In a semiclassical formalism the effective single-electron Hamiltonian which accounts for the spin-orbit interaction term is

$$H = H_0 + H_{SO} \tag{1.64}$$

where H_0 is the self-consistent electron Hamiltonian in the Hartree approximation[3], including also interactions with impurities and phonons. The spin-dependent term H_{SO} may be written as

$$H_{SO} = \frac{\hbar}{2}\mathbf{\Omega_k} \cdot \sigma, \tag{1.65}$$

and can be viewed as the energy of a spin in an effective magnetic field that causes electron spin to precess. $\mathbf{\Omega_k}$ is the spin precession vector depending on the orienta-

[3]The Hartree approximation consists in following some simplifications in the solution of the electronic Schrödinger equation: i) The Born-Oppenheimer adiabatic approximation is inherently assumed. The electron wave function is a function of the coordinates of each of the nuclei, in addition to those of the electrons. ii) Relativistic effects are completely neglected. The momentum operator is assumed to be non-relativistic. iii) The mean field approximation is implied. iv) The permutation symmetry of the electron wave function, which leads to the exchange interaction, is not included [57].

tion of the electron momentum vector with respect to the crystal axes (xyz), σ is the Pauli vector and $\hbar$ is the reduced Planck's constant.

The time reversal symmetry requires that the spin-orbit field is an odd function of the momentum:

$$\mathbf{\Omega}_{\mathbf{k}} = -\mathbf{\Omega}_{-\mathbf{k}}. \tag{1.66}$$

1.5.1 Spin-orbit coupling in bulk GaAs

In zinc-blende-type bulk semiconductors such as GaAs, near the center of Brillouin zone (Γ-point) the zero field splitting caused by the *Spin-Orbit Coupling* (SOC) can depend or cubically on the wave-vector $\mathbf{k}$, due to the bulk inversion asymmetry (BIA) [58, 48], or linearly because of the structure inversion asymmetry (SIA) [59, 60]. Here, we consider only the spin-orbit field due to the BIA.

Near the bottom of each valley, the precession vector can be written as [53]

$$\mathbf{\Omega}_{\Gamma} = \frac{\beta_{\Gamma}}{\hbar}[k_x(k_y^2 - k_z^2)\hat{\mathbf{x}} + k_y(k_z^2 - k_x^2)\hat{\mathbf{y}} + k_z(k_x^2 - k_y^2)\hat{\mathbf{z}}] \tag{1.67}$$

in the Γ-valley,

$$\mathbf{\Omega}_{L} = \frac{\beta_{L}}{\sqrt{3}}[(k_y - k_z)\hat{\mathbf{x}} + (k_z - k_z)\hat{\mathbf{y}} + (k_x - k_y)\hat{\mathbf{z}}] \tag{1.68}$$

in the L-valleys, located along the [111] direction of the crystallographic axes, and

$$\mathbf{\Omega}_{X} = \beta_X[-k_y\hat{\mathbf{y}} + \hat{\mathbf{z}}k_z] \tag{1.69}$$

in the X-valleys located along the [100] direction [45, 61].
In equations (1.67)-(1.69), k_i $(i = x, y, z)$ are the components of the electron wave vector. β_{Γ}, β_L and β_X are the spin-orbit coupling coefficients, crucial parameters for the simulation of spin polarization. In Γ-valley we consider the effects of non-parabolicity on the spin-orbit splitting by using [53],

$$\beta_{\Gamma} = \frac{\alpha\hbar}{m\sqrt{2mE_g}}\left(1 - \frac{E(\mathbf{k})}{E_g}\frac{9 - 7\eta + 2\eta^2}{3 - \eta}\right) \tag{1.70}$$

where $\alpha = 0.029$ is a dimensionless material-specific parameter, $\eta = \Delta/(E_g + \Delta)$, with $\Delta = 0.341$ eV, the spin-orbit splitting of the valence band, E_g the energy separation between the conduction band and the valence band at the Γ point (band gap), m the effective mass and $E(\mathbf{k})$ the electron energy.

Despite of neglecting the nonparabolicity correction, the exact value of β_{Γ} is still in debate. Experimentals results and theoretical calculations based on different

approaches give various values ranging from 8.5 to 34.5 eV·Å^3 (see Refs. [62]). Two kinds of experiments allow to measure the β_Γ value. One, based on the Raman scattering allows the direct measurement of the splitting. Experiments based on this approach show that β_Γ is about 23.5 eV·Å^3 in wide GaAs quantum well [63]. In asymmetric GaAs/AlGaAs heterostructure/quantum well, β_Γ is about ranging between 11.0 and 16.5 eV·Å^3 [64, 65]. The other kind of measurement is indirect and consists of a qualitative calculation of the spin relaxation time or magneto-conductance. Earlier works of this kind estimate that β_Γ is about $20-30$ eV·Å^3 [66].

In real situation, the devices are usually subjected to electric field which can drive the electrons to states far away from Γ-point, or even allow to move towards the other valleys such as L- and/or X-valleys. In previous works investigating the high field spin transport in GaAs [43, 45] the coefficient of spin splitting in higher valleys are approximated by other material, such as GaSb, due to the lack of the data for GaAs.

Recently, Fu et al. [61] have theoretically estimated the spin-orbit coupling in the whole Brillouin zone for GaAs using both the $sp^3s^*d^5$ and sp^3s^* nearest-neighbor tight-binding models [4]. They have reported that, in the X-valleys, the values of β_X obtained from $sp^3s^*d^5$ and sp^3s^* models are close to each other, i.e., $\beta_X = 0.059$ and 0.046 eV/Å·2/$\hbar$, respectively. However, in the L-valley, β_L values, determined from these two models, are very different. For $sp^3s^*d^5$, $\beta_L = 0.26$ eV/Å·2/$\hbar$; while for sp^3s^*, $\beta_L = 0.047$ eV/Å·2/$\hbar$. This difference implies that in L-valleys the d orbit plays an important role in the spin splitting. This is because the more accurate symmetry imposes a d-orbital component in the L-valley and $sp^3s^*d^5$ model can account this symmetry. Moreover, the inclusion of the d orbit greatly improves the accuracy of the effective mass in L-valley [67]-[71]. Therefore in L-valley, we choose as more reliable the coefficients of the spin splitting determined by $sp^3s^*d^5$ model. Exactly, we assume β_L=0.26 eV/Å·2/$\hbar$ and β_X=0.059 eV/Å·2/$\hbar$, while, to avoid confusion, we explicitly indicate the value of α or β_Γ used everytime that is necessary.

[4] In solid-state physics, the tight binding model (or TB model) is an approach to the calculation of electronic band structure using an approximate set of wave functions based upon superposition of wave functions for isolated atoms located at each atomic site. The method is closely related to the Linear Combination of Atomic Orbitals (LCAO) method used in chemistry. TB models are applied to a wide variety of solids.

To the best of our knowledge, there are not experimental measurements or other numerical estimates for the values of β_L and β_X.

Chapter 2

Semiconductor model and semiclassical Monte Carlo approach

In this chapter, the Monte Carlo (MC) approach, used to study the spin dynamics and the transport properties in semiconductor bulk, is introduced. The MC method is one of the most powerful techniques to simulate the transport properties in semiconductor devices beyond the quasi-equilibrium approximations, such as drift-diffusion or linear response approximations. This method has been widely used for modeling charge carrier transport in semiconductor structures and modern devices. Due to its flexibility this approach can easily take into account many scattering mechanisms, specific device design, material properties and boundary conditions in the simulation (for more details see Ref. [72]-[74]).

2.1 Introduction to the problem

In the description of a electronic device, as a transistor or a diode, the usual approach is to consider the electronic current as a fluid but, in the reality, the current consists of single particles free to move through the device. The motion of the particles (electrons) is made from a sequence of free flights ending in collision events. So, the trajectories of these particles are random [74].

The classical description of charge transport in semiconductors is given by the

Boltzmann Transport Equation (BTE) [75]. The BTE is an integral-differential kinetic equation that correctly describes the charge transport also in devices where the sizes are lower than De Broglie's wavelength. In general case, it is not possible to neglect the quantum effects [76]. The study of the transport properties and the spin relaxation process in a semiconductor in the presence of an external field is not simple, especially when the field is very strong. In fact, in these cases, the BTE does not have an analytical solution. To solve this problem, many assumptions can be made, as in the drift-diffusion model and in the hydrodynamic model where the particles are treated as a fluid. However, the validity of these models is limited and they can not applied to most modern devices.

Despite of that, there is an indirect way to solve the problem. Because, the electronic current consists of single particles with own transport sequence, the correct description of a device can be performed following the motion of each particle. The time of free flight and the collision mechanism that causes the end of free flight are distributed in a stochastic way. By generating pseudorandom numbers with a suitable distribution, it is possible to calculate the motion of each particle and to simulate the characteristics of a device [72]-[74].

This method, called *Monte Carlo*, represents a continuous solution in the real space and in the time of Maxwell's equations and of the Boltzmann's equation, and it is very suitable to study the response of a device both in the presence of static fields or in non-stationary fields [77]-[79].

2.2 Boltzmann Transport Equation

The BTE is an equation of motion for the probability distribution function for particles in the 6-dimensional phase space of position and (crystal) momentum

$$\frac{\partial f(\mathbf{r},\mathbf{k},t)}{\partial t} + \frac{1}{\hbar}\nabla_{\mathbf{k}} E(\mathbf{k}) \nabla_{\mathbf{r}} f(\mathbf{r},\mathbf{k},t) + \frac{e\mathbf{F}}{\hbar}\nabla_{\mathbf{k}} f(\mathbf{r},\mathbf{k},t) = \frac{\partial f(\mathbf{r},\mathbf{k},t)}{\partial t}\Big|_{Coll}, \qquad (2.1)$$

where $f(\mathbf{r},\mathbf{k},t)$ is the one-particle distribution function. The right hand side is the rate of change of the distribution function due to randomizing collisions, and it is an integral over the in-scattering and the out-scattering terms in momentum (wavevector) space. Once $f(\mathbf{r},\mathbf{k},t)$ is known, physical observables, such as average velocity or current, are found throught averages over f distribution [75]. Equation (2.1) is

semi-classical in the sense that particles are treated as having distinct position and momentum in violation of the quantum uncertainty relations, but their dynamics and scattering processes are quantum-mechanically treated through the electronic band structure and the use of the time dependent perturbation theory [57, 80].

The BTE is yet an approximation of the underlying many body Liouville equation from a classical point of view, and of the Liouville-von Neumann equation for the density matrix from a quantum-mechanical framework [81]. The main approximations of the BTE are the assumption of instantaneous scattering processes in space and time, the Markov nature of scattering processes (i.e. that they are uncorrelated with the previous scattering events), and the neglecting of multi-particle correlations (i.e. that the system may be characterized by a single particle distribution function). In semi-classical simulation, some of these assumptions are relaxed through the use of molecular dynamics techniques (in the context of device simulations).

The *Monte Carlo* (MC) technique is based on the generation of a random walk in order to simulate the stochastic motion of the particle subject to collision processes in some medium. This process of random walk generation may be used to evaluate integral equations and is connected to the general random sampling technique used in the evaluation of multi-dimensional integrals.

The MC algorithm explicitly consists of generating random free flight times for each particle, choosing the type of scattering occurring at the end of the free flight, changing the final energy and momentum of the particle after scattering, and then repeating the procedure for the next free flight. The sampling of the particle motion at various times throughout the simulation allows the statistical estimation of physically interesting quantities such as the single particle distribution function, the average drift velocity in the presence of an applied electric field, the average energy of the particle, etc.

By simulating an ensemble of particles, representative of the physical system of interest, the non-stationary time-dependent evolution of the electron and hole distributions under the influence of a time-dependent driving force may be simulated.

2.3 Single-Particle Monte Carlo Simulation

In general, the analysis of the carrier transport in a semiconductor is a many-body problem with a large number of carriers mutually interacting; hence it is a very difficult task. However, when the many-body system can be considered an ensemble of independent carriers, it becomes possible to use an approximate method that simulates the ensemble of carriers by monitoring the history of a single carrier undergoing many scattering events.

The *Single-particle Monte Carlo* (SMC) method is straightforward and can be carried out without the need of assuming the shape of the distribution function. It consists in simulating the motion of a single carrier in the momentum space by stochastically selecting the duration of the carrier free flights and the scattering events, making a mapping between the probability density of the given microscopic process and an uniform distribution of random numbers.

2.3.1 Free Flight Generation

In MC method, to simulate the motion of a particle by a random walk process, the probability density $P(t)$ is required, in which $P(t)dt$ is the joint probability that a particle arrives at time t without scattering after the previous collision at $t = 0$, and then suffers a collision in a time interval dt. The probability of scattering in the time interval dt may be written as $\Gamma[\mathbf{k}(t)]dt$, where $\Gamma[\mathbf{k}(t)]$ is the scattering rate of an electron or hole having wavevector $\mathbf{k}$. The scattering rate, $\Gamma[\mathbf{k}(t)]$, represents the sum of the contributions from each individual scattering mechanism, which are usually calculated using perturbation theory. The implicit dependence of $\Gamma[\mathbf{k}(t)]$ on time reflects the change in $\mathbf{k}$ due to acceleration by internal and external fields. For electrons subject to time independent electric and magnetic fields, the time evolution of $\mathbf{k}$ between collisions is described as

$$\mathbf{k}(t) = \mathbf{k}(0) - \frac{e(\mathbf{F} + \mathbf{v} \times \mathbf{B})t}{\hbar}. \tag{2.2}$$

where $\mathbf{F}$ is the electric field, $\mathbf{v}$ is the electron velocity, and $\mathbf{B}$ is the magnetic field.

In terms of the scattering rate, $\Gamma[\mathbf{k}(t)]$, the probability that a particle has not suffered a collision after a time t is given by $\exp(-\int_0^t \Gamma[\mathbf{k}(t')]dt')$. Thus, the probability of scattering in the time interval dt after a free flight of time t may be written

as the joint probability

$$P(t)dt = \Gamma[\mathbf{k}(t)] \exp\left(-\int_0^t \Gamma[\mathbf{k}(t')]dt'\right) dt. \tag{2.3}$$

Random flight times may be generated according to the probability density $P(t)$ by using, for example, a pseudo-random number generator, which uniformly generates distributed random numbers in the range $[0, 1]$. Using a direct method, random flight times may be generated according to

$$r = \int_0^{t_r} P(t)dt, \tag{2.4}$$

where r is a uniformly distributed random number and t_r is the desired free flight time. Integrating (2.4) with $P(t)$ given by (2.3) yields

$$r = 1 - \exp\left(-\int_0^{t_r} \Gamma[\mathbf{k}(t')]dt'\right), \tag{2.5}$$

Since $1 - r$ is statistically the same as r, (2.5) may be simplified to

$$-\ln r = \int_0^{t_r} \Gamma[\mathbf{k}(t')]dt'. \tag{2.6}$$

Equation (2.6) is the fundamental equation used to generate the random free flight time after each scattering event, resulting in a random walk process related to the underlying particle distribution function. If there is no external driving field leading to a change of $\mathbf{k}$ between scattering events, the time dependence vanishes, and the integral is trivially evaluated. In the general case where this simplification is not possible, it is a good expedient to introduce the self-scattering method [82]. In it, a fictitious scattering mechanism, whose rate always adjusts itself in such a way that the total (self-scattering plus real scattering) rate is a constant in time, is introduced

$$\Gamma = \Gamma[\mathbf{k}(t')] + \Gamma_{self}[\mathbf{k}(t')], \tag{2.7}$$

where $\Gamma_{self}[\mathbf{k}(t')]$ is the self-scattering rate. The self-scattering mechanism is defined such that the final state before and after scattering is identical. Hence, when it is selected as terminating scattering mechanism, it has no effect on the free flight trajectory of a particle, but allows the simplification of Eq. (2.6) such that the free flight is given by

$$t_r = -\frac{1}{\Gamma} \ln r. \tag{2.8}$$

The constant total rate (including self-scattering) Γ is chosen *a priori* so that it is larger than the maximum scattering encountered during the simulation interval. In the simplest case, a single value is chosen at the beginning of the entire simulation (constant Γ method), checking to ensure that the real rate during the simulation never exceeds this value.

The inclusion of the electron-electron Coulomb scattering leads impossible the use of the constant gamma method. Hence, everytime that a Coulomb scattering event happens, the value of Γ must be necessarily calculated.

2.3.2 Final State After Scattering

The algorithm described above determines the random free flight time during which the particle dynamics is semi-classically treated according to Eq. (2.2). For the scattering process, we need the type of scattering (i.e. impurity, acoustic phonon, photon emission, etc.) which terminates the free flight, and the final energy and momentum of the particle after scattering. The type of scattering which terminates the free flight is chosen using an uniform random number between 0 and Γ that used as pointer permits to select among the relative total scattering rates of all processes, including self-scattering, at the final energy and momentum of the particle

$$\Gamma = \Gamma_{self}[n, \mathbf{k}] + \Gamma_1[n, \mathbf{k}] + \Gamma_2[n, \mathbf{k}] + ... + \Gamma_N[n, \mathbf{k}], \tag{2.9}$$

with n the band index of the particle (or subband in the case of reduced dimensionality systems), $\mathbf{k}$ the wavevector at the end of the free-flight and M the number of different types of scattering mechanisms. Once the type of scattering terminating the free flight is selected, the final energy and momentum (as well as band or subband) of the particle due to this type of scattering must be selected. For this selection, the scattering rate, $\Gamma_j[n, \mathbf{k}; m, \mathbf{k}']$, of the jth scattering mechanism is necessary, where n and m are the initial and final band (subband) indices, and $\mathbf{k}$ and $\mathbf{k}'$ are the particle wavevectors before and after scattering. Defining a spherical coordinate system around the initial wavevector $\mathbf{k}$, the final wavevector $\mathbf{k}'$ is specified by $|\mathbf{k}'|$ (which depends on conservation of energy) as well as the azimuthal and polar angles, ϕ and θ around $\mathbf{k}$. Typically the scattering rate $\Gamma_j[n, \mathbf{k}; m, \mathbf{k}']$ only depends on the angle θ between $\mathbf{k}$ and $\mathbf{k}'$. Therefore, ϕ may be chosen using an uniform random number between 0 and 2π (i.e. $2\pi r$), while θ is chosen according to the

cross-section for scattering arising from $\Gamma_j[n, \mathbf{k}; m, \mathbf{k}']$. If the probability for scattering into a certain angle $P(\theta)d\theta$ is integrable, then random angles satisfying this probability density may be generated by the direct method through the inversion of Eq. (2.4). Otherwise, a rejection technique may be used to select random angles according to $P(\theta)$[1].

2.4 Ensemble Monte Carlo Simulation

The algorithm described in previous section, may be used to track a single particle over many scattering events in order to simulate the steady-state behavior of a system. Transport transient and spin relaxation simulations require the use of a synchronous ensemble of particles in which the algorithm above described is repeated for each particle in the ensemble representing the system of interest until the simulation is completed.

The conventional *Ensemble Monte Carlo* (EMC) scheme used for electronic device design describes transport of classical *representative* particles, called *superparticles*. Usually, each simulated particle represents a group of real electrons or holes with similar characteristics. In simulation, each particle is simulated as a SMC procedure above described.

Fig. 2.1 illustrates an EMC simulation in which at fixed time-step Δt, the motion of all the carriers in the system is synchronized. The yellow symbols illustrate random, instantaneous, scattering events, which may or may not occur during one time-step. In this picture, τ indicates the random flight time of an individual electron. Basically, each carrier is simulated only up to the end of the time-step, and then the next particle in the ensemble is treated. Within each time-step, the motion of each particle of the ensemble is simulated independently of the other particles. Nonlinear effects such as carrier-carrier interactions are then updated at each scattering event, as discussed in more detail below. The non-stationary one-particle distribution function and related quantities such as drift velocity, valley or subband population, etc., are then taken as averages over the ensemble at fixed time-steps

[1]Rejection tecnhnique is a basic pseudo-random number sampling technique used to generate observations from a distribution and it is usually used in cases where the form of the distribution function $P(\theta)$ makes sampling difficult.

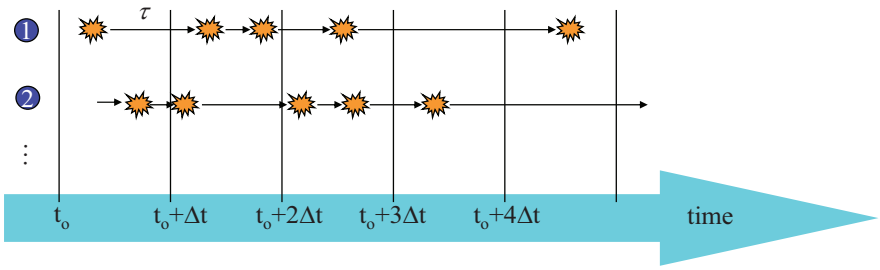

Figure 2.1: Ensemble Monte Carlo simulation in which, the motion of particles is synchronized at each time-step Δt. The yellow symbols represent scattering events.

throughout the simulation. For example, the drift velocity in the presence of the field is given by the ensemble average of the i-component of the velocity at the n^{th} time step as

$$\bar{v}_i(n\Delta t) \cong \frac{1}{N}\sum_{j=1}^{N} v_i^j(n\Delta t), \tag{2.10}$$

where N is the number of simulated particles and j labels the particles in the ensemble. This equation represents an estimator of the true velocity, which has a standard error given by

$$s = \frac{\sigma}{\sqrt{N}}, \tag{2.11}$$

where σ^2 is the variance which may be estimated from

$$\sigma^2 \cong \frac{N}{N-1}\left\{\frac{1}{N}\sum_{j=1}^{N}(v_i^j)^2 - \bar{v}_i^2\right\}. \tag{2.12}$$

Similarly, the distribution functions for the carriers, electrons and holes, may be tabulated by counting their number in cells of **k**-space. From Eq. (2.11), we see that the error in estimated average quantities decreases as the square root of the number of particles in the ensemble, implying the simulation of many particles. Typical ensemble sizes for good statistics are in the range of 10^4 - 10^5 particles.

In the present work of thesis, we have chosen to simulate $5 \cdot 10^4$ superparticles.

2.4.1 Scattering Processes

Free carriers interact with the crystal and with each other through a variety of scattering processes which relax both the energy and the momentum of the particle. Based on first order, time-dependent perturbation theory, the transition rate from

an initial state $\mathbf{k}$ in band n to a final state $\mathbf{k}'$ in band m for the jth scattering mechanism is given by *Fermi's Golden rule*

$$\Gamma_j[n,\mathbf{k}] = \frac{2\pi}{\hbar}\sum_{m,\mathbf{k}'}\left|\left\langle m,\mathbf{k}'|V_j(\mathbf{r})|n,\mathbf{k}\right\rangle\right|^2\delta(E_{\mathbf{k}'}-E_{\mathbf{k}}\mp\hbar\omega). \tag{2.13}$$

where $V_j(\mathbf{r})$ is the scattering potential of this process, $E_{\mathbf{k}}$ and $E_{\mathbf{k}'}$ are the initial and final state energies of the particle. The delta function represents the conservation of energy, with $\hbar\omega$ the energy absorbed (upper sign) or emitted (lower sign) during the process. Fig. 2.2 lists the scattering mechanisms one should consider in a typical MC

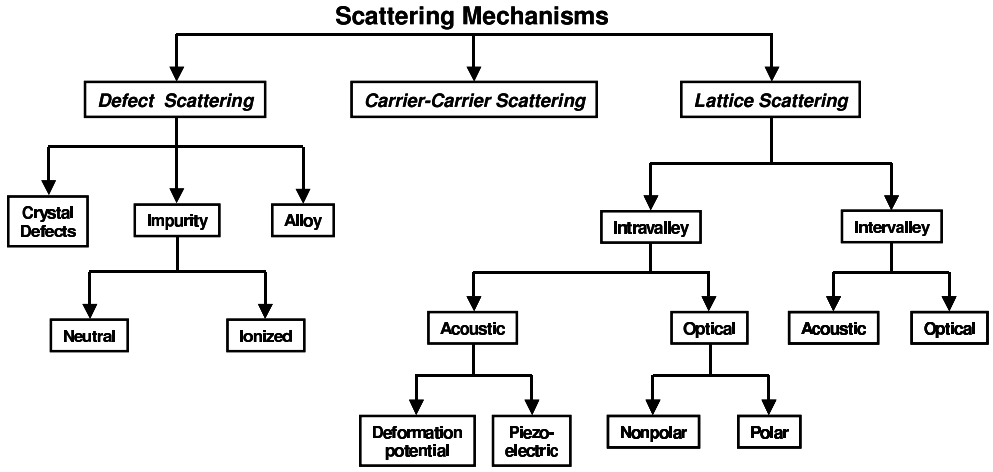

Figure 2.2: Scattering mechanisms in a typical semiconductor.

simulation. They are roughly divided into scattering due to crystal defects, which is primarily elastic in nature, lattice scattering between electrons (holes) and lattice vibrations or phonons, which is inelastic, and finally scattering between the particles themselves, including both single particle and collective type excitations. Phonon scattering involves different modes of vibration, either acoustic or optical, as well as both transverse and longitudinal modes. Carriers may either emit or absorb quanta of energy from the lattice, in the form of phonons, in individual scattering events. The designation of inter- versus intra-valley scattering comes from the multi-valley band structure model, and refers to whether the initial and final states are in the same valley or in different valleys. The scattering rates $\Gamma_j[n,\mathbf{k};m,\mathbf{k}']$ and $\Gamma_j[n,\mathbf{k}]$ are calculated using time dependent perturbation theory using Fermi's rule, Eqs. (2.13), and the calculated rates are then tabulated in a scattering table in order to select the type of scattering and final state after scattering as earlier discussed.

2.4.2 Inclusion of Ensemble Spin Dynamics

In EMC scheme, the spin property can be easily incorporated as an additional parameter, the spin polarization vector [14] or the spin density matrix [41], and calculated for each particle. If spin-dependent interactions between the carriers (dipole-dipole interaction, exchange interaction) are small, then each spin can be considered separately driven by external fields. Therefore, spin dynamics of each particle can be simulated within the classical scheme of the evolution of the classical momentum $\mathbf{S}$ under an effective magnetic field $\mathbf{\Omega_k}$ with the equation of motion

$$\frac{d\mathbf{S}}{dt} = \mathbf{\Omega_k} \times \mathbf{S}. \tag{2.14}$$

which is equivalent to the quantum-mechanical description of the evolution of the expected value of the spin quantum operator.

In Eq. (2.14), the scattering reorients the direction of the precession axis, making the orientation of the effective magnetic field random and trajectory-dependent, thus leading to spin relaxation (dephasing) [48].

2.5 Energy band structure, scattering mechanisms and physical parameters used for the study of GaAs bulk

The properties of electronic transport of a semiconductor material are related to the energy band structure and the kind of scattering events. The shape of energy bands is calculated through the structure of lattice, by approximately solving the Schrödinger's equation for a single electron in a lattice, through the techniques of the *Density Functional Theory* (DFT) [83].

The Fig. 2.4 shows the lattice structure of Gallium Arsenide (GaAs). It has equal numbers of gallium and arsenic ions distributed on a diamond lattice so that each ion has as nearest neighbors four ions of the opposite kind[2].

Usually, the energy bands are showed by making a plot of the electron energy as function of amplitude of electron momentum $\mathbf{k}$ in the interval of values of Brillouin

[2]The diamond lattice consists of two interpenetrating face centered cubic Bravais lattices, displaced along the body diagonal of the cubic cell by one quarter of the length of the diagonal.

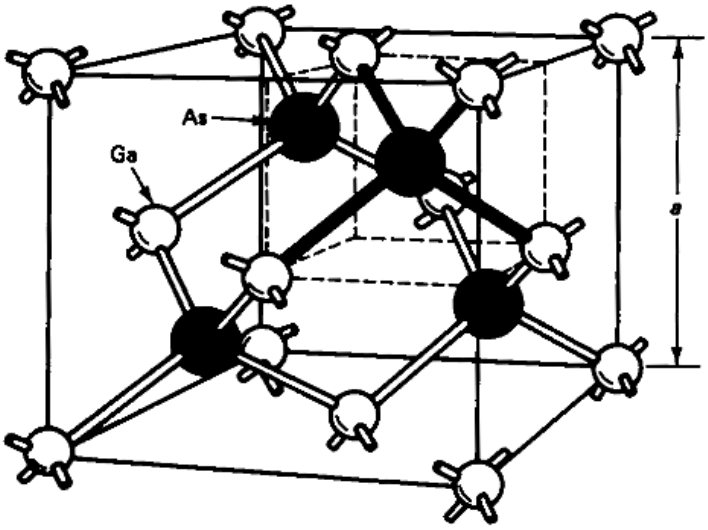

Figure 2.3: GaAs lattice structure.

zone. Since, the crystalline potential depends on the crystal orientation, the energy derives both from the **k**-module and its direction.

In our MC code, the model used for GaAs bulk is known as *three valleys model*. The GaAs band structure is shown in Fig. 2.4. The first conduction band shows three minima. The absolute minimum is at the center of the first Brillouin zone (Γ-valley), the second minimum is along $< 111 >$ direction (L-valley) and the last one, characterized by greater energy, is along $< 100 >$ direction (X-valley).

With the aim to study the electronic transport in presence of electric fields with amplitude not very high ($F < 100$ kV/cm), the inclusion of only these valleys in conduction band is sufficient: one Γ-valley, four equivalent L-valleys and three equivalent X-valleys. The central valley Γ is characterized by a small curvature, and hence, the corresponding effective mass of the electrons is very small. The satellite L and X- valleys are characterized by a low depth and a big value of the effective mass of the electrons. Each valley is assumed to be spherical and nonparabolic, and the *Kane's energy dispersion relation* $\epsilon(\mathbf{k})$ is used

$$\epsilon(\mathbf{k})[1 + \alpha\epsilon(\mathbf{k})] = \gamma(\mathbf{k}) = \frac{\hbar^2\mathbf{k}^2}{2m^*}. \tag{2.15}$$

The equations describing the free flight of the electron are

$$\mathbf{v} = \frac{1}{\hbar}\nabla_{\mathbf{k}}\epsilon = \frac{\hbar\mathbf{k}}{m^*(1 + 2\alpha\epsilon)}, \tag{2.16}$$

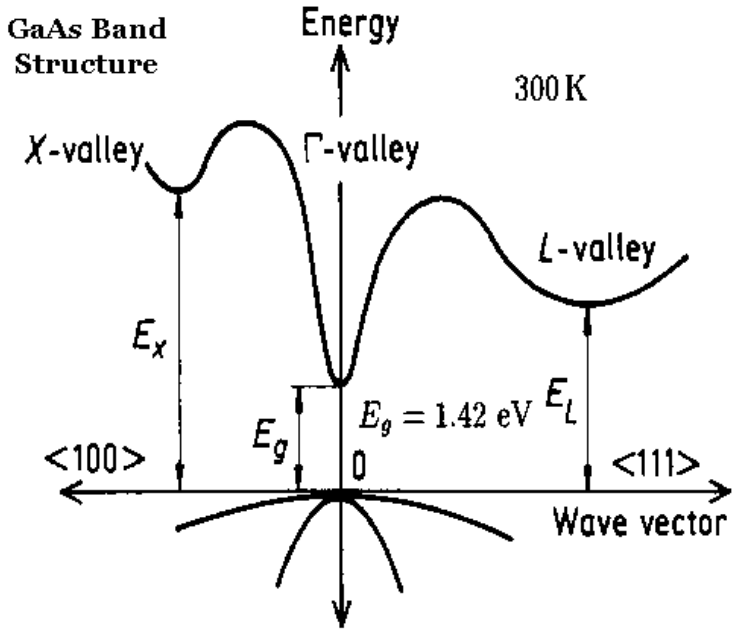

Figure 2.4: GaAs band structure.

$$\mathbf{r} = \mathbf{r}_0 - \frac{e\mathbf{F}t^2}{2m^*(1+2\alpha\epsilon)} + \frac{\hbar\mathbf{k}_0 t}{m^*(1+2\alpha\epsilon)}. \tag{2.17}$$

In our code, we assume that all donors are ionized and that the free electron concentration n is equal to the doping concentration. Moreover, we consider the probabilities of the scattering events to be field-independent. Accordingly, the influence of the external fields is only indirect through the field-modified electron velocities. Nonlinear interactions of the field with the lattice and bound carriers is also neglected.

All simulations are performed in a n-type GaAs bulk with a free electrons concentration varying into the range $10^{13} \div 10^{17}$ cm^3 (nondegenerate regime), by using a temporal step Δt of 10 fs and an ensemble of $5 \cdot 10^4$ electrons to collect spin statistics. All physical quantities of interest are calculated after a transient time of typically 10^4 time steps, long enough to achieve the steady-state transport regime. The spin relaxation simulation starts with all electrons of the ensemble initially polarized ($< \mathbf{S} >= 1$) along $\hat{\mathbf{x}}$-axis of the crystal, at the injection plane ($x_0 = 0$) [4, 13].

The complete set of n-type GaAs parameters used in our calculations is listed in Table 2.1.

Table 2.1: GaAs parameters used in the calculations

Density, kg/m^{-3}	5360
Sound velocity, m/s	5240
Dielectric constant (high frequency)	10.92
Dielectric constant (low frequency)	12.90
Piezoelectric constant, Cm^{-2}	0.0565

	Γ-valley	L-valley	X-valley
Effective mass	0.063	0.222	0.580
Nonparabolicity coefficient, eV^{-1}	0.7	0.5	0.3
Energy gap	0	0.32	0.52
Number of equivalent valleys	1	4	3
Acoustic deformation potential, eVm^{-1}	7	9.2	9.7
Optical deformation potential, $10^{10}eVm^{-1}$	–	3	–
Intervalley deformation potential, $10^{10}eVm^{-1}$			
Γ-valley	–	10	10
L-valley	10	10	5
X-valley	10	5	7
Polar optical phonon energy, eV	0.03613	0.03613	0.03613
Optical nonpolar phonon energy, eV	–	0.03430	–
Intervalley phonon energy, eV			
Γ-valley	–	0.0278	0.0299
L-valley	0.0278	0.0290	0.0293
X-valley	0.0299	0.0293	0.0299

2.6 Electron-electron collisions

Based on the *Random Phase Approximation* (RPA) of Bohm and Pines[3] [84], the effect of the electron-electron (e-e) interactions on electron transport in semiconductors can be studied by solving the Boltzmann transport equation using appropriate scattering rates [85],[72]-[74]. These scattering rates account for the energy conserving collision of electrons, and the transition probabilities are computed by time-dependent perturbation theory.

Here, the electron-electron scattering has been treated as an interaction between two particles using Moško and Mošková approach [95, 87], which is a refinement of previosly existing techniques [88]-[91] adapted to the case of a bulk. .

2.6.1 Derivation of the scattering rate for e-e interaction

Within a semiclassical electron model, the electrons can be described by wave packets with a finite extension smaller than the crystal volume. In this derivation, to simplify the analytical calculations, the energy bands are treated as parabolic. The theory of scattering of identical particles is used [92].

The Hamiltonian operator for the two electrons in the effective mass approximation is

$$\left(-\frac{\hbar^2}{2m_1^*}\Delta_1 - \frac{\hbar^2}{2m_2^*}\Delta_2 + V(\mathbf{r}_1 - \mathbf{r}_2)\right)\Psi(\mathbf{r}_1, \mathbf{r}_2) = E\Psi(\mathbf{r}_1, \mathbf{r}_2) \tag{2.18}$$

where m_i^* is the effective mass of electron i, Δ_i is the Laplace operator for electron i, and V is the interaction potential according to

$$V(\mathbf{r}_1 - \mathbf{r}_2) = \frac{-e}{4\pi\varepsilon_0\varepsilon_\infty}\frac{\exp(-\beta|\mathbf{r}_1 - \mathbf{r}_2|)}{|\mathbf{r}_1 - \mathbf{r}_2|}. \tag{2.19}$$

with e the elementary charge, ε_0 the dielectric constant of vacuum, ε_∞ the relative dielectric constant at the optical frequencies, $\mathbf{r}_1$ and $\mathbf{r}_2$ the coordinates of the couple of interacting electrons. β is the inverse of the screening length determined by

$$\beta^2 = \frac{e^2}{\varepsilon_S k_B}\sum_{i=\Gamma,L,X}\frac{n_i}{T_i} \tag{2.20}$$

[3]The random phase approximation (RPA) is an approximation method in condensed matter physics and in nuclear physics. Bohm and Pines RPA approximation accounts for the weak screened Coulomb interaction, and RPA is commonly used for describing the dynamic linear electronic response of electron systems.

which is valid when the electrons in each valley have a Boltzmann distribution. In this case the screening length coincides with the Debye length. Here ε_S is the static permeability, k_B the Boltzmann constant, n_i and T_i the electron concentration and temperature in valley i, respectively. The index i denotes the Γ, L, and X valleys, respectively.

Similarly to the charged-impurity scattering described in the Brooks-Herring approach, the interaction only depends on the separation distance among the particles [57], hence it is convenient to work with a frame of reference in which one of two particles is at rest. The nonrelativistic transformation in the new frame is achieved by defining the relative velocity $\mathbf{v}_r = \mathbf{v}_1 - \mathbf{v}_2$ and by introducing relative spatial coordinates:

$$\mathbf{r} = \mathbf{r}_1 - \mathbf{r}_2 \qquad \mathbf{R} = \frac{m_1^*\mathbf{r}_1 + m_2^*\mathbf{r}_2}{m_1^* + m_2^*}. \tag{2.21}$$

So, the scattering problem is formulated by

$$\left(-\frac{\hbar^2}{2m}\Delta + V(\mathbf{r})\right)\psi(\mathbf{r}) = E_{\mathbf{r}}\psi(\mathbf{r}) \tag{2.22}$$

with

$$m = \frac{m_1^* m_2^*}{m_1^* + m_2^*} \qquad E_{\mathbf{r}} = \frac{\hbar^2 k_{\mathbf{r}}^2}{2m} \qquad \mathbf{k}_{\mathbf{r}} = \frac{m_2^*\mathbf{k}_1 - m_1^*\mathbf{k}_2}{m_1^* + m_2^*}. \tag{2.23}$$

The equation (2.22) has solution having the following form

$$\psi(\mathbf{r}) = \frac{1}{\sqrt{V}}\left[e^{i\mathbf{k}_{\mathbf{r}}\cdot\mathbf{r}} + f(\Omega)\frac{e^{i\mathbf{k}_{\mathbf{r}}\cdot\mathbf{r}}}{r}\right] \tag{2.24}$$

where $\Omega = (\theta, \psi)$ and V the volume of the electron wave function. Since, the colliding electrons are indistinguishable, the exchange scattering must be taken into account. By introducing the probability p that the spins of colliding electrons are parallel the differential cross section of the particles is obtained as [92, 87]

$$d\sigma/d\Omega = |f(\theta)|^2 + |f(\pi - \theta)|^2 - 2pf(\theta)f(\pi - \theta) \tag{2.25}$$

where θ is the angle between $\mathbf{k}_r^{'}$ and $\mathbf{k}_r$. The probability p is equal 1/2 for spin-randomized electrons and equal to 1 for spin-polarized electrons [87]. Since in our study, the spin depolarization process is simulated, the probability p will be function of the time and will be updated at every time step.

In the first order Born's approximation[4], $f(\theta)$ is a real function given by

$$f(\theta) = -\frac{m}{2\pi\hbar^2}\left|\int_V e^{-i\mathbf{k}'_\mathbf{r}\cdot\mathbf{r}}V(r)e^{i\mathbf{k}_\mathbf{r}\cdot\mathbf{r}}d\mathbf{r}\right|. \tag{2.26}$$

The total cross section for one electron is

$$\sigma_{tot} = \frac{1}{2}\int_{all\ angles}\frac{d\sigma}{d\Omega}d\Omega \tag{2.27}$$

and the scattering rate is given by

$$\lambda(k_r) = (\hbar k_r/mV)\sigma_{tot}. \tag{2.28}$$

At the end of calculation, the scattering rate for a pair of colliding electrons is expressed by

$$\lambda(k_r) = \frac{m_i^* e^4|k_r|n}{\pi\varepsilon_0^2\varepsilon_\infty^2\hbar^3}\left[\frac{1}{(4k_r^2+\beta^2)\beta^2} - \frac{p}{4k_r^2(2k_r^2+\beta^2)}\ln\frac{4k_r^2+\beta^2}{\beta^2}\right], \tag{2.29}$$

with relative momentum vector

$$\mathbf{k}_r = (m_l^*\mathbf{k}_i - m_i^*\mathbf{k}_l)/(m_i^* + m_l^*), \tag{2.30}$$

n the electron density, $\mathbf{k}_i$ the wave vector of the scattered electron and, i and l the indices of the scattered electron and its partner respectively.

Therefore, the total scattering rate Λ of an electron in our Monte Carlo simulation procedure is given by

$$\Lambda = \sum_{j=1}^{M}\lambda^j(\mathbf{k}_i) + \sum_{l=1}^{N-1}\lambda^e(\mathbf{k}_i) + \Lambda_f. \tag{2.31}$$

where M is the number of scattering mechanisms without electron-electron collisions and Λ_f is the fictitious scattering rate [72]-[74].

A random number r $(0 \le r \le \Lambda)$ determines the scattering process which actually takes place. If

$$\sum_{j=1}^{M}\lambda^j(\mathbf{k}_i) + \sum_{q=1}^{l-1}\lambda^e(\mathbf{k}_i) < r < \sum_{j=1}^{M}\lambda^j(\mathbf{k}_i) + \sum_{q=1}^{l}\lambda^e(\mathbf{k}_i) \tag{2.32}$$

[4]The Born's approximation consists in only considering the incident wave and the waves scattered by only one interaction with the potential [93].

with $1 \leq l \leq N$ and $l \neq i$, then the electron is scattered at the partner with wave vector $\mathbf{k}_l$. The direction of the wave vector $\mathbf{k}_i'$ after the scattering process is given by

$$\mathbf{k}_i' = \mathbf{k}_r' + m_i^*(\mathbf{k}_i + \mathbf{k}_l)/(m_i^* + m_l^*), \tag{2.33}$$

where $\mathbf{k}_r'$ is the relative momentum vector after the collision obtained by reorienting the initial relative momentum vector $\mathbf{k}_r$ of the scattering angle α, which is a random quantity distributed between 0 and 2π. The probability distribution $P(\alpha)$ of α is proportional to the integrand in (2.27) and normalized to unity. The angle α can be obtained from the relation $r = \int_0^{\alpha} d\alpha' P(\alpha')$, where r is a random number between 0 and 1 [95]. From the computational point of view $\alpha(r)$ is selected by the von Neumann rejection technique [77, 82].

The wave vector of the scattering partner $\mathbf{k}_l$ is left unaltered due to the fact that its end of flight does not coincide with that one of the electron with wave vector $\mathbf{k}_i$. This causes that in a simulation procedure momentum and energy to be only statistically conserved.

2.6.2 Determination of the scattering partner [94]

In the above described model, when an electron experiences an e-e scattering, the electron partner is chosen in according to the Eq. (2.32). Since, this procedure is very time consuming, often other techniques are used. In our investigation, the electron partner is randomly chosen from the ensemble of all the other electrons. This is understable on the basis of the plane wave nature of electron wave functions considered [95], which specify no information in coordinate space. On the other hand, Kamra and Ghosh have recently proposed the choice of the electron partner as the nearest electron at the time of the scattering, as most logical alternative based on fact that, in a semiclassical model there is a definite coordinate value associated with every electron [96]. Before to begin our calculation, we have compared the results obtained with the two alternative techniques.

In Fig. 2.5(a), we show the average electron spin polarization $\langle S_x \rangle$ as a function of time, in the presence of a driving electric field with amplitude $F = 1$ kV/cm, obtained in a GaAs crystal having impurity density $n = 10^{13}$ cm^{-3} and lattice temperature $T_L = 300$ K. For the same values of parameters, in Fig. 2.5(b) we show the

electron velocity distribution. The curves have been obtained in steady state conditions with a different choice of the electron partner: randomly (red lines) and based on the minimum distance (blue lines). The different choice of the electron partner does not significantly affect the electron velocity distribution (see Fig. 2.5(b)), while the spin relaxation process is found to be slightly slower when the electron partner is randomly chosen, with a discrepancy smaller than 10%. A fitting of the two curves with an exponential function $< S_x > \propto \exp(-t/\tau)$ shows that the random choice of the electron partner leads to a better exponential trend (see Fig. 2.5(a)). For these reasons and with the aim to save computation time we randomly select the electron partner by the ensemble of electrons.

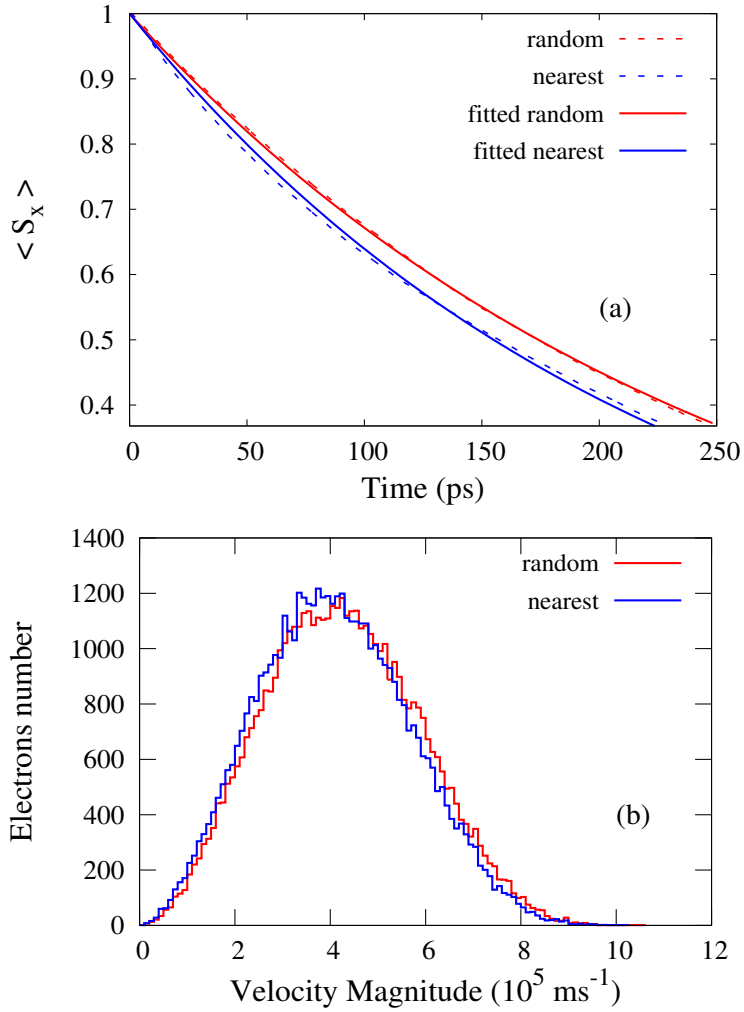

Figure 2.5: (a) Average electron spin polarization $\langle S_x \rangle$ as a function of time and (b) electron velocity distribution, obtained with $F = 1.0$ kV/cm, $n = 10^{13}$ cm^{-3} and $T_L = 300$ K. Each panel shows two curves obtained with a different choice of the Coulomb scattering partner: randomly (red lines) and based on the minimum distance (blue lines). In panel (a) dashed lines represent numerical data and solid lines are the fitting curves with an exponential function (see Eq. (1.59)) [94].

Chapter 3

Electron spin relaxation under low-field conditions

Inducing non-equilibrium spin polarization in a semiconductor, such as GaAs and Si, can be efficiently done and with reasonable current levels by electrical transfer of spins from a ferromagnetic metal across a thin tunnel barrier, at low temperatures ($5 - 150$ K) [7, 8]. Very recently, electrical injection of spin polarization in n-type and p-type silicon at room temperature have been experimentally carried out [11]. These experimental results very promising for development of spintronics devices, suggest that it is important investigate the spin dephasing up to room temperature.

Earlier Monte Carlo simulation has revealed that the presence of an external electric field can accentuate spin relaxation in GaAs bulk materials [14].

In this chapter, the influence of both lattice temperature ($10 < T_L < 300$ K) and low-field transport conditions ($0.1 < F < 2$ kV/cm) on the electron spin relaxation in lightly doped n-type GaAs semiconductors is investigated. Spin relaxation lengths and times are computed through the D'yakonov-Perel process [97]. For amplitudes of electric field lower than the Gunn threshold level, an analytical expression for the inhomogeneous broadening by calculating the average squared precession frequency is derived. Finally, the effect of the impurity density on lifetimes and relaxation lengths of electron spins, is analyzed with and without the inclusion of the electron-electron interaction [98, 99].

The inclusion of the electron-electron Coulomb scattering mechanism in our Monte Carlo procedure and the obtained results have been discussed during my

two-months visiting as reseacher student at the laboratories of Prof. Dr. Ming-Wei Wu in *Hefei's National Laboratory for Physical Sciences at Microscale* and in *Department of Physics* of the *University of Science and Technology of China*.

3.1 Temperature and electric field dependence of spin depolarization times and lengths [97]

The dependence of spin relaxation times and lengths on temperature and driving electric field has been investigated by simulating the relaxation dynamics of the spin of the electrons, and in all runs we have set a free electrons concentration n equal to 10^{13} cm^{-3}.

The initial non-equilibrium spin polarization decays with time as the electrons, driven by a static electric field, move through the medium, experiencing elastic and anelastic collisions. Since scattering events randomize the direction of $\mathbf{\Omega}$, during the motion, the polarization vector of the electron spin experiences a slow angular diffusion. The dephasing of each individual electron spin produces a distribution of spin states that results in an effective depolarization, which is calculated by ensemble-averaging over the spin of all the electrons.

In Fig. 3.1(a), we show the temporal decay of the electron average polarization $\langle S_x \rangle$, in the presence of an electric field, with amplitude $F = 0.1$ kV/cm and directed along the $\hat{\mathbf{x}}$-axis, for three different values of the lattice temperature, namely $T_L = 77$, 170 and 300 K. In Fig. 3.1(b), we show $\langle S_x \rangle$, as a function of the distance traveled by the center of mass of the electron cloud from the injection plane, at $T_L = 77$ K and for three different values of the external field amplitude, namely $F = 0.1$, 1.0 and 1.5 kV/cm. Since $\langle S_x \rangle$ is found to decrease with both time and distance by showing an almost linear trend in a semi-log plot, the spin relaxation times τ and lengths L are estimated by considering the spin depolarization as an exponentially process dependent on time and distance [14]. If $\langle S_x \rangle$ and $\langle x \rangle$ are the mean polarization of the spin along $\hat{\mathbf{x}}$-axis and the mean position of the ensemble of the electrons as a function of time, τ and L are chosen to be characteristic time and distance in according to the equations (1.59)-(1.60).

In Fig. 3.2, we show the spin electron relaxation length L (panel (a)) and the

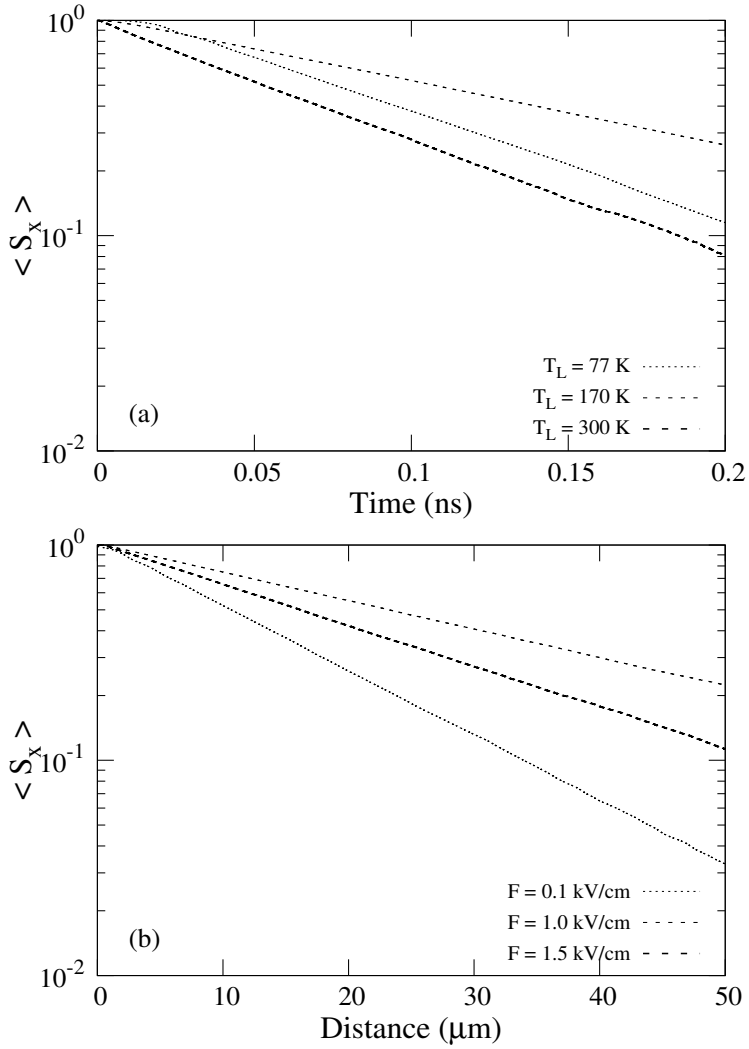

Figure 3.1: (a) Average spin polarization $\langle S_x \rangle$ as a function of time, with field amplitude $F = 0.1$ kV/cm, at three different values of temperature; (b) Average spin polarization $\langle S_x \rangle$ as a function of distance at $T_L = 77$ K, for three different values of the electric field amplitude [97].

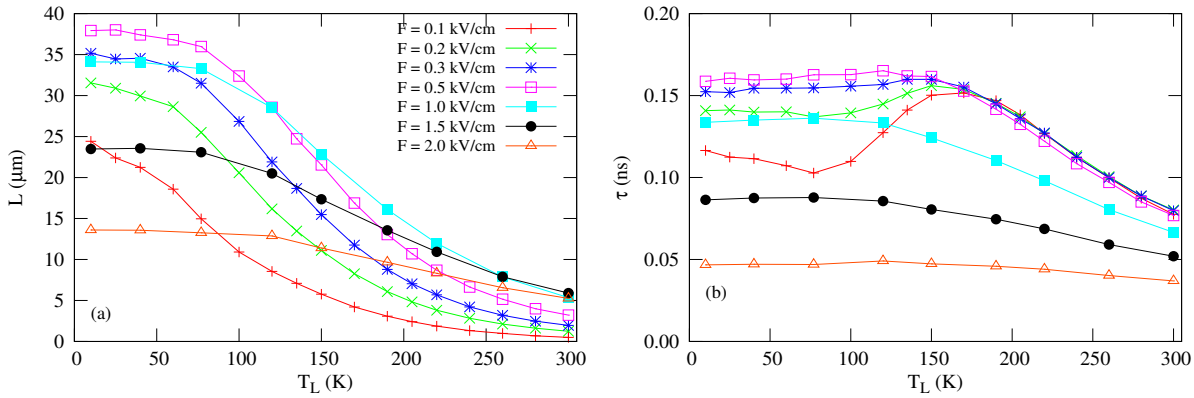

Figure 3.2: (a) Spin depolarization length L and (b) spin depolarization time τ as a function of the temperature T_L, plotted for several values of the electric field amplitude F [97].

spin depolarization time τ (panel (b)) as a function of the lattice temperature T_L, for several values of the electric field amplitude. For a fixed intensity of the electric field, the spin electron relaxation length is a monotonic decreasing function of T_L. When $F = 0.5$ kV/cm, L shows its maximum value, remaining greater than 35 μm up to $T_L \simeq 80$ K. Furthermore, for field amplitudes greater than 1 kV/cm, the spin depolarization length remains almost constant for $T_L < 100$ K. At room temperature the maximum value of L (~ 6 μm) is obtained for F≥ 1 kV/cm.

The relaxation time τ shows, instead, a nonmonotonic behavior with the lattice temperature (see Fig. 3.2(b)). In particular, the curves obtained with $F = 0.1$ and 0.2 kV/cm exhibit a minimum at $T_L \sim 80$ K and an increase in the range $100 - 170$ K. For temperatures greater than 170 K, all curves with a field amplitude up to 0.5 kV/cm show a common decreasing trend. The longest value of spin dephasing time ($\tau > 0.15$ ns) is achieved for the field amplitude $F = 0.5$ kV/cm up to temperatures $T_L \leq 150$ K. For higher values of F, the spin depolarization time strongly decreases, becoming nearly temperature-independent for $F > 1.5$ kV/cm.

As the lattice temperature increases, the scattering rate increases too, and hence the ensemble of spins loses its spatial order faster, resulting in a faster spin relaxation. This temperature dependence becomes less evident at higher amplitudes of the driving electric field, where, because of the greater drift velocities, the polarization loss is mainly due to the strong effective magnetic field. At very low electric

fields, the spin dephasing is, instead, primarily caused by the multiple scattering events. The nonmonotonicity of τ can be ascribed by the progressive change, with the increase of the temperature, of the dominant scattering mechanism from acoustic phonons and ionized impurities to polar optical phonons [22]. Following the main result of theory of D'yakonov-Perel, τ^{-1} is proportional to the third power of the electrons temperature T_e and linearly depends on the momentum relaxation time τ_p [48]. An increase of the temperature initially leads to a slightly decrease of τ; for temperatures greater than ~ 100 K the electrons start to experience scattering by polar optical phonons. This switching on leads to an abrupt decrease of τ_p that, for lattice temperatures in the range $100 - 150$ K, results more effective than the increase of T_L, giving rise to the observed increase of τ. For temperatures greater than 150 K this latter effect is no more relevant.

In Fig. 3.3, we plot the spin depolarization length L (panel (a)) and the spin

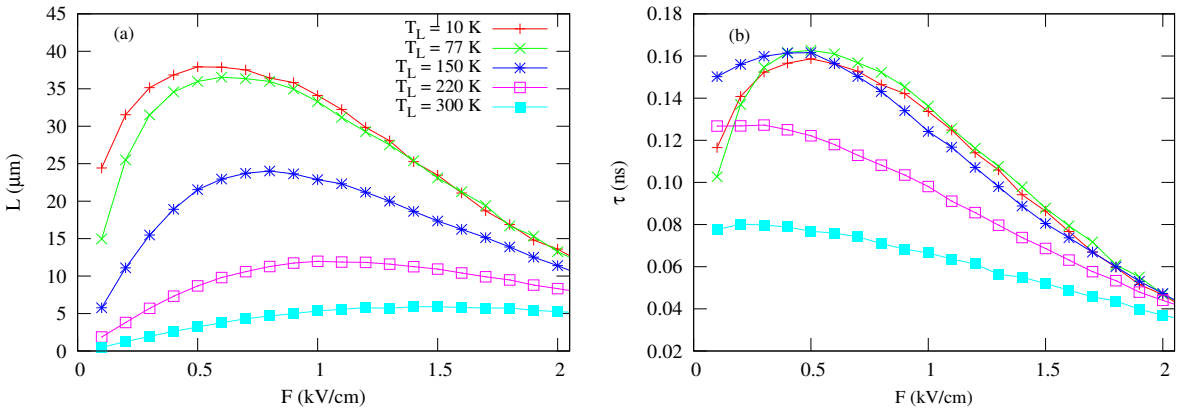

Figure 3.3: (a) Spin depolarization length L and (b) Spin depolarization time τ as a function of the electric field amplitude F, plotted for several values of the lattice temperature T_L [97].

depolarization time τ (panel (b)) as a function of the electric field amplitude, for different values of the lattice temperature. The spin relaxation lengths show a marked maximum that rapidly reduces its intensity, widens and moves towards higher electric field amplitudes with the increasing of T_L. For temperatures $T_L \leq 150$ K the spin lifetimes plotted in Fig. 3.3 (b) show a nonmonotonic behavior. For $F > 0.5$ kV/cm, τ lightly depends on the temperature up to $T_L \sim 150$ K.

The presence of a maximum in the spin depolarization time can be explained

by the interplay between two competing factors, both due to the increase of the electric field. In the momentum space, at greater field amplitudes, the electrons occupy states with larger $\mathbf{k}$, characterized by a stronger spin-orbit coupling, causing an enhancement of the spin inhomogeneous broadening (spatial variation of the precession frequency). On the other hand, a larger electric field also brings about an increase of the number of scattering events, giving rise to a reduction of the momentum relaxation time. This in turn causes an increase of the spin relaxation time as follows from Eq. (1.61).

At low values of temperature and for electric field amplitudes $0.1 \leq F \leq 0.5$ kV/cm the inhomogeneous broadening is still marginal and the spin relaxation phenomenon is dominated by the momentum scattering. In particular, the number of electron scattering events, which are mainly due to interactions with acoustic phonons at very weak electric fields, increases its value because of the triggering of the scattering mechanism by ionized impurities, causing a reduction of τ_p. For field amplitudes greater than ≈ 0.5 kV/cm, the enhancement of the spin-orbit coupling, which is $\mathbf{k}$-cubic dependent, is faster than the decrease on τ_p. Consequently, the spin lifetime starts to decrease with the increasing of the electric field. The nonmonotonic electric field dependence of τ is not observed for $T_L > 150$ K where, because of the greater drift electron velocities, the loss of spin polarization is mainly due to the strong effective magnetic field.

At higher temperatures, the spin electron relaxation time becomes a monotonic decreasing function of the electric field intensity.

The presence of maxima in the spin depolarization length at intermediate fields can be explained by the interplay between two competing factors: in the linear regime, as the field becomes larger, the electron momentum and the drift velocity increase in the direction of the field. On the other hand, the increased electron momentum also brings about a stronger effective magnetic field, as shown in Eq. (1.67) [14]. Consequently, the electron precession frequency becomes higher, resulting in faster spin relaxation (i.e., shorter spin relaxation time). For $F < 0.5$ kV/cm and $T_L \leq 150$ K the nonmonotonic behavior of the relaxation time reflects the complex scenario described above, caused by the triggering of scattering mechanisms having different rates of occurrence.

3.2 Doping and field dependence of the inhomogeneous broadening [99]

In absence of an applied electric field, the spin relaxation length is the diffusion length $L_s = \sqrt{D_s \tau}$ where D_s is the diffusion constant and τ is the spin relaxation time. An applied electric field can significantly change the relaxation length by dragging or pulling the electrons. When a semiconductor is in contact with a spin polarization source at $x = 0$, in absence of magnetic field ($\mathbf{B} = \mathbf{0}$) and with a static electric field ($\mathbf{F} = F\hat{\mathbf{x}}$) directed along the $\hat{\mathbf{x}}$-direction, the drift-diffusion model predicts spin accumulation with an exponential decay in the semiconductor $S(x) = S_0 \cdot \exp[-x/L]$ (see paragraph 1.4), in which L is the electric-field-dependent spin depolarization length [27, 28]. For electric field amplitudes, such that the diffusive contribution to the spin depolarization length can be neglected, the electrons move in average with the drift velocity v_d within the spin lifetime τ and [27, 28],

$$L = v_d \tau = \mu F \tau = \frac{eF\tau_p \tau}{m^*}, \tag{3.1}$$

where $\mu = e\tau_p/m^*$ is the electron mobility, e the elementary charge, m^* the electron effective mass and τ_p the momentum relaxation time (including the contributions due to several kind of scattering) [13]. In downstream case, the inequality $L_s < L$ is valid.

The spin relaxation process due to the DP mechanism is well explained by the random and trajectory-dependent orientation of the effective magnetic field caused by the unavoidable coupling with the fluctuating environment, such as the phonons, impurities and other carriers. These lead the spin precession frequencies $\mathbf{\Omega}(\mathbf{k})$ or their directions to vary from part to part within the electron spin ensemble, and so the total spin polarization undergoes a free-induction-decay due to destructive interference. This spatial variation, induced by $\mathbf{k}$-dependent spin-orbit coupling [100], is called *inhomogeneous broadening* (IB). It can be quantified by the average squared precession frequency ($<\mid \mathbf{\Omega}(\mathbf{k}) \mid^2>$) that is one of key factors of the D'yakonov-Perel's formula (see Eq. (1.61)), where the second important factor is τ_c, the correlation time of the random angular diffusion of spin precession vector.

In according to this formula, DP spin relaxation time decreases both with increasing τ_c and with increasing inhomogeneous broadening.

Since, in our case, we include the electron-electron interaction mechanism, one needs to distinguish between the momentum relaxation time τ_p and the momentum redistribution time $\tau_p^{'}$, which is practically equal to τ_c. This distinction is necessary because, although electron-electron scattering contributes to momentum redistribution, it does not directly lead to momentum relaxation [101]-[103].

By using Eqs. (3.1) and (1.61), the spin depolarization length can be expressed as

$$L = \frac{eF}{m^*} \frac{1}{<\mid \mathbf{\Omega}(\mathbf{k}) \mid^2>} \frac{\tau_p}{\tau_p^{'}}. \tag{3.2}$$

Hence, the spin injection length L results to be directly proportional to the applied electric field amplitude F and to the ratio $\tau_p/\tau_p^{'}$, while it is inversely proportional to the inhomogeneous broadening $<\mid \mathbf{\Omega}(\mathbf{k}) \mid^2>$.

At fixed value of F, the doping dependence of the spin injection length L can be studied by analyzing both $<\mid \mathbf{\Omega}(\mathbf{k}) \mid^2>$ and the ratio $\tau_p/\tau_p^{'}$ as a function of the electron density n.

3.2.1 Maxwell's distribution: zero electric field case ($F = 0$)

The main result of the theory of D'yakonov and Perel for spin relaxation in bulk system is [48, 53, 104]

$$\tau_{DP}^{-1} \simeq Q\tau_p\alpha^2 < \epsilon_{\mathbf{k}}^3 > /E_g. \tag{3.3}$$

Here, $\alpha = 2\beta_\Gamma\sqrt{2m^{*3}E_g}$ is a dimensionless parameter, E_g is the energy gap, $\epsilon_{\mathbf{k}}$ is the momentum-dependent energy and $Q \sim 1$ is a parameter depending on relevant scattering, $Q \simeq 1.5$ for ionized impurity scattering, $Q \simeq 3$ for longitudinal optical phonon scattering [22], $Q \simeq 0.8$ for piezoelectric acoustic phonon scattering, and $Q \sim 2.7$ for acoustic phonon scattering due to the deformation potential [4].

From Eq. (3.3), derived using the elastic-scattering approximation and in absence of a driving electric field, the spin relaxation time is independent on the doping density n. The elastic-scattering approximation artificially confines the random-walk-like spin precession, due to the $\mathbf{k}$-dependent spin-orbit field, only within the same energy states. However, when the inelastic electron-phonon scattering (i.e. the electron-LO-phonon scattering) as well as the electron-electron Coulomb scattering are taken into account, the random spin precession (*the inhomogeneous broadening*) should be fully counted for the whole $\mathbf{k}$ space, instead that only within the same

energy states [36]. On the other hand, both semiclassical Monte Carlo (MC) and Kinetic Spin Bloch Equations (KSBEs) approaches, which self-consistently solve spin precession and momentum scattering, take into account all scattering effects on the inhomogeneous broadening [36, 105]. In this case, Jiang and Wu [36] have found that, in absence of an applied electric field, the inhomogeneous broadening $<\mid \mathbf{\Omega}(\mathbf{k}) \mid^2>$ is little sensitive to n.

The same temperature dependence of the D'yakonov-Perel formula can be obtained by deriving the expression for the inhomogeneous broadening. With the use of the Maxwell-Boltzmann distribution for the momentum vector $f(\mathbf{k})$, which is a good assumption in nondegenerate regime, we find

$$<\mid \mathbf{\Omega}(\mathbf{k}) \mid^2>= \int_{\mathbf{k}} \mid \mathbf{\Omega}(\mathbf{k}) \mid^2 f(\mathbf{k}) d^3(\mathbf{k}) = \frac{12\beta_\Gamma^2}{\hbar^6}(m^* k_B T_e)^3. \tag{3.4}$$

Here T_e is the electron temperature, which is in general greater than the lattice temperature T_L, but for $F = 0$ the hot electron effect is absent and it is possible to replace T_e with T_L in the Eq. (3.4).

3.2.2 Drifted Maxwell's distribution, case: $F \neq 0$

In Ref. [14], Barry et al. have considered the electric field dependence of spin relaxation by using an approximate functional form of the Eq. (1.67). Their findings indicate that the common assumption of dependence on the third power of the electron temperature, provided by the Eq. (3.3), overestimates the spin relaxation rates in the drift regime. They suggest that a T_e^2 scaling may be more appropriate, but do not give an explicit analytical relation that includes the drift effect [14]. The presence of an applied electric field accelerates the electrons, so that their average velocity increases until reaches a stationary value v_d. The resulting distribution for the electron momentum is the drifted Maxwell-Boltzmann distribution [80, 75]

$$f_d(\mathbf{k}) = \left(\frac{\hbar^2}{2\pi m^* k_B T_e}\right)^{3/2} \exp\left[-\frac{\hbar^2}{2m^* k_B T_e} \sum_{i=x,y,z} \left(k_i - \frac{m^* \mu \mathbf{F} \cdot \hat{i}}{\hbar}\right)^2\right], \tag{3.5}$$

where $\mathbf{F} = F\hat{\mathbf{x}}$. By using Eq. (3.5), we calculate the ensemble average value of the squared precession frequency, obtaining

$$<\mid \mathbf{\Omega}(\mathbf{k}) \mid^2>_d = \frac{\beta_\Gamma^2}{\hbar^8}(m^* k_B T_e)\left[12(m^* k_B T_e)^2 + 12(m^* \mu F)^2 (m^* k_B T_e) + 2(m^* \mu F)^4\right]. \tag{3.6}$$

Eq. (3.6) generalizes the expression for the inhomogeneous broadening, by taking into account the drift effect. By putting $F = 0$ in Eq. (3.6), the zero field case is recovered (see Eq. (3.4)). With respect to Eq. (3.4), Eq. (3.6) contains two additive terms which are proportional to T_e^2 and T_e, respectively, confirming that, in the presence of an applied electric field, the dependence on electron temperature is not a simple T_e^3 scaling. Moreover, the ensemble average value of $\mid \mathbf{\Omega}(\mathbf{k}) \mid^2$ depends on the electron density n through the electron mobility μ that, in general, is a decreasing function of n [75].

3.3 Effect of doping density [98]

Until now, the experimental investigation of the doping density influence on the ultrafast spin dynamics in bulk semiconductors have been performed at low temperature ($T < 80$ K) [17, 25],[106]-[108]. In the detailed work of Dzhioev et al. [106], the dependence of the spin lifetime on the donor concentration shows at very low temperatures ($T < 5$ K) a very unusual behavior, characterized by the presence of two maxima, ascribed to the predominance of one of three different spin-relaxation mechanisms: hyperfine interaction, anisotropic exchange interaction, and D'yakonov-Perel (DP) mechanism. Recently, Römer et al. [107] have measured the electron-spin relaxation in bulk GaAs for doping densities close to the metal-to-insulator transition finding that, at temperatures higher than 30 K and densities lower than $8.8 \cdot 10^{16}$ cm^{-3}, all measurements are consistent with DP spin relaxation of free electrons since all electrons are delocalized and other spin-relaxation mechanisms can be neglected.

From a theoretical point of view, by using a fully microscopic kinetic spin Bloch equation approach, Jiang and Wu have predicted a nonmonotonic dependence of the spin relaxation time on the donor concentration, showing that the maximum spin relaxation time occurs at the crossing between degenerate regime and nondegenerate regime [36, 109].

In this section, we show the impurity density effect on the fast process of relaxation of non-equilibrium electron spin polarization in GaAs bulks for $10^{13} < n < 10^{17}$, $0.1 < F < 1$ kV/cm and $40 < T_L < 300$ K [98, 99].

In Fig. 3.4, we show the electron spin lifetime τ as a function of the doping density n, for different values of applied electric field F, namely 0.1, 0.5 and 1.0 kV/cm. In

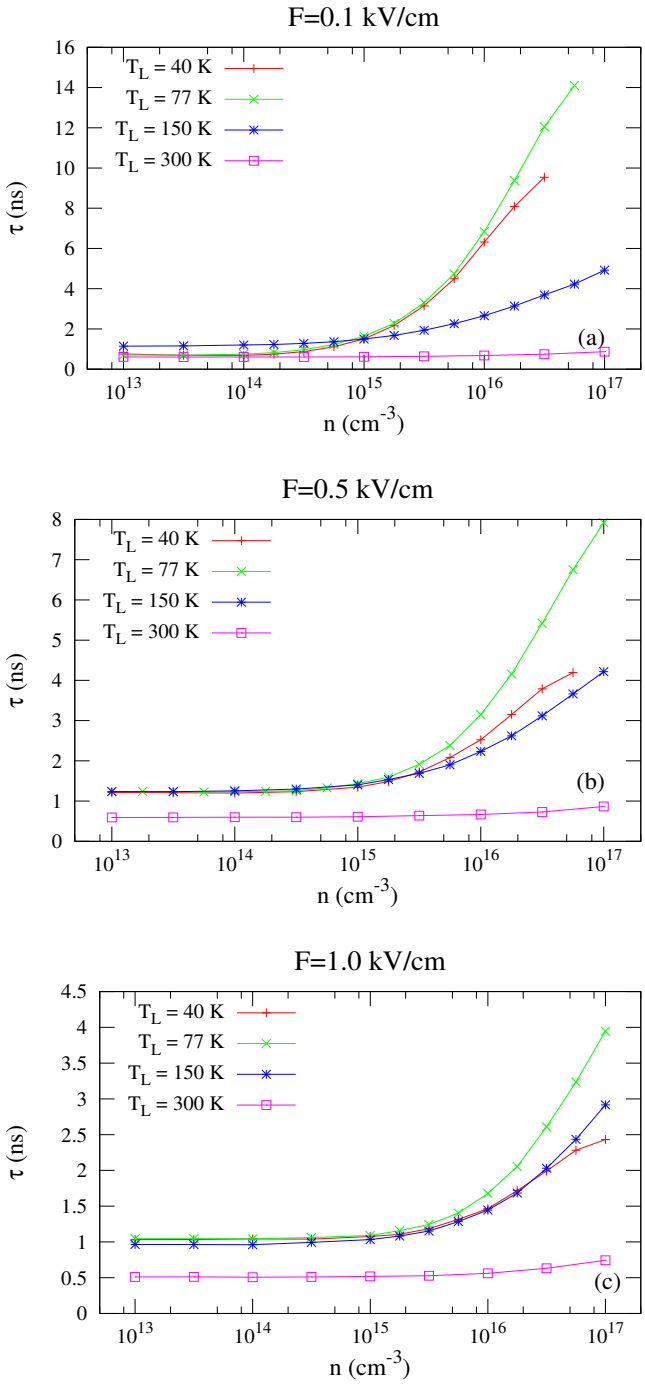

Figure 3.4: Electron spin lifetimes τ as a function of the doping density at different amplitudes of the applied electric field F (a) 0.1 kV/cm, (b) 0.5 kV/cm and (c) 1.0 kV/cm, and four different values of lattice temperature, namely T_L = 40, 77, 150, 300 K [98].

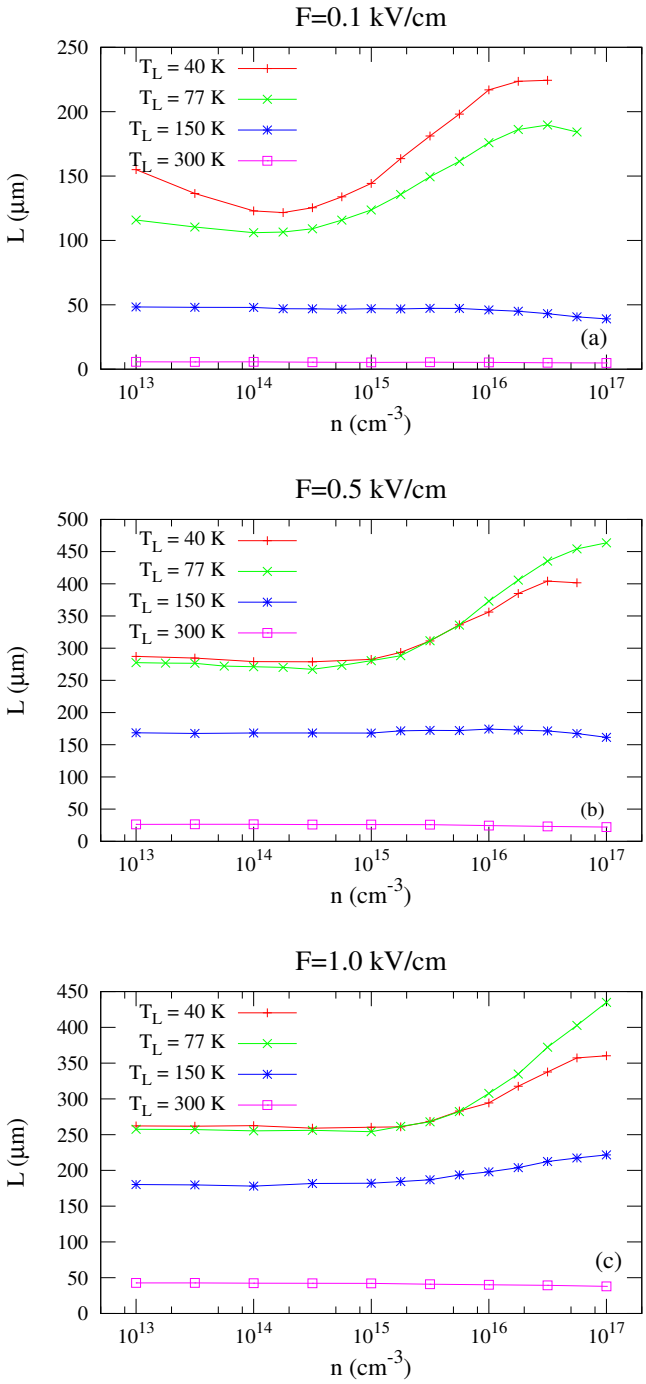

Figure 3.5: Electron spin depolarization length L as a function of the doping density at different amplitudes of the applied electric field F (a) 0.1 kV/cm, (b) 0.5 kV/cm and (c) 1.0 kV/cm, and four different values of lattice temperature, namely $T_L = 40$, 77, 150, 300 K [98].

each panel, we show four curves at the following values of lattice temperature T_L: 40, 77, 150 and 300 K.

Up to $T = 150$ K, the electron spin lifetime is nearly independent on n until $\sim 10^{15}$ cm^{-3}, then τ increases with the doping density. For $n > 10^{15}$ cm^{-3} and for each value of the applied field, the longest value of τ is obtained at $T_L = 77$ K (≈ 14 ns at $F = 0.1$ kV/cm). At the room temperature (300 K), the spin lifetimes are almost insensitive to the impurity density. In the investigated range of n, the system is nondegenerate, i.e. the electron plasma temperature is much greater than the Fermi's temperature T_F ($T_e \gg T_F$). Hence the inhomogeneous broadening $<| \mathbf{\Omega}(\mathbf{k}) |^2>$ is little sensitive to n, while the momentum scattering rate τ_p^{-1} is proportional to a linear function of n [36]. So, in accordance with the DP formula (Eq. (1.61)), for high values of n the spin lifetime τ increases with the doping density [48]. Moreover, for all the investigated intensities of the driving field, the relaxation time τ has a nonmonotonic behavior as a function of the temperature.

In Fig. 3.5, we show the electron spin depolarization length L as a function of the doping density n at the same values of applied electric fields and lattice temperatures used in Fig. 3.4. In particular, in panel (a), i.e. for $F = 0.1$ kV/cm and $T_L < 150$ K, L appear to be a nonmonotonic function of n, by showing a minimum at $\approx 2 \cdot 10^{14}$ cm^{-3}. At higher temperatures, L is nearly independent on the doping density. For higher amplitudes of the electric field (panels (b) and (c)), up to $T_L = 77$ K, L is insensitive to both the temperature and the doping density until $n \approx 10^{15}$ cm^{-3} and slightly increasing for higher values of n. For $T_L \geq 150$ K the effect of the doping density is marginal.

To understand the behaviour of L as a function of n, it is necessary to consider the interplay between τ and v_d in the relation $L = v_d\tau$. In fact, in the investigated range of n, the spin lifetime τ always increases with n; on the contrary v_d is a decreasing function of n. The nonmonotonic behavior of L, observed at $F = 0.1$ kV/cm and T_L in the range $40 \div 77$ K, arises from the fact that for $10^{13} < n < 2 \cdot 10^{14}$ cm^{-3}, v_d decreases more rapidly than τ increases. Viceversa, for $n > 2 \cdot 10^{14}$ cm^{-3}, τ increases more quickly and hence L increases too.

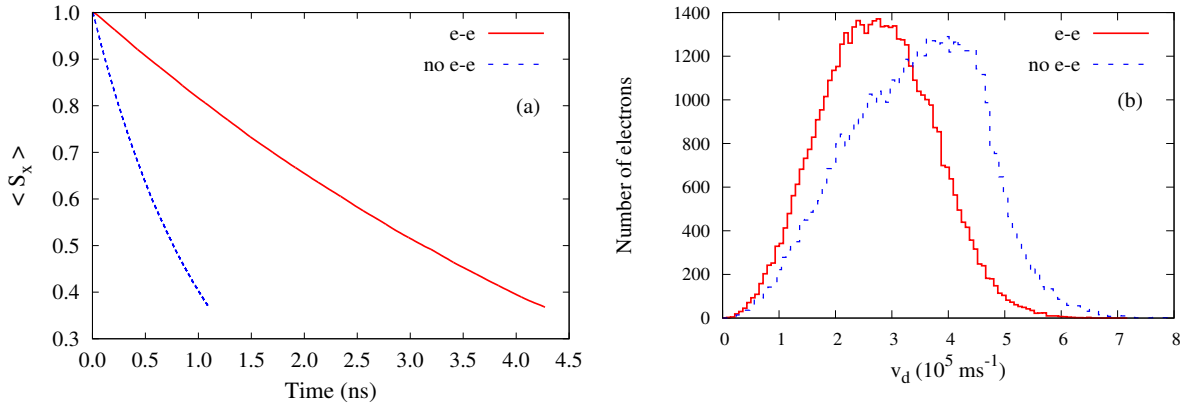

Figure 3.6: (a) Average electron spin polarization $\langle S_x \rangle$ as a function of time and (b) electron velocity distribution, with and without the Coulomb scattering, obtained with amplitude of applied electric field $F = 1.0$ kV/cm, electron density $n = 10^{13}$ cm^{-3} and lattice temperature $T_L = 40$ K [99].

3.3.1 Influence of electron-electron scattering [99]

In the previous section, we have reported and discussed the effect of doping density on both spin relaxation time and length without to take into account the electron-electron Coulomb scattering. In this subsection, we will give the discussion of the results obtained when the Coulomb interaction is considered.

Although it has long been believed that the electron-electron (e-e) Coulomb scattering does not contribute to the spin relaxation/dephasing [110], in the presence of inhomogeneous broadening in spin precession, any scattering, including spin-conserving scattering, can cause irreversible spin dephasing [111]. The inhomogeneous broadening can come from the energy-dependent g-factor [111], the D'yakonov-Perel term [100], the random spin-orbit coupling [112], and even the momentum dependence of the spin diffusion rate along the spatial gradient [113].

In [001]-grown n-doped quantum wells, the role of the Coulomb scattering in spin relaxation/dephasing was proved by Glazov and Ivchenko by using the perturbation theory, but its importance compared with all the other scattering mechanisms has not been addressed [101]-[103]. By using a fully microscopic kinetic approach, based on the spin Bloch equations, to study the effect of the Coulomb interaction on the spin dynamics in high-mobility low-density n-doped [001] quantum well, a peak in the temperature dependence of the spin relaxation time has been pre-

dicted [114, 115]. This temperature dependence of the spin dephasing has been experimentally verified [116, 117].

Despite the role of the electron-electron Coulomb scattering in spin dynamics has been extensively investigated in two dimensional systems, only recently has been shown that it is also very relevant for spin relaxation in bulk structures [36]. Nevertheless, to the best of our knowledge, a complete theoretical investigation of the spin depolarization in semiconductor bulk crystals, including the electron-electron scattering via MC method, is still lacking.

In Fig. 3.6a, we show the average electron spin polarization $\langle S_x \rangle$ as a function of time, in the presence of a driving electric field with amplitude $F = 1$ kV/cm, obtained in a GaAs crystal having impurity density $n = 10^{13}$ cm^{-3} and lattice temperature $T_L = 40$ K. For the same values of parameters, in Fig. 3.6b we show the electron velocity distribution. The curves have been obtained in steady state conditions with (red solid line) and without (blue dashed line) the inclusion of the electron-electron scattering. The spin lifetime τ, calculated with the inclusion of the e-e scattering, is about 4 times greater than the corresponding quantity obtained without it. This increase of the electron spin lifetime is in agreement with the numerical results obtained on 2DEG structures [34, 96] and on bulks [101, 36].

The increase of the spin relaxation time τ is due to the cooperative action of two factors. Firstly, the electron-electron scattering leads to a narrower distribution in the $\mathbf{k}$-space, which gives rise to an electron velocity distribution nearly Maxwellian (see Fig. 4.3b, red line). This involves a reduction in DP spin relaxation since τ^{-1} depends on $<| \mathbf{\Omega}(\mathbf{k}) |^2>$. Secondly, as shown by the Eq. (1.61), the DP spin relaxation rate is directly proportional to the correlation time τ_c, which is strongly reduced by electron-electron interaction mechanism.

In Fig. 3.7, we show the electron spin lifetime τ as a function of the doping density n, for different values of lattice temperature, (a) $T_L = 40$, (b) 77, and (c) 300 K. In panel (d), we show the electron spin lifetimes τ as a function of the lattice temperature T_L for three values of the electron density, namely $n = 10^{14}, 10^{15}$ and 10^{16} cm^{-3}. Up to $T_L = 77$ K, the electron spin lifetime τ is nearly independent on n until $n \approx 10^{14}$ cm^{-3}, then it increases with the doping density. The longest values of τ are obtained at $T_L = 77$ K. At room temperature, spin lifetimes are almost insensitive to the impurity density. These numerical findings are explained

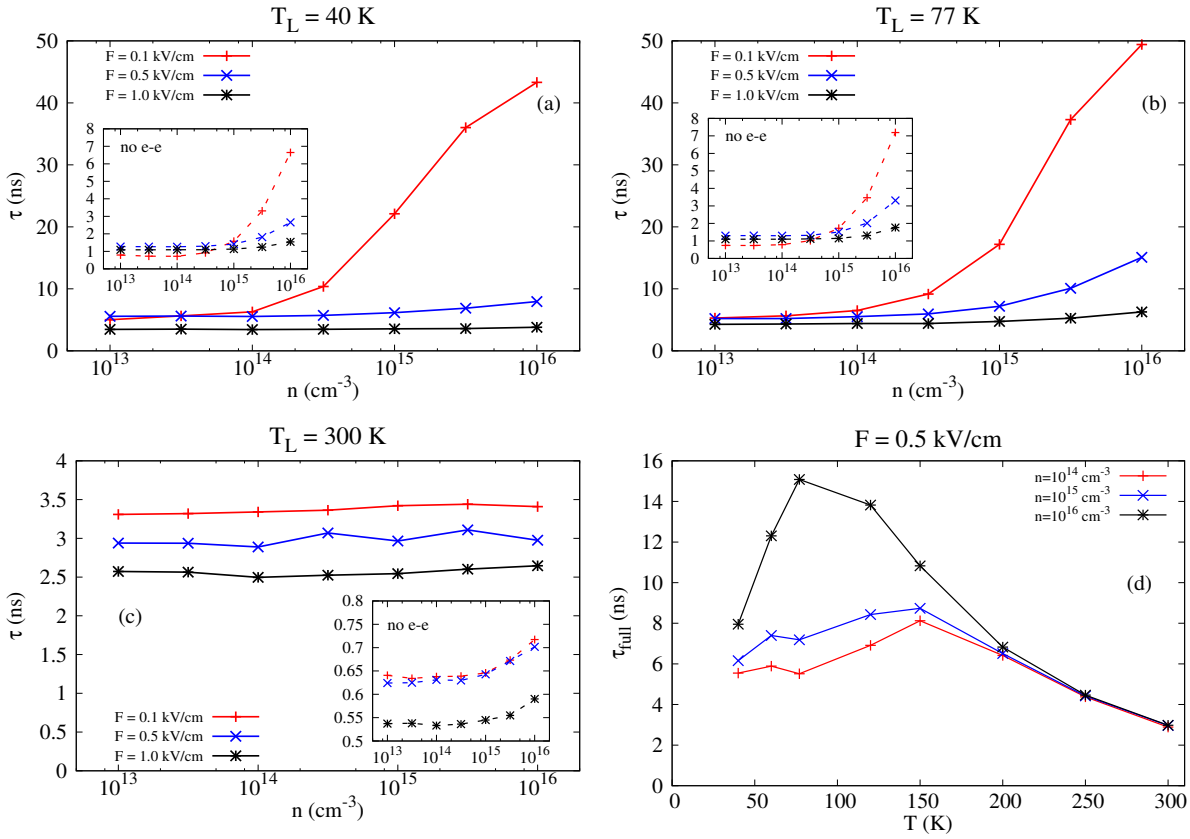

Figure 3.7: Electron spin lifetime τ as a function of the doping density n at different values of lattice temperature, namely (a) $T_L = 40$, (b) 77, and (c) 300 K, and three different values of electric field amplitude, namely $F = 0.1$, 0.5 and 1.0 kV/cm (solid lines). The insets show τ vs n without the inclusion of electron-electron scattering (dashed lines). (d) Electron spin lifetime τ as a function of the lattice temperature T_L for $F = 0.5$ kV/cm and three values of the electron density, namely $n = 10^{14}$, $n = 10^{15}$ and $n = 10^{16}$ cm^{-3} [99].

in accordance with the DP classical relation (see Eq. (1.61)). In fact, according to Eq. (3.6), $<| \mathbf{\Omega}(\mathbf{k}) |^2>$ is a decreasing function of n. Moreover, with the inclusion of Coulomb interaction $\tau_c^{-1} \approx < \lambda^e >$ (see Eq. (2.29)). Therefore, the correlation time τ_c of the random angular diffusion of the spin vector is inversely proportional to n and hence, the spin lifetime τ increases with the doping density.

The trends of the spin lifetime τ as a function of n, calculated without the electron-electron scattering (dashed lines), are similar to those obtained with full calculations, but the numerical values are significantly lower (see insets). The discrepancy is due to the reduction of the correlation time τ_c of DP relaxation process from τ_p to $\tau_p^{'}$, caused by the electron-electron interaction.

Panel (d) of Fig. 3.7 shows that spin relaxation time has a nonmonotonic behavior as a function of the lattice temperature for all the investigated values of electron density. In particular, the curve at the highest doping density ($n = 10^{16}$ cm^{-3}) shows a marked maximum around $T_L = 77$ K, while the other curves are wider and show reduced maxima around $T_L = 150$ K. This nonmonotonic behavior is in qualitative agreement with the results obtained in quantum wells, by using different theoretical approaches [114, 115] and with the recent experimental results of Leyland et al. [116]. From Eq. (3.6), at low temperatures the term $<| \mathbf{\Omega}(\mathbf{k}) |^2>$ increases approximately as $k_B T_e$, while at high temperatures increases as $(k_B T_e)^3$. Moreover, $\tau_c \propto T_e^{-2}$, therefore from Eq. (1.61) τ first increases and then decreases with the temperature. By further increasing the temperature, the terms proportional to $k_B T_e$ and $(k_B T_e)^2$ in Eq. (3.6) can be neglected. As a consequence $<| \mathbf{\Omega}(\mathbf{k}) |^2>$ becomes independent on the electron density. Therefore, at high lattice temperatures the lattice-electrons interaction prevails and the behavior of the electron spin lifetime versus the lattice temperature becomes independent on the electron density n. All the curves of Fig. 5.2(d), obtained for different values of n, collapse into a single curve.

In Fig. 3.8, we show the electron spin depolarization length L as a function of the doping density n at a fixed value of electric field amplitude $F = 0.1$ kV/cm and three values of lattice temperature, namely $T_L = 40$, 77 and 300 K, obtained with the inclusion of the e-e scattering. In the insets we show the results obtained without e-e scattering. Up to $T_L = 77$ K, the curves obtained in the presence of Coulomb interaction show that L is a nonmonotonic function of n, with a maximum at values

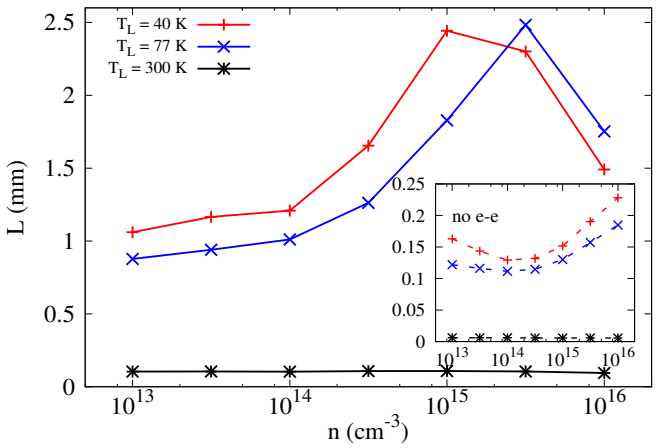

Figure 3.8: Electron spin depolarization length L as a function of the doping density n at $F = 0.1$ kV/cm and three different values of lattice temperature, namely $T_L = 40$, 77 and 300 K (solid lines). The inset shows L vs n without the inclusion of electron-electron scattering (dashed lines) [99].

of n within the range $10^{15} \div 3 \cdot 10^{15}$ cm^{-3}. At room temperature, L is independent on the doping density. Moreover, with the inclusion of the electron-electron scattering, also the spin depolarization length L is found to be significantly greater than that obtained by neglecting it.

In the presence of the Coulomb interaction, the behaviour of L as a function of n is described by the Eq. (3.2), where all quantities, that is the inhomogeneous broadening $<| \mathbf{\Omega}(\mathbf{k}) |^2>$, $\tau_p = e\mu/m^*$ and $\tau_p^{'}$ depend on n. The momentum redistribution time $\tau_p^{'}$ is equal to $< \lambda^e >^{-1}$, and hence inversely proportional to the electron density n (see Eq. (2.29)). Theoretical calculations [118, 119], that well describe the experimental results, show that at room temperature both τ_p and μ decrease with n. It is possible to approximate the mobility dependence on n by using the relation $\mu \propto n^{-a}$, characterized by an exponent a that changes with n. By best fitting our numerical calculations with this empirical law we have found that, at temperatures lower than 77 K, $a > 1$ for the highest electron densities ($10^{15} \div 10^{16}$ cm^{-3}) and $a < 1$ for the lowest ones ($10^{13} \div 10^{15}$ cm^{-3}). The inhomogeneous broadening $<| \mathbf{\Omega}(\mathbf{k}) |^2>$ also depends on n through the electron mobility μ. In particular, $<| \mathbf{\Omega}(\mathbf{k}) |^2>$ is approximately proportional to $k_1 + k_2 n^{-2a} + k_3 n^{-4a}$, where k_1, k_2 and k_3 are constants of proportionality. Hence $L \sim n^{1-a}/(k_1 + k_2 n^{-2a} + k_3 n^{-4a})$.

The nonmonotonic behavior of L could be ascribed to the fact that for values of n lower than 10^{15} $(3 \cdot 10^{15})$ cm^{-3} at $T_L = 40$ (77) K, respectively, $<|\ \mathbf{\Omega}(\mathbf{k})\ |^2>$ decreases and $\tau_p/\tau_p^{'}$ increases with n, while for greater values of n, $\tau_p/\tau_p^{'}$ decreases with n more rapidly than $<|\ \mathbf{\Omega}(\mathbf{k})\ |^2>$ decreases. At higher temperatures, the ratio $\tau_p/\tau_p^{'}$ remains almost constant with the electron density and the dominant term in Eq. (3.6) is independent on n. Therefore, from Eq. (3.2), L is nearly independent on n.

The behavior of L as a function of n, without the inclusion of the electron-electron scattering mechanism, is shown in the inset of Fig. 3.8. We see a minimum in the spin depolarization length, for low values of temperature T_L [98]. This false dependence on n is due to the fact that, when the spin relaxation process is simulated both at low temperatures and doping densities, the assumption to neglect the electron-electron Coulomb interaction is not more acceptable, since leads to a non-Maxwellian electron momentum distribution. With the aim to show that, the inclusion of the electron-electron scattering allows to obtain a Maxwellian distribution of the electron momentum, we have compared the distributions obtained with and without the Coulomb interaction. For purpose of comparison, we fit each electrons distribution with the expression

$$f_g(k_i) = C \exp\left[-r\left|k_i - \frac{m^*\mu\mathbf{F}\cdot\hat{\mathbf{i}}}{\hbar}\right|^s\right], \tag{3.7}$$

where $\mathbf{F} = F\hat{\mathbf{x}}$ and k_i is the $\hat{\mathbf{i}}$-component of electron momentum vector $\mathbf{k}$ (i=x,y,z). C, r and s are real and positive parameters. The definition of r is given from the expression

$$r = \left(\frac{\hbar^2}{2m^*k_BT_e}\right)^{s/2} \tag{3.8}$$

and the value of C is obtained from the normalization condition $\int_{-\infty}^{\infty} f_g(k_i)dk_i = 1$ as

$$C = \frac{r^{1/s}s}{2\Gamma(1/s)}. \tag{3.9}$$

The parameter s is the order of the exponential tails of $f_g(k_i)$, and Γ is the *Euler's Gamma function* defined as $\Gamma(z) = \int_0^{\infty} t^{z-1}e^{-t}\,\mathrm{d}t$ in the set of complex numbers z with positive real part $\Re(z) > 0$ [120].

The Eq. (3.7) is a generalization of the exponential function with the stretching

exponent s, and it is usually called *stretched exponential function* or *Kohlrausch's function* [121]. When $s < 2$, the graph of this generalized exponential function is characteristically stretched, with fat tails, while when $s > 2$, its shape has leaner tails with respect to case of the Maxwell-Boltzmann distribution. For $s = 2$, f_g becomes the drifted Maxwell-Boltzmann distribution for the $\hat{\mathbf{i}}$-component of $\mathbf{k}$. Moreover, f_g preserves the following important properties:

$$< k_x >= m^* \mu F/\hbar, \qquad < k_y >=< k_z >= 0, \tag{3.10}$$

and both C and r parameters depend on the hot-electron temperature T_e. In Fig. 3.9 we show the results of the comparison between the electron momentum distributions along the three directions $\hat{\mathbf{x}}$, $\hat{\mathbf{y}}$ and $\hat{\mathbf{z}}$ in momentum space, for fixed value of amplitude of the applied electric field $F = 0.1$ kV/cm and different values of doping density n and lattice temperature T_L. In particular, in panels (a), (b) and (c) $n = 10^{13}$ cm^{-3}, $T_L = 40$ K; in panels (d), (e) and (f) $n = 10^{13}$ cm^{-3}, $T_L = 300$ K; in panels (g), (h) and (i) $n = 10^{16}$ cm^{-3}, $T_L = 40$ K; and (j), (k), and (l) $n = 10^{16}$ cm^{-3}, $T_L = 300$ K. In each panel, the fitting curves have been removed and only the values of the parameter s, obtained by fitting the electron distribution, are shown. The parameters s_{full} and s are obtained, respectively, with and without the inclusion of the e-e scattering mechanism. The parameter s_{full} is always nearly equal to 2, while s ranges from a value lightly greater than 1 up to a value greater than 7. Thus, the inclusion of the Coulomb scattering gives rise to Maxwell-Boltzmann distribution curves. Moreover, by neglecting the electron-electron interation mechanism, even the $\hat{\mathbf{y}}$- and $\hat{\mathbf{z}}$-components show a value of s always lower than 2, and the distribution curves are characterized by higher peaks centered at zero, as expected. The $\mathbf{k}_x$ distributions are strongly dependent also on the lattice temperature T_L, especially at the lowest value of electron density. In particular, for $T_L = 40$ K and $n = 10^{13}$ cm^{-3}, the value of s reaches 7.31 and the associated distribution shows a shortened peak centered on the average value of $\mathbf{k}_x$ (see Fig. 3.9(a)). The curves reported in panels (d), (g) and (j) are not centered too in zero because of the drift effect, but the shift is clearly reduced, because the electron mobility μ is lower than that of case (a).

In conclusion, our analytical and numerical calculations demonstrate that, the inclusion of the electron-electron Coulomb interaction leads to a Maxwell-Boltzmann

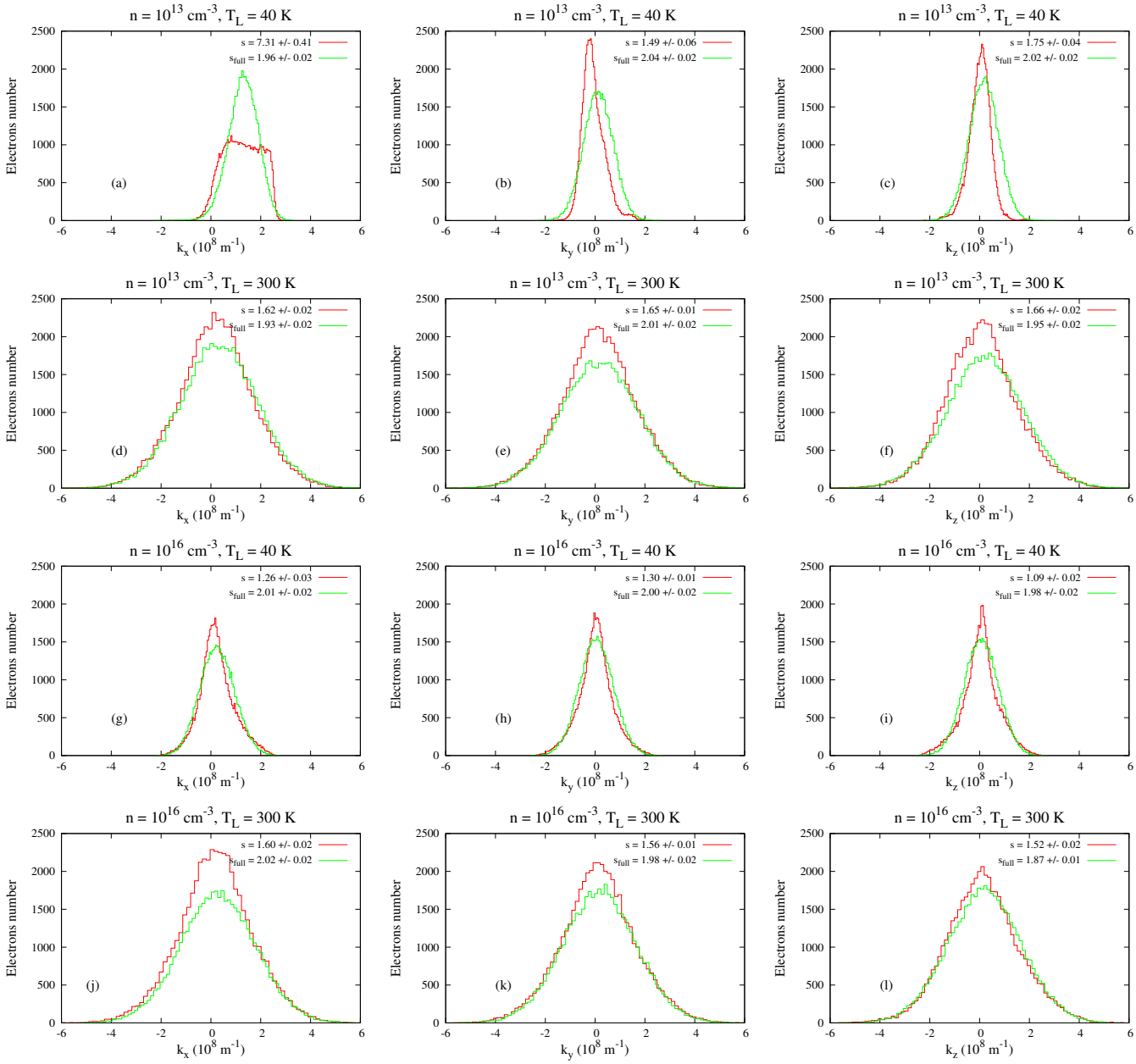

Figure 3.9: Electron momentum distributions along the three directions (a,d,g,j) $\hat{\mathbf{x}}$, (b,e,h,k) $\hat{\mathbf{y}}$ and (c,f,i,l) $\hat{\mathbf{z}}$ in momentum space at the fixed value of amplitude of applied electric field $F = 0.1$ kV/cm, and for different couples of values of doping density n and lattice temperature T_L. Namely (a,b,c) $n = 10^{13}$ cm^{-3}, $T_L = 40$ K; (d,e,f) $n = 10^{13}$ cm^{-3}, $T_L = 300$ K; (g,h,i) $n = 10^{16}$ cm^{-3}, $T_L = 40$ K; and (j,k,l) $n = 10^{16}$ cm^{-3}, $T_L = 300$ K [99].

distribution of the electrons in the **k**-space. Moreover, when the electron-electron scattering mechanism is taken into account, analytical results show that the average squared precession frequency decreases with the doping density, while increases with the electric field amplitude.

In the whole range of investigated values of applied electric field, spin lifetime and depolarization length are increased by the inclusion of the electron-electron scattering mechanism, in agreement with the effect of the e-e Coulomb interaction reported in previous work on semiconductor structures. In particular, in low electric field conditions and for lattice temperatures up to $T_L = 77$ K, the electron spin lifetime is an increasing function of the doping density. Moreover, for very low strengths of the driving field, the spin depolarization length shows a nonmonotonic behaviour with the density. At room temperature, spin relaxation tends to be insensitive to the donor concentration. These numerical results can be explained by using the analytical relation derived for the inhomogeneous broadening, and the ratio between the momentum relaxation time and the momentum redistribution time.

3.4 Comparison with experiments and with other theoretical approaches [99, 105]

Unfortunately, to the best of our knowledge experimental investigations on the relaxation of electron spin during drift transport in bulk semiconductors, at both sample temperatures higher than 30 K and applied field amplitudes greater than 0.1 kV/cm are still lacking.

Therefore, with the aim to validate the prediction capability of our MC code, we have performed a comparison between our numerical spin lifetimes and very recent experimental measurements of the electron spin relaxation rate, reported in Ref. [107]. The experiments were carried out by performing spin noise spectroscopy[1] on a sample of n-type GaAs at a doping concentration of $n = 2.7 \cdot 10^{15}$ cm^{-3}, without any driving field and for lattice temperatures T_L between 4 and 80 K. In Fig. 3.10 we plot the temperature dependence of the spin relaxation rate calculated from our

[1] Spin noise spectroscopy in semiconductors is an optical method that allows nearly perturbation free measurements of the spin dynamics of electrons in thermal equilibrium.

code with (solid line) and without (dashed line) electron-electron Coulomb scattering, together with the experimental data (full circles, sample B in Ref. [107]). In order to best fit the experimental points with our numerical prediction, we have utilized the spin-orbit coupling coefficient in Γ-valley β_Γ as a free parameter, obtaining the best agreement with $\beta_\Gamma^{no\,e-e}$=19 eV·Å^3 and β_Γ^{e-e}=51 eV·Å^3. The value of $\beta_\Gamma^{no\,e-e}$ is only slightly different from the value (23.8 eV·Å^3), recently estimated by using the tight binding theory [61], and within the reasonable range of values calculated and measured via various methods, as reported in Ref. [62]. Dashed line shows that, for sample temperatures in the range $50 \div 80$ K, our numerical trend well agrees with the experimental data, while out of this range of temperatures a considerable discrepancy is found, due to the neglecting the electron-electron scattering mechanism [105]. This discrepancy disappears when the Coulomb interaction is taken into account (solid line). Even taking into account the large spread among the published values for β_Γ, we find the best fitting value of β_Γ^{e-e} just out of the range of values listed in Ref. [62]. The finding of a large value of β_Γ^{e-e} could be ascribed to the fact that, in our investigations, the e-e interaction mechanism has been treated within the approximation of parabolic energy bands. Indeed, the inclusion of nonparabolic conduction bands could produce a larger e-e scattering rate, and cause the reduction of the value of β_Γ^{e-e} in the best fit.

In order to further test the effectiveness of our code we have compared our one-valley numerical data with the calculation of the effects of a low amplitude electric field ($F \leq 2$ kV/cm) on spin relaxation in n-type III-V semiconductor bulks, lately obtained from the fully microscopic kinetic spin Bloch equation (KSBE) approach [36, 122]. In Fig. 3.11 we plot the ratio of the spin relaxation time under electric field to the electric-field-free one $\tau(F)/\tau(F=0)$ and the ratio between the hot electron temperature and the lattice temperature T_e/T_L, as a function of the applied field obtained from our MC code for a GaAs bulk with $n = 10^{16}$ cm^{-3} at T_L=300 K. These results are compared with the calculation from the KSBEs (see Fig. 2(b) of Ref. [122]). Our findings for both spin lifetime and electron temperature are in very good agreement with the theoretical results obtained from the KSBE approach in all the investigated range (see Fig. 2(b) of Ref [122]). Moreover, we observe that, the values of the electron temperature obtained without including the electron-electron scattering are systematically slightly lower than those that ob-

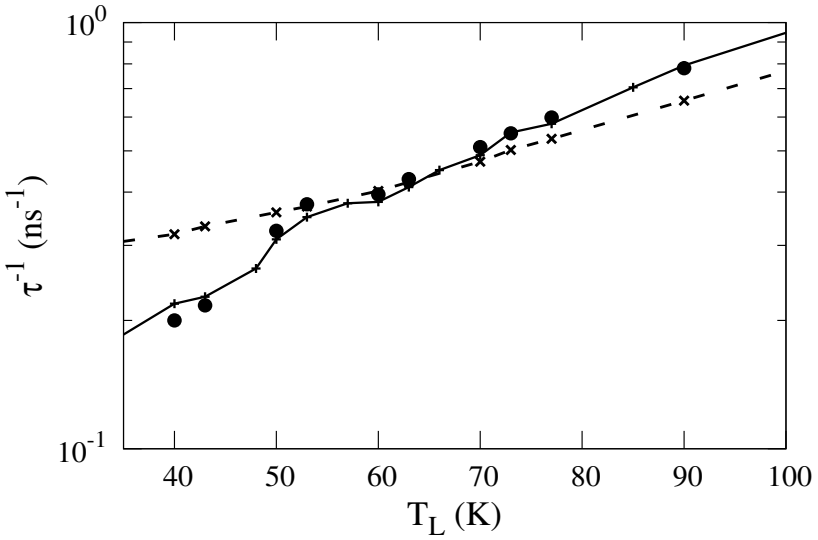

Figure 3.10: Temperature-dependent measurements of the spin-relaxation rate from the experiment (sample B) in Ref. [107] (circles) and numerical data obtained from our Monte Carlo code with (solid line) and without (dashed line) electron-electron Coulomb scattering, $n = 2.7 \cdot 10^{15}$ cm^{-3}, $\beta_\Gamma^{no\,e-e}$=19 eV·Å^3 and β_Γ^{e-e}=51 eV·Å^3 [99].

tained with the e-e scattering inclusion. Hence, electron-electron scattering is very important in determining the correct hot electron temperature. The hot electron temperature influences both the electron-longitudinal optical (e-LO) phonon and the electron-impurity scattering causing e-e scattering effectively influences spin relaxation.

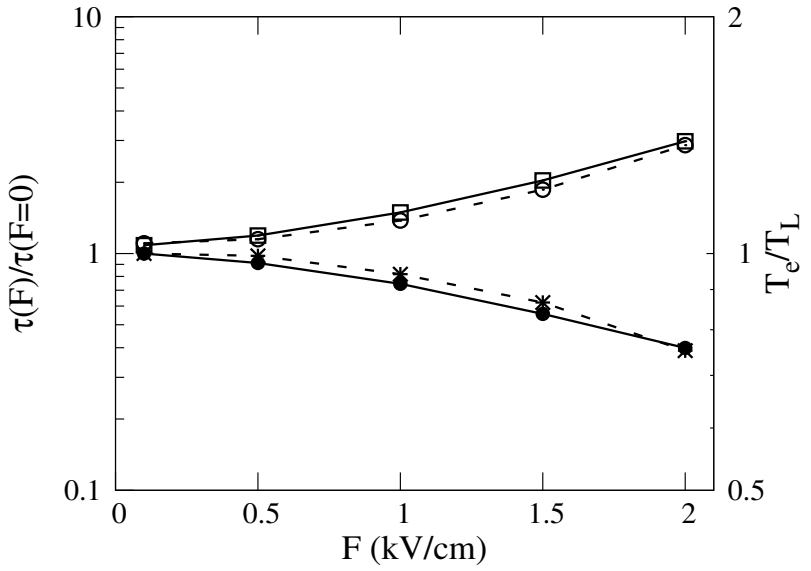

Figure 3.11: Lower curves: ratio of the spin relaxation time under electric field to the electric-field-free one $\tau(F)/\tau(F=0)$, in the presence (filled circles) and in the absence (stars) of the e-e scattering, respectively. Upper curves: ratio between the hot electron temperature and the lattice temperature T_e/T_L as a function of the applied field in the presence (squares) and in the absence (empty circles) of the e-e scattering, respectively. These behaviors have been obtained from our Monte Carlo code, with $n = 10^{16}$ cm^{-3} and $T_L = 300$ K [99].

Chapter 4

Electron spin relaxation under high-field conditions

In this chapter, the multivalley spin relaxation of drifting electrons in a doped n-type GaAs bulk semiconductor under high-field transport conditions is investigated, by considering the spin dynamics of electrons in both the Γ and the upper valleys of the semiconductor [105]. Spin dephasing times are calculated in a wide range of lattice temperature and doping density. Finally, the effect of the electron-electron Coulomb scattering on lifetimes and relaxation lengths of electron spins is investigated and the results obtained with and without the electron-electron interaction are compared [99].

We find a significant reduction of the average spin polarization lifetime at high intensities of the electric field, caused by the stronger spin-orbit coupling of electrons in the L-valleys. Moreover, for field amplitudes greater than 2.5 kV/cm, we observe at room lattice temperatures spin lifetimes longer than those observed at $T_L = 77$ K.

Our results show that the electron spin lifetime is not marginally influenced by the driving electric field, the lattice temperature and the impurity density, which hence represent key parameters into the depolarization process.

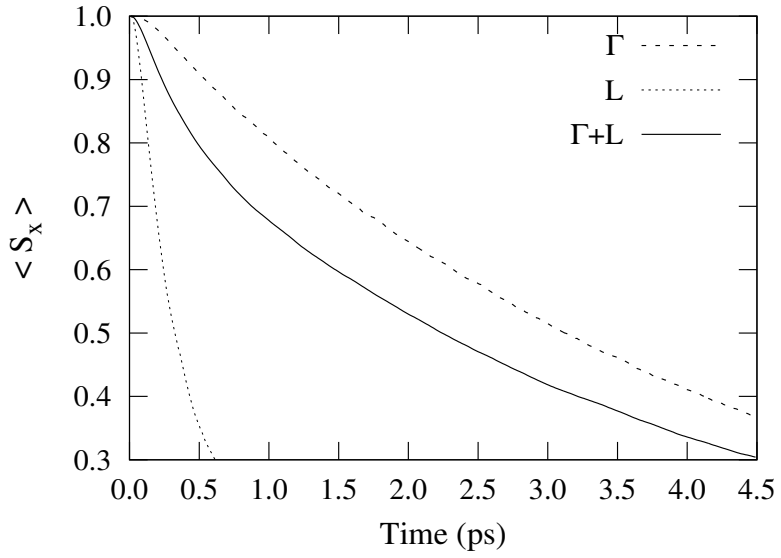

Figure 4.1: Average electron spin polarization $\langle S_x \rangle$ as a function of time, by only considering the electrons drifting into the Γ-valley (dashed line), into the L-valleys (dotted line) and into the $(\Gamma + L)$-valleys (solid line). $F = 5$ kV/cm, $n = 10^{13}$ cm^{-3} and $T_L = 300$ K [105].

4.1 Multivalley electron spin evolution

The miniaturization process forces the system to experience very intense electric fields, even when the applied voltages are very low. Hence, in this section, we consider electric field amplitudes higher than that of the Gunn field and discuss the influence of these fields on the spin dynamics. In our calculations, we calculate the value of the spin-orbit coupling parameter β_Γ by Eq. (1.70).

In Fig. 4.1 we show the average electron spin polarization $\langle S_x \rangle$, in the presence of a driving electric field, with amplitude $F = 5$ kV/cm and directed along the $\hat{\mathbf{x}}$-axis, with density $n = 10^{13}$ cm^{-3} and lattice temperature $T_L = 300$ K. This value of field amplitude is high enough to allow almost 21% of all electrons to visit the L valleys. The curves represent the decreasing trend of $\langle S_x \rangle$ vs. time by firstly considering only the electrons drifting into the Γ-valley (dashed line), secondly, by solely taking into account the electrons moving into the L-valleys (dotted line) and, finally, by considering the electrons moving into both the Γ and the L-valleys (solid line). We find a significant reduction of the average spin polarization lifetime caused by the

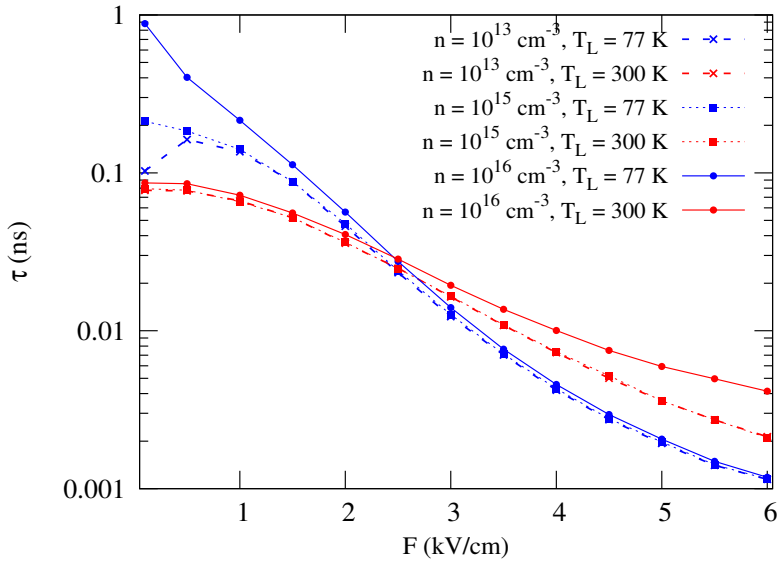

Figure 4.2: Spin lifetime τ as a function of the electric field amplitude F, at T_L=77 K (blue lines) and T_L=300 K (red lines), for three values of doping density, namely $n = 10^{13}$ cm^{-3}, $n = 10^{15}$ cm^{-3} and $n = 10^{16}$ cm^{-3}, with the electrons drifting in both the Γ and the L-valleys [105].

spin-orbit coupling in L-valleys stronger with respect to that in Γ-valley, according to the theoretical results obtained by Zhang et al. [35] on quantum wells. The transition of about 21% of electrons to the L-valleys leads to an increase of efficacy of the dephasing mechanism, which brings to a reduction of $\langle S_x \rangle$ over time in the range $15 \div 20\%$

4.2 Effects of temperature and doping density on spin relaxation [105]

In Fig. 4.2, we show the spin depolarization time τ as a function of the electric field amplitude F, for two values of the lattice temperature, namely $T_L = 77$ (blue curves) and 300 K (red curves) and three values of doping density $n = 10^{13}, 10^{15}$ and 10^{16} cm^{-3}, respectively, leaving the electrons free to drift in both the Γ and the L-valleys. Except for the case at the doping density $n = 10^{13}$ cm^{-3} and $T_L = 77$ K, we find that τ is always a monotonic decreasing function of F. In fact, when the field amplitude becomes larger, the electron momentum $\mathbf{k}$ increases, causing a stronger

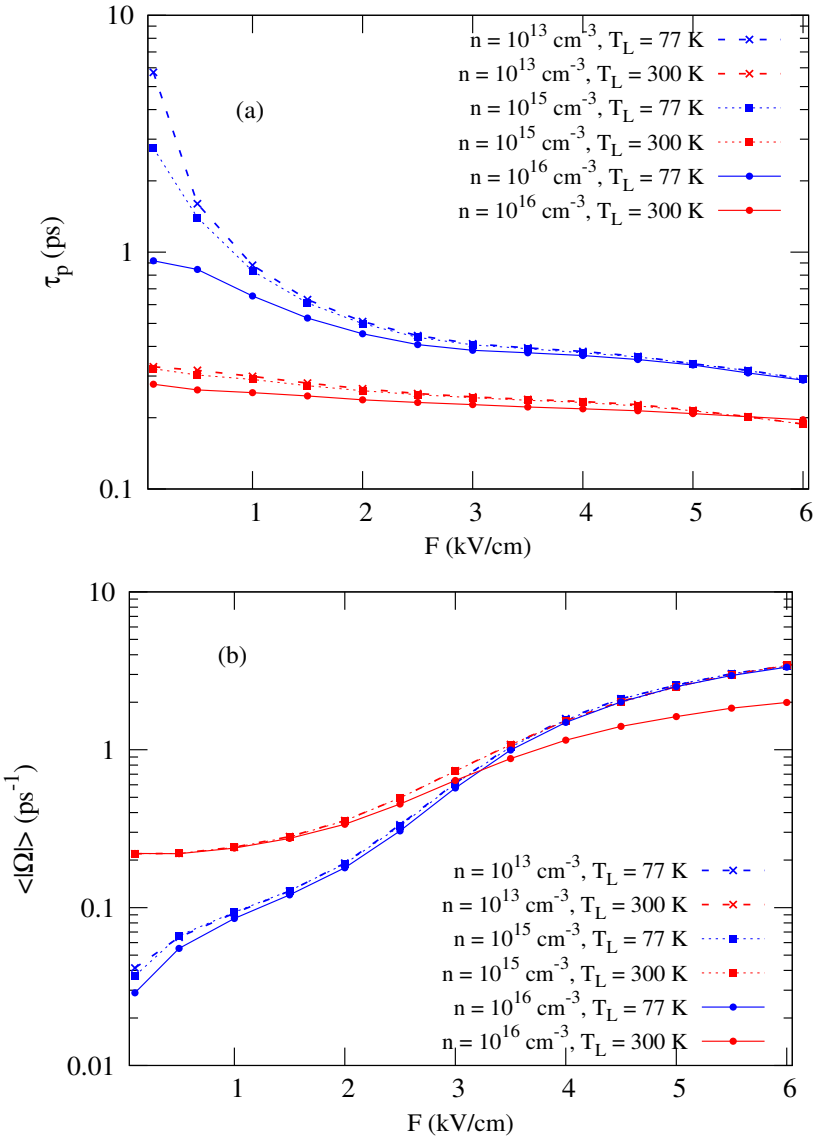

Figure 4.3: (a) Momentum scattering time τ_p and (b) spin precession frequency $<|\,\Omega\,|>$ as a function of the electric field amplitude F, at $T_L = 77$ K (blue lines) and $T_L = 300$ K (red lines), for three values of doping density, namely $n = 10^{13}, 10^{15}$ and 10^{16} cm^{-3} [105].

effective magnetic field, as expected by Equations (1.67)-(1.68). Consequently, the electron precession frequency becomes higher, inducing a faster spin relaxation [48].

For field amplitudes greater than 2.5 kV/cm, at $T_L = 300$ K we find depolarization times longer than those obtained at $T_L = 77$ K. In order to avoid that the observed behaviour could be ascribed only to stochastic fluctuations of MC computations, we have calculated the statistical error associated to our simulated data. We have repeated our simulations ten times, finding a maximum spread of 0.05 ps, which corresponds to about 1% of the observed variation of τ with the temperature.

We have investigated the counterintuitive behavior of longer average spin lifetimes obtained for hotter electrons, by adopting the DP proportionality law (1.61). We have calculated the spin precession frequency and the momentum characteristic scattering time for each electron of our ensemble and in Fig. 4.3, we show the average momentum scattering time τ_p (panel (a)) and the average spin precession frequency $<|\ \Omega\ |>$ (panel (b)) as a function of the electric field amplitude F, at $T_L = 77$ and 300 K, for the three values of doping density $n = 10^{13}, 10^{15}$ and 10^{16} cm^{-3}.

The panel (a) of Fig. 4.3 shows that τ_p is a monotonically decreasing function of F for every values of n and T_L. At the higher temperature ($T_L = 300$ K) we find low values of τ_p, because electrons experience a greater number of scattering events, both in the Γ-valley and in L-valleys. Moreover, the curves at room temperature are characterized by only a slight slope, because in this case the thermal energy of the electrons is dominant with respect to the drift kinetic energy. At $T_L = 77$ K and for very low values of the electric field amplitude, since the scattering events are mainly due to ionized impurities, τ_p is greatly dependent on n, increasing its value at lower densities. At $T_L = 300$ K, τ_p is nearly independent on the doping density since the dominant scattering mechanism is due to the optical phonons.

The panel (b) of Fig. 4.3 shows that the spin precession frequency $<|\ \Omega\ |>$ is an increasing monotonic function of F. For $F < 3$ kV/cm, independently from the values of the doping density, the values of $<|\ \Omega\ |>$ obtained at room temperature are larger than those obtained at $T_L = 77$ K. The increase of the spin precession frequency for electrons moving at higher temperatures is explained by the increasing number of electron transitions from the Γ to L valleys, being the value of the spin-orbit coupling coefficient in the L-valleys one order of magnitude greater than that of Γ-valley. At $T_L = 77$ K, for $F < 3$ kV/cm, the percentage of electrons in the

central valley Γ is practically unitary and the spin precession frequency increases as the third power of electron momentum, which increases with F according to the Eq. (1.67). When F is greater than 3 kV/cm, the percentage of electrons in the L-valley is high enough to lead Ω for having a nearly linear trend (see Eq. (1.68)). At $T_L = 300$ K, for $F < 3$ kV/cm, the term of thermal energy is dominant with respect to the drift kinetic energy and $<|\ \Omega\ |>$ vs. F shows a more slight increase.

For $F > 3$ kV/cm, independently from the values of T_L and n, the action of F wins on the disorder due to the lattice temperature. In fact, except for the data obtained at $T_L = 300$ K and $n = 10^{16}$ cm^{-3}, which show lower values of Ω, all curves coincide.

The calculation of the square of the spin precession frequency times the momentum relaxation time as a function of the electron energy for each electron of the ensemble shows that for $F > 2.5$ kV/cm the average value of $\Omega^2\tau_p$ obtained at $T_L = 77$ K is greater than that at $T_L = 300$ K. This finding explains the longer lifetimes observed at higher temperatures for field amplitudes greater than 2.5 kV/cm.

4.3 Influence of electron-electron scattering [99]

In Fig. 4.4(a), we show the spin lifetime τ obtained with and without the Coulomb scattering, as a function of the electric field amplitude F, at $T_L = 77$ K and 300 K, and for a fixed value of the doping density $n = 10^{15}$ cm^{-3}. The spin lifetime is a monotonic decreasing function of F. Moreover, for field amplitudes F greater than 2.5 kV/cm, spin lifetimes increase with the lattice temperature T_L, as previously found neglecting the electron-electron interaction. With the aim to quantitatively highlight the effect of the electron-electron scattering on the spin relaxation, we show in Figs. 4.4(b) and (c), the inhomogeneous broadening $<|\ \mathbf{\Omega}\ |^2>$ and the correlation time of DP process τ_c, respectively, as a function of the electric field amplitude F with and without the Coulomb scattering, at T_L=77 and 300 K, with $n = 10^{15}$ cm^{-3}. The values of $<|\ \mathbf{\Omega}\ |^2>$ increase with the lattice temperature T_L. Moreover, these quantities with the inclusion of the electron-electron scattering are found to be greater than those obtained in absence of this interaction. In panel (c) of Fig. 4.4, we observe that the correlation time τ_c of DP process as a function of the amplitude

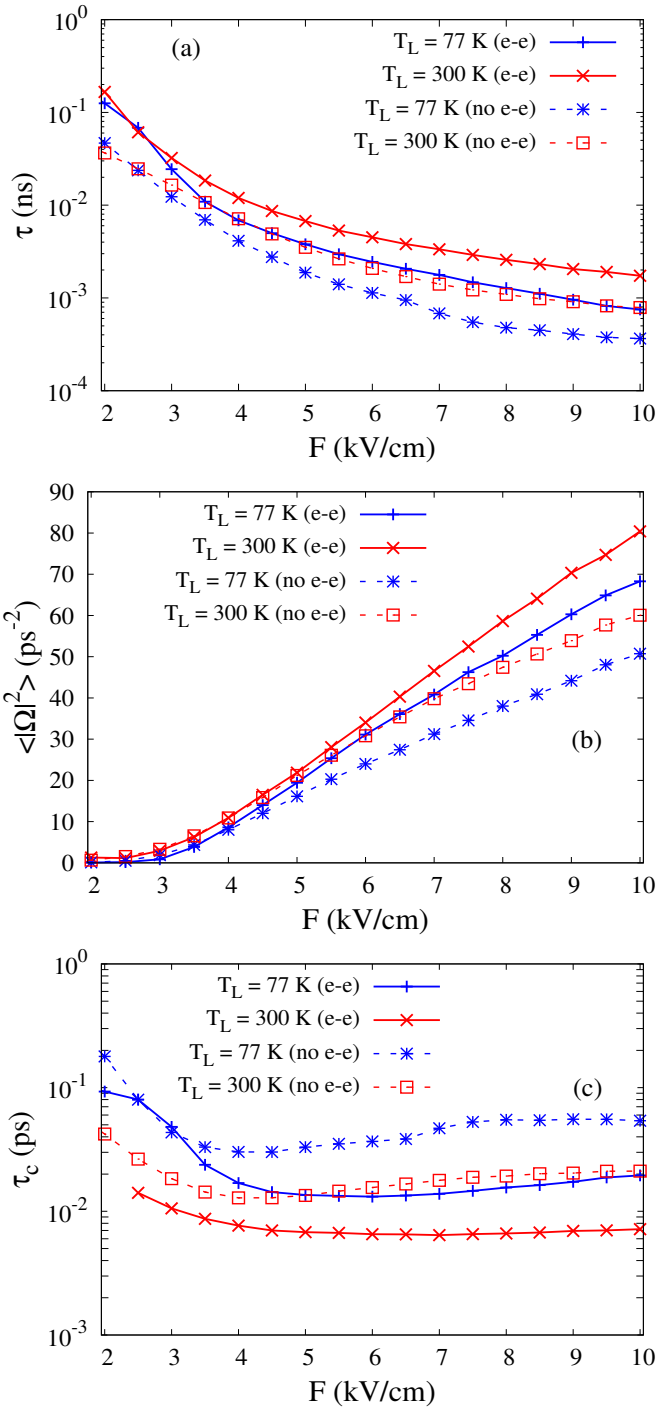

Figure 4.4: (a) Spin lifetime τ, (b) inhomogeneous broadening $<|\,\mathbf{\Omega}\,|^2>$ and (c) correlation time of DP process τ_c obtained with and without the inclusion of the electron-electron interaction mechanism, as a function of the electric field amplitude F, at T_L=77 K and T_L=300 K, and for a fixed value of the doping density, $n = 10^{15}$ cm^{-3} [99].

of the electric field F shows a decreasing behavior for $F < 4.5$ kV/cm, while it becomes nearly constant for higher values of F. Moreover, τ_c is strongly reduced when the electron-electron interaction is taken into account ($\tau_p^{'} \ll \tau_p$). Although both the inclusion of the e-e scattering mechanism and the increase of the lattice temperature give rise to an enhancement of $<|\ \mathbf{\Omega}\ |^2>$ (see Fig 4.4(b)), the correlation time of the DP process decreases with T_L (see Fig 4.4(c)) so strongly that this reduction becomes dominant in Eq. (1.61). This fact explains why the spin lifetimes obtained at room temperature are greater than those obtained at $T_L = 77$ K.

In conclusion, for high values of the electric field amplitudes, the spin depolarization process has been explored including the upper L and X valleys into the spin dephasing dynamics. Results obtained in the presence and in the absence of the electron-electron interaction have been compared, showing that the spin lifetimes obtained with the inclusion of the e-e scattering are greater than those obtained without it. Furthermore, spin lifetimes obtained at room temperature are greater than the corresponding values obtained at $T_L = 77$ K.

Chapter 5

Noise effect on electron spin relaxation [123]

The results discussed in this chapter are born from the idea to continue the investigation of the effects induced by external noise in semiconductor devices, which has been started some year ago by my supervisor Prof. Dr. Dominique Persano Adorno et al. [124]-[126]. The main goal of these studies is to demonstrate that the noise can assume a control role in transport phenomena, particularly relevant in nano-scale systems and devices.

In spin-based devices, the information stored in a system of polarized electron spins, must be transferred, as attached, to mobile carriers by applying an external electric field [2]-[5],[12]-[13]. In order to avoid nonlinear response, applied voltages are very low. Since, low voltages are more subjected to the background noise, in the design of spintronic devices is essential to understand the influence of fluctuations of the electric field on the spin depolarization process. Moreover, externally added noise could assume a control role also in spin relaxation process.

In this chapter, we focus our attention on the calculation of the modifications of the spin depolarization length caused by the addition of an external source of correlated noise in zinc-blende bulk semiconductors, for different values of the static field strength, noise amplitude and correlation time. The influence of the electron-electron scattering mechanism is also shown and discussed [123].

This study has been possible thank to an one-year HPC 2010 Grant received from *CASPUR Consortium (Interuniversity Consortium for Supercomputing Appli-*

cations for Universities and Research).

5.1 A brief introduction to the problem

Over the last twenty years the tendency to use the noise in nonlinear systems out of equilibrium has been established. It has been discovered that there are some interesting cases in which the simultaneous presence of noise and nonlinearities may lead to situations of greater order, giving rise to some constructive effects, such as *Stochastic Resonance* (SR), *Noise Enhanced Stability* (NES), *Resonant Activation* (RA), etc. [127]-[130]. Moreover, the analysis of the phenomena induced by noise in systems far from equilibrium allows to understand the behavior of complex physical systems.

The presence of noise in experiments is generally considered a disturbance, especially in determining the performance of semiconductor-based devices, where strong fluctuations could affect their response. The existence of fluctuations, for example, can limit the lifetime of the information stored in a memory cell, it bothers the opening (or closure) of random logic gates and it causes the enlargement of the distribution of arrival times of signals on transmission lines. One of fundamental problems in quantum computation is related to the destruction of entangled states of qubits caused by interaction with the environment. This event is characterized by loss of coherence, which is not suitable for the design of quantum computers [131].

Recently, an increasing interest has been directed towards the constructive aspects of fluctuations on the dynamical response of semiconductor systems. In bulk materials the possibility to reduce the diffusion noise by adding a correlated random contribution to a driving static electric field has been investigated by Varani and collaborators. Their numerical results, obtained by including energetic considerations in the theoretical analysis, have shown that, under specific conditions of the fluctuating electric field, it is possible to suppress the intrinsic noise in n-type GaAs semiconductors [132]. A less noisy response in the presence of a driving periodic electric field containing time-correlated or random telegraph fluctuations has been observed in GaAs bulks by studying the changes of the spectrum of fluctuations of the electrons velocity [124]-[126]. A clear reduction of the peak of the power spec-

tral density at the operating frequency has been observed for a wide range of noise amplitude and noise correlation times lower than duration of a cycle of the driving periodic electric field [124, 125]. This reduction effect arises from the fact that the transport dynamics of electrons in the semiconductor receives a benefit by the constructive interplay between the random fluctuating electric field and the intrinsic noise of the system.

Theoretical works which discuss the way to improve the ultra-fast magnetization dynamics of magnetic spin systems by including random fields have been recently published [133]-[135]. Nevertheless, to the best of our knowledge, the investigation of the role of noise on the electron spin dynamics in semiconductors is still missing.

5.2 Noise modeling

In our simulations the semiconductor bulk is driven by a fluctuating electric field

$$F(t) = F_0 + \eta(t) \tag{5.1}$$

where F_0 is the amplitude of the deterministic part and $\eta(t)$ is a random term, modeled by a stochastic process. Here, $\eta(t)$ is modeled as an Ornstein-Uhlenbeck (OU) process, which obeys the stochastic differential equation [136]

$$\frac{\mathrm{d}\eta(t)}{\mathrm{d}t} = -\frac{\eta(t)}{\tau_D} + \sqrt{\frac{2D}{\tau_D}}\xi(t) \tag{5.2}$$

where τ_D and D are, respectively, the correlation time and the intensity of the noise described by the OU process which has the autocorrelation function expressed by $\langle \eta(t)\eta(t') \rangle = D \exp(-|t-t'|/\tau_D)$. $\xi(t)$ is a Gaussian white noise with zero mean $< \xi(t) >= 0$, and autocorrelation function $\langle \xi(t)\xi(t') \rangle = \delta(t-t')$. Within the framework of the Ito's calculus, the general solution of the equation (5.2) leads to the following complete expression for the stochastic evolution of the amplitude of the electric field

$$F(t) = F_0 + \eta(0)e^{-t/\tau_D} + \sqrt{\frac{2D}{\tau_D}} \int_0^t e^{-\frac{t-t'}{\tau_D}} dW(t'), \tag{5.3}$$

where the initial condition is $\eta(0) = 0$, and $W(t)$ is the Wiener process [136].

In a practical system, $\eta(t)$ could be generated by a RC circuit driven by a source

of Gaussian white noise, with correlation time $\tau_D = (RC)^{-1}$ (see equation (5.2)). The Gaussian white noise can be generated either by the Zener breakdown phenomenon in a diode or in a inversely polarized base-collector junction of a BJT, either by amplifying the thermal noise in a resistor [137]. The correlation time τ_D is tunable by using a diode (varicap) with a voltage-dependent variable capacitance; the noise intensity D can be chosen, for example, by suitably amplifying the noise produced through the Zener stochastic process.

5.3 Effects of a fluctuating electric field on spin relaxation

In this section, all simulations have been performed in a GaAs crystal with a free electrons concentration n equal to 10^{13} cm^{-3} and lattice temperature T_L equal to 77 K. All physical quantities of interest are collected in steady-state transport regime. The spin lifetime τ and the spin depolarization length L are calculated by extracting, respectively, the time and the distance from the injection plane of the center of mass of the electron ensemble, corresponding to a reduction of the initial spin polarization by a factor $1/e$.

In Fig. 5.1, we show electron spin average polarization $\langle S_x \rangle$ as a function of the distance traveled by the center of mass of the electron cloud from the injection point, obtained by applying a fluctuating field characterized by a deterministic component with amplitude F_0 and a random component with standard deviation $D^{1/2}$, for three different values of noise correlation time τ_D: $10^{-4}\tau_0$, $10^{-1}\tau_0$, $10^{2}\tau_0$ and in absence of noise; τ_0 is the spin relaxation time obtained in absence of noise at the same value of F_0. In panel (a): $F_0 = 1$ kV/cm and $D^{1/2} = 0.6$ kV/cm; in panel (b): $F_0 = 6$ kV/cm and $D^{1/2} = 3.6$ kV/cm.

When $\tau_D << \tau_0$, the spin dephasing process is not affected by the fluctuations of the electric field, which have a negligible memory (τ_D) with respect to the characteristic time τ_0 of the system. In particular, under low electric field condition (panel (a)), the spin relaxation process is significantly influenced by the fluctuating field only for values of noise correlation time comparable with τ_0, while the process becomes quasi-deterministic when $\tau_D >> \tau_0$. Differently, under high electric field condition (panel (b)) when $\tau_D \sim \tau_0$ and $\tau_D >> \tau_0$, a slow down of the spin relaxation

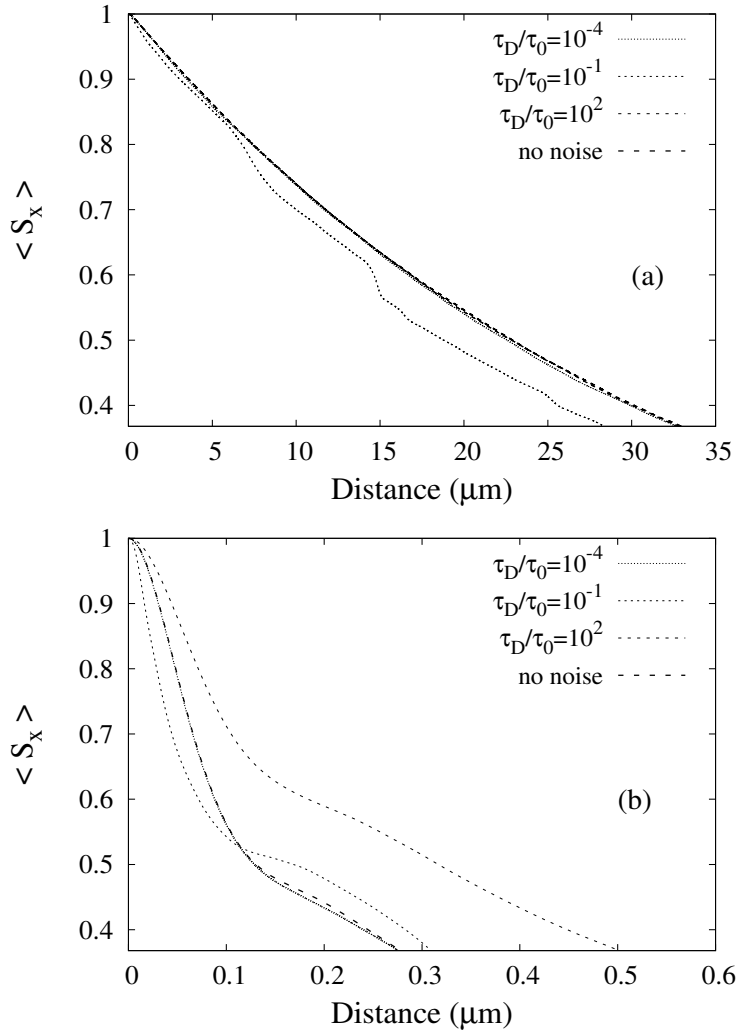

Figure 5.1: Spin polarization $\langle S_x \rangle$ as a function of the distance from the injection point ($x = 0$) obtained by applying a fluctuating field characterized by a deterministic component F_0 and a random component with standard deviation $D^{1/2}$, for different values of noise correlation time τ_D: $10^{-4}\tau_0$, $10^{-1}\tau_0$, $10^{2}\tau_0$, and in absence of external noise. (a) $F_0 = 1$ kV/cm, $D^{1/2} = 0.6$ kV/cm and (b) $F_0 = 6$ kV/cm, $D^{1/2} = 3.6$ kV/cm [123].

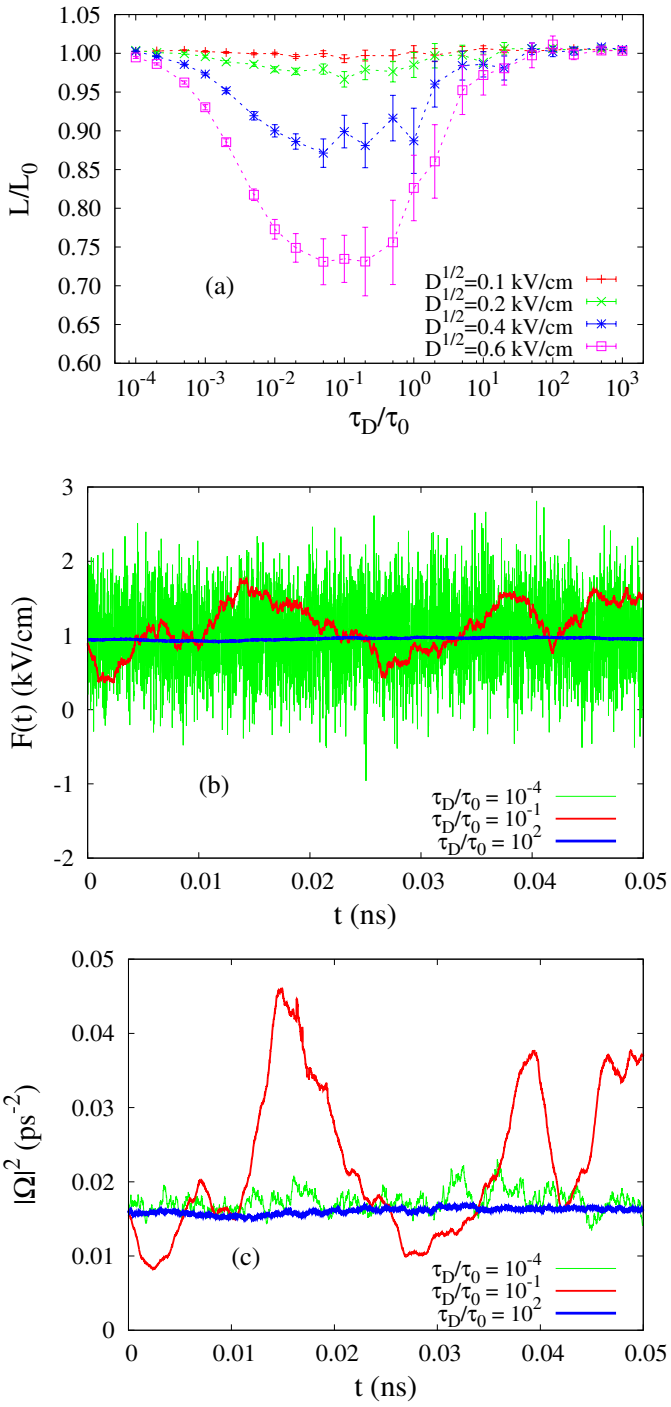

Figure 5.2: (a) Ratio between the spin depolarization length L in the presence of noise and L_0, obtained in absence of noise, as a function of the ratio between the noise correlation time τ_D and the spin relaxation time in absence of noise τ_0, at different values of noise intensity D at fixed $F_0 = 1$ kV/cm. (b) Electric field amplitude $F(t)$ and (c) electron spin squared precession frequency $|\,\mathbf{\Omega}(\mathbf{k})\,|^2$ as a function of time t for $D^{1/2} = 0.4$ kV/cm [123].

process is observed.

With the aim of investigating the effects of the correlated noise source on the spin depolarization process, we performed 100 different realizations and evaluated both average values and error bars of the extracted spin depolarization lengths.

In panel (a) of Fig. 5.2, we show the ratio between the spin depolarization length L in the presence of noise and L_0, obtained in absence of noise, as a function of the ratio between the noise correlation time τ_D and τ_0, at different values of noise intensity D and with $F_0 = 1$ kV/cm. For these values of parameters, $L_0 = 32.6$ μm and $\tau_0 = 0.16$ ns. The addition of a source of correlated fluctuations, characterized by $10^{-2}\tau_0 < \tau_D < \tau_0$, reduces the values of the spin depolarization length L up to 25%. In particular, L/L_0 is a nonmonotonic function of τ_D/τ_0 which exhibits a minimum for $\tau_D/\tau_0 \approx 0.1$. For both $\tau_D << \tau_0$ and $\tau_D >> \tau_0$, the values of L coincide with those of L_0. The presence of the minimum, which becomes deeper with the increasing of the noise amplitude, can be explained by analyzing the temporal evolution of the quantities related to the electron transport and to the spin relaxation process. In panels (b) and (c) of Fig. 5.2, we report the electric field amplitude $F(t)$ and the squared precession frequency $\mid \mathbf{\Omega}(\mathbf{k}) \mid^2$, respectively, as a function of time t. For very low values of τ_D/τ_0, $\mid \mathbf{\Omega}(\mathbf{k}) \mid^2$ symmetrically fluctuates around its average value, corresponding to that obtained in absence of noise. By increasing the value of τ_D, the effective electric field felt by electrons, within a time window comparable with the spin relaxation time, becomes very different from the value F_0 (panel (b)). As a consequence, the temporal evolution of $\mid \mathbf{\Omega}(\mathbf{k}) \mid^2$ shows an evident asymmetry in the same temporal window (panel (c)). Because of the proportionality between the electron momentum k_x and the electric field $F(t)$, the equation (1.67) leads to a quadratic relation between $F(t)$ and $\mid \mathbf{\Omega}(\mathbf{k}) \mid^2$ on the $k_x^2(k_y^2 - k_z^2)^2$ term and at fourth power on the other two terms. Hence, the values of F greater than F_0 give rise to values of $\mid \mathbf{\Omega}(\mathbf{k}) \mid^2$ much greater than those obtained for $F < F_0$. So, in accordance with equation (1.61), the asymmetry of $\mid \mathbf{\Omega}(\mathbf{k}) \mid^2$ is responsible for the observed reduction of spin lifetime. By further increasing the value of τ_D, the random fluctuating term $\eta(t)$ of the electric field tends to its initial value $\eta(0) = 0$ (see equation (5.2)), and $F(t) \to F_0$. Therefore, the behavior of system becomes quasi-deterministic and the spin dephasing length L approaches its deterministic value L_0.

In Fig. 5.3(a), we show the ratio L/L_0 as a function of τ_D/τ_0 for $F_0 = 6$ kV/cm, at different values of noise intensity D. For these values of parameters, $L_0 = 279$ nm and $\tau_0 = 1.13$ ps. In the presence of a driving electric field greater than the necessary static field to allow the electrons to move towards the upper energy valleys, the Gunn field $E_G = 3.25$ kV/cm, we find a positive effect of the field fluctuations. In fact, despite the error bars are large, our findings show that the addition of correlated fluctuations, characterized by $10^{-1}\tau_0 < \tau_D < \tau_0$, can increase the value of the spin depolarization length L up to the 20% of L_0. This effect is maximum for $\tau_D/\tau_0 \approx 1$. For the reasons discussed above, even in the high field case, both for very high and very low values of noise correlation time τ_D, the value of L approaches L_0. The presence of a positive effect of noise can be ascribed to the reduction of the electron occupation percentage in L-valleys, shown in panel (b) of Fig. 5.3. This finding, which can be considered as a further example of Noise Enhanced Stability (NES) [125],[138]-[139], leads a greater number of electrons to experience a spin-orbit coupling in Γ-valley at least of one order of magnitude weaker than that present in L-valleys [105], causing a decrease of efficacy of the DP dephasing mechanism.

5.3.1 The effect of the electron-electron scattering inclusion

In this subsection, in order to quantify the effect of the Coulomb interaction on the spin depolarization process in the presence of external noise, we show a comparison between the results obtained with the e-e scattering mechanism and without it, analyzing the behavior of L/L_0, as a function of the ratio between the noise standard deviation $D^{1/2}$ and the deterministic value of the driving field F_0 (see Fig. 5.4). We show the comparison at the values of noise correlation time corresponding with the maximum of the noise effect observed by neglecting the Coulomb interaction. Each panel of Fig. 5.4 shows the *'ee-points'*, obtained through full calculations including the electron-electron scattering mechanism, and the *'no ee-points'*, calculated without the electron-electron interaction. In panel (a): $\tau_D = 0.1\tau_0$ and $F_0 = 1$ kV/cm, with $L_0 = 127$ μm and $\tau_0 = 0.49$ ns; in panel (b): $\tau_D = \tau_0$ and $F_0 = 6$ kV/cm, with $L_0 = 666$ nm and $\tau_0 = 2.42$ ps; the new values of τ_0 and L_0 have been obtained by including the Coulomb scattering. For $\tau_D = 0.1\tau_0$, the reduction of the spin depolarization length, caused by fluctuations, is slightly affected from the inclusion of electron-electron scattering mechanism up to values of $D^{1/2}$ lower than 40% of

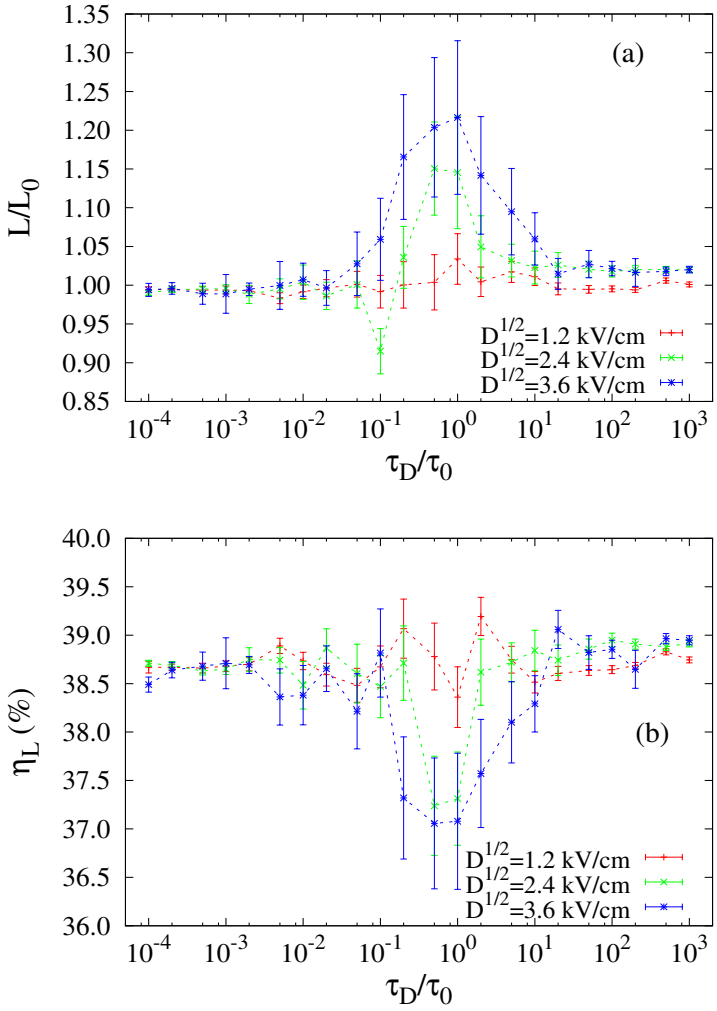

Figure 5.3: (a) Ratio between the spin depolarization length L in the presence of noise and L_0, obtained in absence of noise, as a function of the ratio between the noise correlation time τ_D and the spin relaxation time in absence of noise τ_0 and (b) electrons occupation percentage in L-valleys η_L as a function of τ_D/τ_0, at different values of noise intensity D. $F_0 = 6$ kV/cm [123].

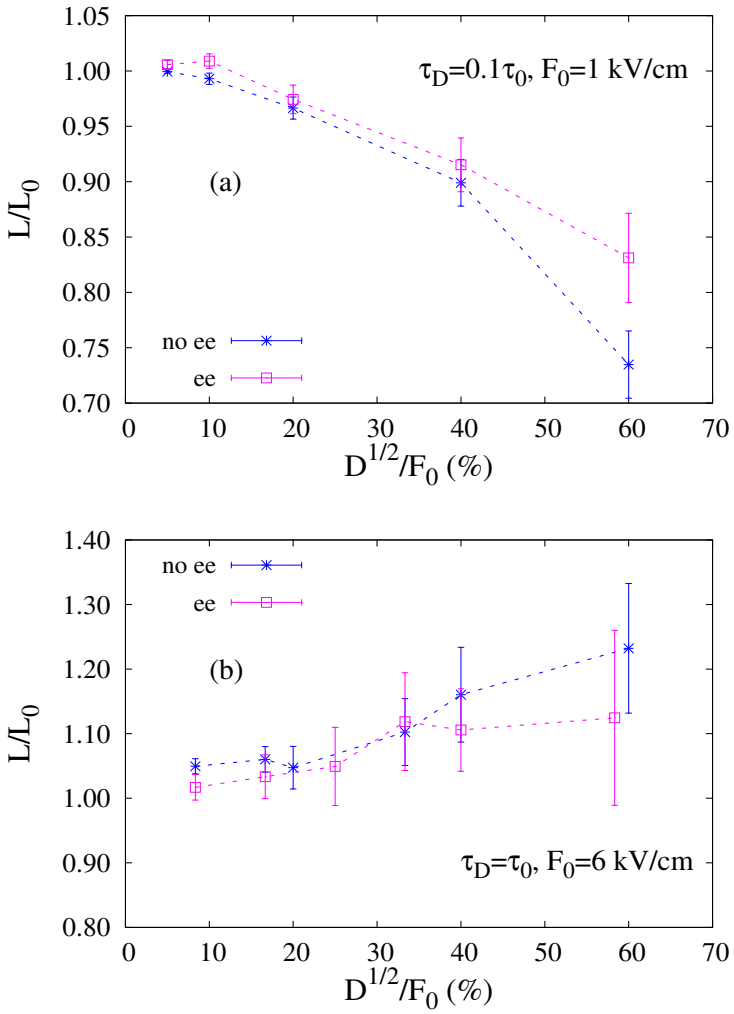

Figure 5.4: Ratio between the spin depolarization length L in the presence of noise and L_0, obtained in absence of noise, as a function of the ratio between the noise amplitude $D^{1/2}$ and F_0. The *'ee-points'* are obtained through full calculations including the electron-electron scattering mechanism; the *'no ee-points'* are calculated without the electron-electron interaction. (a) $\tau_D = 10^{-1}\tau_0$ and $F_0 = 1$ kV/cm, (b) $\tau_D = \tau_0$ and $F_0 = 6$ kV/cm [123].

the value of F_0. For values of $D^{1/2}/F_0$ greater than 0.4, the inclusion of the e-e scattering leads to a longer spin dephasing length, i.e. the electron-electron scattering mechanism reduces the negative effect of noise. This effect of the Coulomb interaction could be ascribed to the frequent momentum redistribution experienced from the electrons ensemble [13]. Unfortunately, the Coulomb interaction inclusion seems to randomize the system also for field amplitude greater than the Gunn field. Under high electric field conditions, in fact, up to values of $D^{1/2}$ lower than 33% of the value of F_0, the quantity L/L_0 is almost not influenced by the inclusion of the e-e mechanism. By increasing the noise amplitude, a slight noise-induced positive effect on spin relaxation length is found. In this case, the addition of a source of correlated fluctuations, having correlation time comparable with the spin lifetime, enhances the value of the spin depolarization length L of only about 10-15%.

In this chapter, we have investigated the noise influence on the electron spin relaxation process in lightly n-doped GaAs semiconductor bulks by also including the electron-electron interaction. The findings show that a fluctuating electric field, obtained by adding a correlated source of noise to a static field, can modify the spin depolarization length. For electric fields lower than the Gunn field and values of the noise correlation time $\tau_D \sim \tau_0$, a reduction of the spin depolarization length up to 15% has been observed, strongly dependent on the noise intensity. This behavior can be explained by the different effective electric field experienced by the electron ensemble, within a time window comparable with τ_0. On the contrary, in the high electric field regime, for τ_D=τ_0, we find an enhancement of the spin relaxation length up to 15%. This positive effect can be explained by the decrease of the occupation of the L-valleys, where the strength of spin-orbit coupling felt by electrons is at least one order of magnitude greater than that present in Γ-valley and represents an example of NES in spin depolarization process.

Conclusions

A promising area of nano-technology, very attractive in terms of miniaturization, and currently explored, is *Spintronics*, in which electron spin degrees of freedom will be used to encode information [13]. Among the possible applications, hybrid devices that combine traditional electronics based on semiconductors with the use of the spin are currently the focus of research for the increased functionality and ease of integration. However, in semiconductors, the spin states of electrons depolarize (relaxation) due to scattering by lattice imperfections and the elementary excitations due to other carriers and phonons. Because of that, the understanding and the control over the relaxation of intrinsic angular momenta of the electrons in a spintronic device, are necessary. This knowledge is also relevant from a technological point of view. In fact, it could improve the performances of electronic devices and allow advanced technological applications, with the challenge to replace the existing micro-electronic technology.

This thesis has been focused on the study of the relaxation dynamics of the spins of conduction electrons in n-doped GaAs bulk crystals subjected to static electric fields. In fact, the possibility of using spin-based devices can not neglect the knowledge of their response in the presence of electric fields. For this reason, in recent years, there has been a great proliferation of experimental works in which, indirectly, the influence of transport conditions on the relaxation of the spins in semiconductors has been studied [9]. However, it has been paid few attention from theoretical/numerical standpoint [14].

The research activity of Ph. D. period has included: (i) the study of the electron spin relaxation, under low-field conditions, by estimating both the spin lifetimes and the depolarization lengths as a function of the values of lattice temperature, electric field amplitude and doping density; (ii) the study of the electron spin relaxation

in the presence of electric field having amplitude greater than the Gunn threshold; (iii) the analysis of the influence of the inclusion of the electron-electron scattering mechanism on the spin depolarization process and (iv) the investigation of the role played by the addition of an external source of correlated noise to the static electric field. The main purposes of this study were:

1. to find the better conditions that minimize the spin relaxation rate and maximize spin lifetimes and depolarization lengths, by exploring a wide interval of values of lattice temperature, doping density and electric field amplitude;

2. to understand the dynamical response in the presence of external fluctuations, with the aim to verify in what working conditions, the fluctuations could lead to longer spin relaxation times and lengths.

In our studies, we have used a numerical code Monte Carlo to simulate transport and spin dynamics of the electrons in homogeneous semiconductors, in the presence of a static electric field. This code has been built by using, as a starting point, a Monte Carlo code developed and tested in previous work related to the simulation of linear and nonlinear properties of the response to intense electromagnetic radiation from bulk semiconductors [140]. With the goal to allow the simultaneous study of spin dynamics and electron transport, the code has been modified to include the simulation of the evolution of the electron spin average polarization.

We have studied the relaxation of electronic spin states, caused of scattering events with impurities, phonons and other carriers by only considering the spin-orbit coupling mechanism of D'yakonov-Perel, which is the unique relevant relaxation process for spin dynamics in III-V semiconductors.

Before to calculate electron spin lifetimes and depolarization lengths under several conditions of temperature and applied electric field, we have studied the curves of the electron spin polarization averaged over all the electrons of the ensemble, as a function of both time and distance from the injection point. This analysis allowed us to obtain information about the shape of the temporal and spatial trend of the average spin polarization, with the aim to validate the use of exponential fitting functions to estimate the values of spin relaxation times and lengths.

In the presence of static electric field having amplitude lower than the Gunn threshold, i.e. with all electrons in the central Γ-valley, we have found that, at

fixed electric field intensity, the spin relaxation length is a decreasing function of the lattice temperature. The observed dependence was expected, because with the increasing of the temperature, the scattering probability increases too, and hence, the ensemble of the electrons faster looses its spatial order, that is a stronger inhomogeneous broadening causing a faster spin depolarization. Instead, the spin relaxation time shows a nonmonotonic behaviour with a minimum and a wide maximum, that is explained by the progressive changing of dominant scattering mechanism, from acoustical phonons and ionized impurities at low temperatures, to optical polar phonons at higher temperatures.

At fixed value of the lattice temperature, the spin depolarization length is a nonmonotonic function of electric field amplitude, which shows a maximum that shorten and moves itself toward stronger electric fields with the increase of temperature. The presence of the maximum for intermediate values of the electric field intensity, can be ascribed to the interplay of two competing factors: in linear regime, the electron wave vector and the drift velocity increase along the direction of electric field. On the other hand, the increase of the momentum vector leads to a stronger effective magnetic field, causing an enlargement of spin relaxation rate. The same trend is observed for the spin lifetimes.

The recent estimate of the coefficients of spin-orbit coupling in upper energy valleys allowed us to extend the spin dynamics inside to our numerical code, including the D'yakonov-Perel mechanism in L- and X-valleys which is momentum-linear dependent [61]. By using the updated model of spin dynamics, the influence of high electric fields on spin relaxation process has been investigated.

Our findings have showed that, for electric field amplitudes greater to Gunn threshold field, the spin depolarization times increase with the growing up of the lattice temperature. This unexepected result has been explained by means of the D'yakonov-Perel formula, by calculating the average precession frequency of the spin and the average value of momentum relaxation time of the electrons [48].

Since, the study of low field transport conditions has showed that, the doping density is a fundamental parameter on spin relaxation process, we have extended our analysis by varying the electron density under nondegenerate regime. Our findings show that, for values of lattice temperature lower than 150 K, the spin depolarization time is a increasing function of the doping density, in accordance with both the

results obtained by KSBE approach by Jiang et al. and the experimental measurements by Romër et al.

The more important results of this thesis have been obtained with the inclusion of the electron-electron scattering mechanism in our Monte Carlo code. Because the taking into account for electron-electron Coulomb scattering process requires very time consuming computations, Monte Carlo code has been updated to run in a parallel way.

Although, it has longer been believed that, this interaction mechanism does not contribute on the spin relaxation of the electrons [110], recently it has been proved that, in the presence of inhomogeneous broadening, any scattering mechanism can lead to the decoherence of the electron spin [13]. The results of our calculations show that the electron-electron scattering is fundamental to obtain energy and momentum of the electrons distributed as a Maxwell-Boltzmann curve.

For each investigated value of doping density, the average spin lifetime shows a nonmonotonic behaviour as a function of the lattice temperature with a more marked maximum at the highest value of electron density. This finding is in accordance with the results obtained on quantum wells by using different numerical approaches [114, 115] and with the experimental measurements by Leyland et al. [116].

By using values of amplitude of the static electric field up to 10 kV/cm, we have observed that, spin lifetimes and depolarization lengths show a significant increase caused by including the Coulomb interaction mechanism. This increase has been explained by considering the strong reduction of the correlation time of the spin precession vector caused by reciprocal interaction mechanism of the electrons.

We have validated our Monte Carlo code by comparing the spin relaxation rate, numerically calculated by including the electron-electron scattering mechanism, with the results of the measurements reported by Romër et al. via spin noise spectroscopy [107]. The results of our comparison show a very good qualitative and quantitative agreement on the entire interval of values of lattice temperature. Moreover, we have compared our results with those obtained by a fully microscopic method based on *Kinetic Spin Bloch Equations* (KSBE) by Jiang et al. [36, 122]. The results of this comparison show a full agreement for both the spin lifetimes and the electrons temperature.

Finally, the influence of fluctuations of the electric field on spin relaxation process has been studied, by adding a term of correlated noise to the static electric field. The results of numerical simulations show that a fluctuating electric field can significantly change both spin relaxation times and spin depolarization lengths. In particular, when the applied electric field is weak and for values of noise correlation time comparable with the spin relaxation time obtained in absence of fluctuations, we have observed a reduction of spin depolarization length, which increases with the intensity of added noise. This result has been explained by examinating the effective electric field felt from the electrons ensemble within a time window comparable with the time of relaxation of the spin.

When the intensity of the applied electric field is greater than Gunn threshold level, we have found that, the noise effect which increases with its intensity, consists in a significant increase of the spin depolarization length. This positive effect by noise has been explained in terms of the reduction of occupation percentage in L-valleys, where the strengh of spin-orbit coupling is a order of magnitude lower than in the Γ-valley. Lastly, our findings show that the noise induced effects on spin dynamics are not significantly affected by the inclusion of the electron-electron scattering mechanism. In conclusion, our preliminary results show that the presence of fluctuations in the applied voltage changes the maintenance of long spin depolarization lengths in a way strongly dependent on both the strength of the applied electric field and the noise correlation time.

The future of this research is directed toward both the extension of the obtained results at nanostructures and the study of spin dynamics in different semiconductor materials, such as Silicon (Si) or Gallium Nitride (GaN).

As it is well known the silicon is the core material for the information technology. Unlike in III-V semiconductors, in which the most important mechanism is the D'yakonov-Perel [36], spin depolarization in silicon is caused by the EY mechanism [6, 46, 47, 141].

Recently, for wide-gap nitride semiconductors, as like GaN, long spin relaxation times and lengths have been predicted due to their spin-orbit coupling relatively weak as compared to III-V compounds with smaller band gap, such as GaAs. In particular, GaN shows anisotropic spin dynamics [142] and, to the best of our knowl-

edge, a theoretical-numerical investigation of the influence of this anisotropy on the spin relaxation process during electric field transport is still missing.

Moreover, our investigation of the effects induced by external source of noise on spin dynamics in semiconductors will be continued by using different sources of noise, i.e. dichotomic noise and Lévy noise.

Bibliography

[1] F. Meie, B.P. Zakharchenya (Eds.), *'Optical Orientation'* North-Holland, New York, 1984.

[2] J. Fabian, S. Das Sarma, *'Spin relaxation of conduction electrons'* J. Vac. Sci. Technol. B **17**, 1708-1715 (1999).

[3] S.A. Wolf, D.D. Awschalom, R.A. Buhrman, J.M. Daughton, S. von Molnár, M.L. Roukes, A.Y. Chtchelkanova, D.M. Treger, *'Spintronics: A Spin-Based Electronics Vision for the Future'* Science **294**, 1488-1495 (2001).

[4] I. Žutič, J. Fabian, S. Das Sarma, *'Spintronics: Fundamentals and Applications'* Rev. Mod. Phys. **76**, 323-410 (2004).

[5] D.D. Awschalom, M.E. Flatté, *'Challenges for semiconductor spintronics'* Nature Phys. **3**, 153-159 (2007).

[6] J. Fabian, A. Matos-Abiage, C. Ertler, P. Stano, I. Žutić, *'Semiconductor Spintronics'* Acta Phys. Slov. **57**, 565-907 (2007).

[7] X. Lou, C. Adelmann, S.A. Crooker, E.S. Garlid, J. Zhang, K.S. Madhukar Reddy, S.D. Flexner, C.J. Palmstrøm, P.A. Crowell, *'Electrical detection of spin transport in lateral ferromagnetsemiconductor devices'* Nature Phys. **3**, 197-202 (2007).

[8] B.T. Jonker, G. Kioseoglou, A.T. Hanbicki, C.H. Li, P.E. Thompson, *'Electrical spin-injection into silicon from a ferromagnetic metal/tunnel barrier contact'* Nature Phys. **3**, 542-546 (2007).

[9] M.I. D'yakonov (Ed.), *'Spin Physics in Semiconductors'* Solid-State Sciences Vol 110, Springer, Berlin 2008.

[10] Yu.V. Gulayev, P.E. Zilberman, A. I. Panas, E. M. Epshtein, *'Spintronics: exchange switching of ferromagnetic metallic junctions at a low current density'* Usp. Fiz. Nauk **52** (4), 335-343 (2009).

[11] S.P. Dash, S. Sharma, R.S. Patel, M.P. de Jong, R. Jansen, *'Electrical creation of spin polarization in silicon at room temperature'* Nature **462**, 491-494 (2009).

[12] M.E. Flatté, *'Silicon spintronics warms up'* Nature **462**, 419-420 (2009).

[13] M.W. Wu, J.H. Jiang, M.Q. Weng, *'Spin dynamics in semiconductors'* Physics Reports **493**, 61-236 (2010).

[14] E.A. Barry, A.A. Kiselev, K.W. Kim, *'Electron spin relaxation under drift in GaAs'* Appl. Phys. Lett. **82**, 3686-3688 (2003).

[15] G. Lampel, *'Nuclear dynamic polarization by optical electronic saturation and optical pumping in semiconductors'* Phys. Rev. Lett. **20**, 491-493 (1968).

[16] R.R. Parsons, *'Band-to-band optical pumping in solids and polarized photoluminescence'* Phys. Rev. Lett. **23**, 1152-1154 (1969).

[17] J.M. Kikkawa, D.D. Awschalom, *'Resonant spin amplification in n-type GaAs'* Phys. Rev. Lett. **80**, 4313-4316 (1998).

[18] J.M. Kikkawa, D.D. Awschalom, *'Lateral drag of spin coherence in gallium arsenide'* Nature **397**, 139-141 (1999).

[19] D. Hägele, M. Oestreich, W.W. Rühle, N. Nestle, K. Eberl, *'Spin transport in GaAs'* Appl. Phys. Lett. **73**, 1580-1582 (1998).

[20] H. Sanada, I. Arata, Y. Ohno, Z. Chen, K. Kayanuma, Y. Oka, F. Matsukura, H. Ohno, *'Relaxation of photoinjected spins during drift transport in GaAs'* Appl. Phys. Lett. **81**, 2788-2790 (2002).

[21] Y. Sato, Y. Takahashi, Y. Kawamura, H. Kawaguchi,*'Field Dependence of Electron Spin Relaxation during Transport in GaAs'* Jpn. J. Appl. Phys **43**, L230-L232 (2004).

[22] R.I. Dzhioev, K.V. Kavokin, V.L. Korenev, M.V. Lazarev, N.K. Poletaev, B.P. Zakharchenya, E.A. Stinaff, D. Gammon, A.S. Bracker, M.E. Ware, *'Suppression of D'yakonov-Perel Spin Relaxation in High-Mobility n-GaAs'* Phys. Rev. Lett. **93**, 216402 (2004).

[23] Y. Kato, R.C. Myers, A.C. Gossard, D.D. Awschalom, *'Coherent spin manipulation without magnetic fields in strained semiconductors'* Nature **427**, 50-53 (2004).

[24] M. Beck, C. Metzner, S. Malzer, G.H. Döhler, *'Spin lifetimes and strain-controlled spin precession of drifting electrons in GaAs'* Europhys. Lett. **75**, 597-603 (2006).

[25] M. Furis, D.L. Smith, S.A. Crooker, J.L. Reno, *'Bias-dependent electron spin lifetimes in n-GaAs and the role of donor impact ionization'* Appl. Phys. Lett. **89**, 102102 (2006).

[26] M. Hruška, Š. Kos, S.A. Crooker, A. Saxena, D.L. Smith, *'Effects of strain, electric, and magnetic fields on lateral electron-spin transport in semiconductor epilayers'* Phys. Rev. B **73**, 075306 (2006); *'Erratum: Effects of strain, electric, and magnetic fields on lateral electron-spin transport in semiconductor epilayers'* [Phys. Rev. B **73**, 075306 (2006)], Phys. Rev. B **76**, 169903 (2007).

[27] Z.G. Yu, M. E. Flatté, *'Electric-field dependent spin diffusion and spin injection into semiconductors'* Phys. Rev. B **66**, 201202 (2002).

[28] Z.G. Yu, M. E. Flatté, *'Spin diffusion and injection in semiconductor structures: Electric field effects'* Phys. Rev. B **66**, 235302 (2002).

[29] I. Martin, *'Spin-drift transport and its applications'* Phys. Rev. B **67**, 014421 (2003).

[30] S. Saikin, Y.V. Pershin, V. Privman, *'Modeling for semiconductor spintronics'* IEE Proc.-Circuits Devices Syst., **152** 366-376 (2005).

[31] E.L. Ivchenko, Y.B. Lyanda-Geller, G.E. Pikus, *'Current of thermalized spin-oriented photocarriers'* Sov. Phys.-JEPT, **71**, 550-557 (1990).

[32] M.W. Wu, C.Z. Ning, *'D'yakonov-Perel Effect on Spin Dephasing in n-Type GaAs'* Phys. Status Solidi B **222**, 523-534 (2000).

[33] M.Q. Wen, M.W. Wu, *'Kinetic theory of spin transport in n-type semiconductor quantum wells'* J. Appl. Phys. **93**, 410-420 (2003).

[34] M.Q. Weng, M.W. Wu, L. Jiang, *'Hot-electron effect in spin dephasing in n-type GaAs quantum wells'* Phys. Rew. B **69**, 245320 (2004).

[35] P. Zhang, J. Zhou, M.W. Wu, *'Multivalley spin relaxation in the presence of high in-plane electric fields in n-type GaAs quantum wells'* Phys. Rev. B **77**, 235323 (2008).

[36] J.H. Jiang, M.W. Wu, *'Electron-spin relaxation in bulk III-V semiconductors from a fully microscopic kinetic spin Bloch equation approach'* Phys. Rev. B **79**, 125206 (2009).

[37] E.G. Mishchenko, B.I. Halperin, *'Transport equations for a two-dimensional electron gas with spin-orbit interaction'* Phys. Rev. B **68**, 045317 (2003).

[38] S. Saikin, *'A drift-diffusion model for spin-polarized transport in a two-dimensional non-degenerate electron gas controlled by spinorbit interaction'* J. Phys.: Condens. Matter **16**, 5071 (2004).

[39] A.A. Kiselev, K.W. Kim, *'Progressive suppression of spin relaxation in two-dimensional channels of finite width'* Phys. Rev. B **61**, 13115-13120 (2000).

[40] A. Bournel, P. Dollfus, E. Cassan, P. Hesto, *'Monte Carlo study of spin relaxation in AlGaAs/GaAs quantum wells'* Appl. Phys. Lett. **77**, 2346-2348 (2000).

[41] S. Saikin, M. Shen, M.C. Cheng, V. Privman, *'Semiclassical Monte Carlo model for in-plane transport of spin-polarized electrons in III-V heterostructures'* J. Appl. Phys. **94**, 1769-1775 (2003).

[42] S. Pramanik, S. Bandyopadhyay, M. Cahay, *'Spin dephasing in quantum wires'* Phys. Rev. B **68**, 075313 (2003).

[43] M. Shen, S. Saikin, M.C. Cheng, V. Privman, *'Monte Carlo Modeling of Spin FETs Controlled by Spin-Orbit Interaction'* Mathematics and Computers in Simulation **65**, 351-363 (2004).

[44] Y. Pershin, *'Long-lived spin coherence states in semiconductor heterostructures'* Phys. Rev. B **71**, 155317 (2005).

[45] S. Saikin, M. Shen, M.C. Cheng *'Spin dynamics in a compound semiconductor spintronic structure with a Schottky barrier'* J. Phys.: Condens. Matter **18**, 1535-1544 (2006).

[46] R.J. Elliott, *'Theory of the Effect of Spin-Orbit Coupling on Magnetic Resonance in Some Semiconductors'* Phys. Rev. **96**, 266-279 (1954).

[47] Y. Yafet, *'g Factors and Spin-Lattice Relaxation of Conduction Electrons'* Solid State Physics Vol. 14, edited by F. Seitz and D. Academic, Turnbull New York, 1963.

[48] N.I. D'yakonov, V.I. Perel, *'Spin relaxation of conduction electrons in noncentrosymmetric semiconductors'* Sov. Phys. - Solid State **13**, 3023-3026 (1971).

[49] M.I. D'yakonov, *'Introduction to spin physics in semiconductors'* Physica E **35**, 246-250 (2006).

[50] G.L. Bir, A.G. Aronov, G.E. Pikus, *'Spin relaxation of electrons due to scattering by holes'* Sov. Phys. - JETP **42**, 705-712 (1976).

[51] A. Abragam, *'The Principles of Nuclear Magnetism'*, Clarendon Press, Oxford, 1961.

[52] D. Paget, G. Lampel, B. Sapoval, V.I. Safarov, *'Low field electron-nuclear spin coupling in gallium arsenide under optical pumping conditions'* Phys. Rev. B **15**, 5780-5796 (1977).

[53] G.E. Pikus, A.N. Titkov, *Optical Orientation*, edited by F. Meyer, Nauka, Leningrad, 1989.

[54] K.V. Kavokin, *'Anisotropic exchange interaction of localized conduction-band electrons in semiconductors'* Phys. Rev. B **64**, 075305 (2001).

[55] K.L. Litvinenko, M.A. Leontiadou, J. Li, S.K. Clowes, M.T. Emeny, T. Ashley, C.R. Pidgeon, L.F. Cohen, B.N. Murdin, *'Strong dependence of spin dynamics on the orientation of an external magnetic field for InSb and InAs'* Appl. Phys. Lett. **96**, 111107 (2010).

[56] H. A. Kramers, *'Théorie générale de la rotation paramagnétique dans les cristaux'* Proc. Amst. Acad. **33**, 959-972 (1930).

[57] B.K. Ridley, *'Quantum Processes in Semiconductors'*, Clarendon Press, Oxford, 1999.

[58] G. Dresselhaus, *'Spin-Orbit Coupling Effects in Zinc Blende Structures'* Phys. Rev **100**, 580-586 (1955).

[59] Y.A. Bychkov, E.I. Rashba, *'Properties of a 2D electron gas with lifted spectral degeneracy'* J. Exp. Theor. Phys. Lett. **39**, 78-81 (1984).

[60] Y.A. Bychkov, E.I. Rashba, *'Oscillatory effects and the magnetic susceptibility of carriers in inversion layers'* J. Phys. C **17**, 6039-6045 (1984).

[61] J.Y. Fu, M.Q. Weng, M.W. Wu, *'Spin-orbit coupling in bulk GaAs'* Physica E **40**, 2890-2893 (2008).

[62] J.J. Krich, B.I. Halperin, *'Cubic Dresselhaus Spin-Orbit Coupling in 2D Electron Quantum Dots'* Phys. Rev. Lett. **98**, 226802 (2007).

[63] D. Richards, B. Jusserand, H. Peric, B. Etienne, *'Intrasubband excitations and spin-splitting anisotropy in GaAs modulation-doped quantum wells'* Phys. Rev. B **47**, 16028 (1993).

[64] B. Jusserand, D. Richards, G. Allan, C. Priester, B. Etienne, *'Spin orientation at semiconductor heterointerfaces'* Phys. Rev. B **51**, 4707 (1995).

[65] D. Richards, B. Jusserand, G. Allan, C. Priester, B. Etienne, *'Electron spin-flip Raman scattering in asymmetric quantum wells: Spin orientation'* Solid-State Electron. **40**, 127-131 (1996).

[66] J.B. Miller, D.M. Zumbühl, C.M. Marcus, Y.B. Lyanda-Geller, D. Goldhaber-Gordon, K. Campman, A.C. Gossard, *'Gate-Controlled Spin-Orbit Quantum Interference Effects in Lateral Transport'* Phys. Rev. Lett. **90**, 076807 (2003).

[67] J.M. Jancu, R. Scholz, F. Beltram, F. Bassani, *'Empirical spds* tight-binding calculation for cubic semiconductors: General method and material parameters'* Phys. Rev. B **57**, 6493-6507 (1998).

[68] S.B. Singh, C.A. Singh, *'Extensions of the Feynman-Hellman theorem and applications'* Am. J. Phys. **57**, 894 (1989).

[69] Y.C. Chang, D.E. Aspnes, *'Theory of dielectric-function anisotropies of (001) GaAs (21) surfaces'* Phys. Rev. B **41**, 12002-12012 (1990).

[70] S.L. Richardson, M.L. Cohen, S.G. Louie, J.R. Chelikowsky, *'Electron charge densities at conduction-band edges of semiconductors'* Phys. Rev. B **33**, 1177-1182 (1986).

[71] P. Boguslawsky, I. Gorczyca, *'Atomic-orbital interpretation of electronic structure of III-V semiconductors: GaAs versus AlAs'* Semicond. Sci. Technol. **9**, 2169 (1994)

[72] C. Jacoboni, P. Lugli, *'The Monte Carlo Method for Semiconductor Device Simulation'*, edited by S. Selberherr, Springer, Wien, 1989

[73] C. Moglestue, *'Monte Carlo Simulation of Semiconductor Devices'*, Chapman and Hall, London, 1993.

[74] K. Tomizawa, *'Numerical simulation of submicron semiconductor devices'*, Artech House, London, 1993.

[75] M. Lundstrom, *'Fundamentals of carrier transport'*, University Press, Cambridge, 2000.

[76] D.K. Ferry, C. Jacoboni, *'Quantum Transport in Semiconductor Devices'*, Chapman and Hall, Cambridge, 1993.

[77] C. Jacoboni, L. Reggiani, *'The Monte Carlo method for the solution of charge transport in semiconductors with applications to covalent materials'* Rev. Mod. Phys. **55**, 645-705 (1983).

[78] D. Persano Adorno, M. Zarcone, G. Ferrante, *'Far-infrared harmonic generation in semiconductors: A Monte Carlo simulation.'* Laser Phys. **10**, 310-315 (2000)

[79] D. Persano Adorno, M. Zarcone, G. Ferrante, P. Shiktorov, E. Starikov, V. Gružinskis, S. Pérez, T. González, L. Reggiani, L. Varani, J. C. Vaissière, *'Monte Carlo simulation of high-order harmonics generation in bulk semiconductors and submicron structures'* Phys. Status Solidi C **1**, 1367-1376 (2004).

[80] P.Y. Yu, M. Cardona,*'Fundamentals of Semiconductors, Physics and Material Properties'*, Springer-Verlag, Berlin, 2003.

[81] C. Jacoboni, *'Theory of Electron Transport in Semiconductors'*, Springer-Verlag, Berlin Heidelberg, 2010.

[82] W. Fawcett, A.D. Boardman, S. Swain, *'Monte Carlo Determination of Electron Transport in Gallium Arsenide'* J. Phys. Chem. Solids **31**, 1963-1990 (1990).

[83] R.M. Dreizler, E.K.U. Gross, *'Density Functional Theory - An Approach to the Quantum Many-Body Problem'*, Springer-Verlag, Berlin Heidelberg, 1990.

[84] D. Bohm, D. Pines, *'A Collective Description of Electron Interactions: III. Coulomb Interactions in a Degenerate Electron Gas'* Phys. Rev. **92** 609 (1953).

[85] W. Takenaka, M. Inoue, Y. Inuishi, *'Influence of Inter-Carrier Scattering on Hot Electron Distribution Function in GaAs'* J. Phys. Soc. Japan **47**, 861-868 (1979).

[86] M. Moško, A. Mošková, *'Ensemble Monte Carlo simulation of electron-electron scattering: Improvements of conventional methods'* Phys. Rev. B **44**, 10794-10803 (1991).

[87] A. Mošková, M. Moško, *'Exchange carrier-carrier scattering of photoexcited spin-polarized carriers in GaAs quantum wells: Monte Carlo study'* Phys. Rev. B **49**, 7443-7452 (1994).

[88] P. Lugli, D.K. Ferry, *'Effect of electron-electron scattering on Monte Carlo studies of transport in submicron semiconductors devices'* Physica B **117**, 251-253 (1983).

[89] R. Brunetti, C. Jacoboni, V. Dienys, A. Matulionis, *'Effect of interparticle collisions on energy relaxation of carriers in semiconductors'* Physica B **134**, 369-373 (1985).

[90] A. Hasegava, K. Miyatsuji, K. Taniguchi, C. Hamaguchi, *'A new Monte Carlo simulation of hot electron transport with electron-electron scattering'* Solid State Electron. **31**, 547-550 (1988).

[91] L. Rota, P. Lugli, *'Energy exchange via electron-electron scattering in many-valley semiconductors'* Solid State Electron. **32** 1423-1427 (1989).

[92] A. Messiah, *'Quantum Mechanics'*, North-Holland Publishing Company, Amsterdam, 1961.

[93] C. Cohen-Tannoudji, B. Diu, F. Laloë, *'Quantum Mechanics'*, Wiley-Vch, Paris, 2005.

[94] D. Persano Adorno, S. Spezia, N. Pizzolato, B. Spagnolo, *'Monte Carlo investigation of electron spin relaxation in GaAs crystals during low-field transport'*, submitted to Rep. Math. Phys.

[95] M. Mosko, A. Moskova, *'Ensemble Monte Carlo simulation of electron-electron scattering: Improvements of conventional methods'* Phys. Rev. B **44** 10794-10803 (1991).

[96] A. Kamra, B. Ghosh, *'The role of electron-electron scattering in spin transport'* J. Appl. Phys. **109** 024501 (2011).

[97] S. Spezia, D. Persano Adorno, N. Pizzolato, B. Spagnolo, *'Temperature dependence of spin depolarization of drifting electrons in n-type GaAs bulks'* Acta Physica Polonica B **41**, 1172-1180 (2010).

[98] S. Spezia, D. Persano Adorno, N. Pizzolato, B. Spagnolo, *'Doping Dependence of Spin Dynamics of Drifting Electrons in GaAs Bulks'* Acta Physica Polonica A **119**, 250-252 (2011).

[99] S. Spezia, D. Persano Adorno, N. Pizzolato, B. Spagnolo, *'Electron-Electron Scattering Influence on Electron Spin Relaxation in n-type GaAs crystals'*, Submitted to Phys. Rev. B.

[100] M.W. Wu, *'Spin Dephasing Induced by Inhomogeneous Broadening in D'yakonov-Perel' Effect in a n-doped GaAs Quantum Well'* J. Phys. Soc. Japan **70**, 2195-2198 (2001).

[101] M.M. Glazov, E.L. Ivchenko, *'Precession Spin Relaxation Mechanism Caused by Frequent ElectronElectron Collisions'* J. Exp. Theor. Phys. Lett. **75**, 403-405 (2002).

[102] M.M. Glazov, E.L. Ivchenko, *'D'yakonovPerel' Spin Relaxation Controlled by ElectronElectron Scattering'* Journal of Superconductivity: Incorporating Novel Magnetism **16**, 735-742 (2003).

[103] M.M. Glazov, E.L. Ivchenko, *'Effect of ElectronElectron Interaction on Spin Relaxation of Charge Carriers in Semiconductors'* J. Exp. Theor. Phys. Lett. **99**, 1279-1290 (2004).

[104] P.H. Song, K.W. Kim, *'Spin relaxation of conduction electrons in bulk III-V semiconductors'* Phys. Rev. B **66**, 035207 (2002).

[105] S. Spezia, D. Persano Adorno, N. Pizzolato, B. Spagnolo, *'Relaxation of electron spin during high-field transport in GaAs bulk'* J. Stat. Mech. **P11033**, 1-13 (2010).

[106] R.I. Dzhioev, K.V. Kavokin, V.L. Korenev, M.V. Lazarev, B. Ya Meltser, M.N. Stepanova, B.P. Zakharchenya, D. Gammon, D. S.Katzer *'Low-temperature spin relaxation in n-type GaAs'* Phys. Rev. B **66**, 245204 (2002).

[107] M. Römer, H. Bernien, G. Müller, D. Schuh, J. Hübner, M. Oestreich, *'Electron-spin relaxation in bulk GaAs for doping densities close to the metal-to-insulator transition'* Phys. Rev. B **81**, 075216 (2010).

[108] M. Krauß, H.C. Schneider, R. Bratschitsch, Z. Chen, S.T. Cundiff, *'Ultrafast spin dynamics in optically excited bulk GaAs at low temperature'* Phys. Rev. B **81**, 035213 (2010).

[109] K. Shen, *'A Peak in Density Dependence of Electron Spin Relaxation Time in n-Type Bulk GaAs in the Metallic Regime'* Chin. Phys. Lett. **26**, 067201 (2009).

[110] M.E. Flatté, J.M. Byers, W.H. Lau, *'Spin Dynamics in Semiconductors'* Springer, Berlin, 2002.

[111] M.W. Wu, C.Z. Ning, *'A novel mechanism for spin dephasing due to spin-conserving scatterings'* Eur. Phys. J. B **18**, 373-376 (2000).

[112] E.Y. Sherman, *'Random spin-orbit coupling and spin relaxation in symmetric quantum wells'* Appl. Phys. Lett. **82**, 209 (2003).

[113] M.Q. Weng, M.W. Wu, *'Longitudinal spin decoherence in spin diffusion in semiconductors'* Phys. Rev. B **66**, 235109 (2002).

[114] F.X. Bronold, A. Saxena, D.L. Smith, *'Semiclassical kinetic theory of electron spin relaxation in semiconductors'* Phys. Rev. B **70**, 245210 (2004).

[115] J. Zhou, J.L. Cheng, M.W. Wu, *'Spin relaxation in n-type GaAs quantum wells from a fully microscopic approach'* Phys. Rev. B **75**, 045305 (2007).

[116] W.J.H. Leyland, G.H. John, R.T. Harley, M.M. Glazov, E.L. Ivchenko, D.A. Ritchie, I. Farrer, A.J. Shields, M. Henini, *'Enhanced spin-relaxation time due to electron-electron scattering in semiconductor quantum wells'* Phys. Rev. B **75**, 165309 (2007).

[117] X.Z. Ruan, H.H. Luo, Y. Ji, Z.Y. Xu, V. Umansky, *'Effect of electron-electron scattering on spin dephasing in a high-mobility low-density two-dimensional electron gas'* Phys. Rev. B **77**, 193307 (2008).

[118] W. Walukiewicz, J. Lagowski, L.Jastrzebski, M. Lichtensteiger, H. C. Gatos, *'Electron mobility and free-carrier absorption in GaAs: Determination of the compensation ratio'* J. Appl. Phys. **50**, 899-908 (1979).

[119] A. Islam, K. Kalna, *'Monte Carlo simulations of mobility in n-doped GaAs using self-consistent Fermi-Dirac statistics'* Semicond. Sci. Technol. **26**, 055007 (2011).

[120] M. Abramowitz, I.A. Stegun, *'Handbook of Mathematical Functions'*, DC, Washington, (1970).

[121] A.V. Bobylev, I.M. Gamba, V.A. Panferov, *'On Some Properties of Kinetic and Hydrodynamic Equations for Inelastic Interactions'* J. Stat. Phys. **98**, 743-773 (2004).

[122] J.H. Jiang, M.W. Wu, *'Electron-spin relaxation in bulk III-V semiconductors from a fully microscopic kinetic spin Bloch equation approach [Phys. Rev. B 79, 125206 (2009)]'* Phys. Rev. B **83**, 239906(E) (2011).

[123] S. Spezia, D. Persano Adorno, N. Pizzolato, B. Spagnolo, *'New insight into electron spin dynamics in the presence of correlated noise'*, J. Phys.: Condens. Matter. **24**, 052204 (2012)

[124] D. Persano Adorno, N. Pizzolato, B. Spagnolo, *'External noise effects on the electron velocity fluctuations in semiconductors'* Acta Physica Polonica A **113**, 985-988 (2008).

[125] D. Persano Adorno, N. Pizzolato, B. Spagnolo, *'The influence of noise on electron dynamics in semiconductors driven by a periodic electric field'* J. Stat. Mech. **P01039**, 1-10 (2009).

[126] D. Persano Adorno, N. Pizzolato, D. Valenti, B. Spagnolo: *'External Noise Effects in doped semiconductors operating under sub-THz signals'*, submitted to Reports on Mathematical Physics.

[127] J.M.G. Vilar, J.M. Rubí, *'Noise Suppression by Noise'* Phys. Rev. Lett. **86**, 950-953 (2001).

[128] R.N. Mantegna, B. Spagnolo, *'Noise Enhanced Stability in an Unstable System'* Phys. Rev. Lett. **76**, 563-566 (1996).

[129] L. Gammaitoni, P. Hänggi, P. Jung, F. Marchesoni, *'Stochastic resonance'* Rev. Mod. Phys. **70**, 223-287 (1998).

[130] N. Pizzolato, A. Fiasconaro, D. Persano Adorno, B Spagnolo, *'Resonant activation in polymer translocation: new insights into the escape dynamics of molecules driven by an oscillating field'* Phys. Biol. **7**, 034001 (2010).

[131] G.M. Palma, K.A. Suominen, A.K. Ekert, *'Quantum Computers and Dissipation'* Proc. Roy. Soc. Lond. **A452**, 567-584 (1996).

[132] L. Varani, C. Palermo, C. De Vasconselos, J.F. Millithaler, J.C. Vaissiére, J.P. Nouger, E. Starikov, P. Shiktorov, V. Gruzinskis, *'Is It Possible To Suppress Noise By Noise In Semiconductors?'* Proc. Int. Conf. on Unsolved Problems of Noise and Fluctuations, Melville, New York, AIP Conf. Proc. 800, p. 474-479 (2005).

[133] N. Kazantseva, U. Nowak, R.W. Chantrell, J. Hohlfeld, A. Rebei, *'Slow recovery of the magnetisation after a sub-picosecond heat pulse '* Europhys. Lett. **81**, 27004 (2008).

[134] U. Atxitia, O. Chubykalo-Fesenko, R.W. Chantrell, U. Nowak, A. Rebei, *'Ultrafast Spin Dynamics: The Effect of Colored Noise'* Phys. Rev. Lett. **102**, 057203 (2009).

[135] T. Bose, S. Trimper, *'Correlation effects in the stochastic Landau-Lifshitz-Gilbert equation'* Phys. Rev. B **81**, 104413 (2010).

[136] C.W. Gardiner, *'Handbook of stochastic methods for physics, chemistry and the natural sciences'*, Springer-Verlag, Berlin, 1993.

[137] Askari G, Ghasemi K, Sadeghi HM, *Microwave and Millimeter Wave Technologies Modern UWB antennas and equipment*, edited by I Minin, Rijeka, In-Tech, 2010.

[138] N. Agudov, B. Spagnolo, *'Noise-enhanced stability of periodically driven metastable states'* Phys. Rev. E **64**, 035102(R) (2001).

[139] A. Fiasconaro, B. Spagnolo, *'Stability measures in metastable states with Gaussian colored noise'* Phys. Rev. E **80**, 041110(6) (2009).

[140] D. Persano Adorno, M.C. Capizzo, M. Zarcone, *'Changes of electronic noise induced by oscillating fields in bulk GaAs semiconductors'* Fluct. Noise Lett., **8**, L11 (2008).

[141] J.L. Cheng, M.W. Wu, J. Fabian, *'Theory of the Spin Relaxation of Conduction Electrons in Silicon'* Phys. Rev. Lett. **104**, 016601 (2010)

[142] J.H. Buß, J. Rudolph, F. Natali, F. Semond, D. Hägele, *'Anisotropic electron spin relaxation in bulk GaN'* Appl. Phys. Lett. **95**, 192107 (2009).

[143] A.S. Pikovsky, J. Kurths, *'Coherence Resonance in a Noise-Driven Excitable System'* Phys. Rev. Lett. **78**, 775-778 (1997).

[144] Y. Seol, K. Visscher, D.B. Walton, *'Suppression of Noise in a Noisy Optical Trap'* Phys. Rev. Lett. **93**, 160602 (2004).

Appendix A

A.1 List of Pubblications

A.1.1 Papers in ISI Journals

1. S. Spezia, D. Persano Adorno, N. Pizzolato and B. Spagnolo *'Temperature dependence of spin depolarization of drifting electrons in n-type GaAs bulks'* Acta Physica Polonica B, **41** No 5 1171-1180 (2010).

2. S. Spezia, D. Persano Adorno, N. Pizzolato and B. Spagnolo *'Relaxation of Electron Spin during High-Field Transport in GaAs Bulk'* J. Stat. Mech.: Theo Exp P11033 (2010).

3. S. Spezia, D. Persano Adorno, N. Pizzolato and B. Spagnolo *'Doping dependence of spin dynamics of drifting electrons in GaAs bulks'* Acta Physica Polonica A, **119** 250-252 (2011).

4. S. Spezia, D. Persano Adorno, N. Pizzolato, B. Spagnolo, *'Electron-Electron Scattering Influence on Electron Spin Relaxation in n-type GaAs crystals'*, submitted to Phys. Rev. B.

5. S. Spezia, D. Persano Adorno, N. Pizzolato, B. Spagnolo, *'New insight in electron spin dynamics in the presence of correlated noise'*, J. Phys.: Condens. Matter. **24**, 052204 (2011).

6. D. Persano Adorno, S. Spezia, N. Pizzolato, B. Spagnolo, *'Monte Carlo investigation of electron spin relaxation in GaAs crystals during low-field transport'*, submitted to Rep. Math. Phys.

7. S. Spezia, D. Persano Adorno, N. Pizzolato, B. Spagnolo, *'Effect of a fluctuating electric field on electron spin dephasing in III-V semiconductors'*, submitted to Acta Physica Polonica B.

8. S. Spezia, D. Persano Adorno, B. Spagnolo, *'Electric Field Orientation Dependence of Electron Spin Relaxation in Wurtzite GaN'*, in preparation.

A.2 International conferences

1. Poster presentation: *'Nonlinear Dependence on Temperature and Field of Electron Spin Depolarization in GaAs Semiconductors'* al *22nd Marian Smoluchowski Symposium on Statistical Physics*, S. Spezia, D. Persano Adorno, N. Pizzolato, B. Spagnolo, held in Zakopane, Poland on 2009 September 12-17.
http://th-www.if.uj.edu.pl/zfs/smoluchowski/2009/

2. Poster presentation: *'Doping dependence of spin lifetime of drifting electrons in GaAs bulks'* at *14th International Symposium on Ultrafast Phenomena in Semiconductors* pag. 66 in Abstracts ISBN 978-9955-750-08-6, S. Spezia, D. Persano Adorno, N. Pizzolato, B. Spagnolo, held in Vilnius, Lithuania on 2010 August 23-25.
http://www.pfi.lt/conf/ufps/ufps14/

3. Invited talk at *4th IRC-CoSiM Workshop on Advanced Computational Techniques in the Microworld* (Tryavna, Bulgaria, 2011 April 28-2011 May 1), *'Relaxation of Electron Spin during Field Transport in GaAs Bulk'*, S. Spezia, D. Persano Adorno, N. Pizzolato, B. Spagnolo.
http://www.irc-cosim.uni-sofia.bg/events/workshops/fourth-irc-cosim-workshop

4. Poster presentation: *'Monte Carlo investigation of electron spin relaxation in GaAs crystals during low-field transport'* by D. Persano Adorno, S. Spezia, N. Pizzolato, B. Spagnolo, at the *International Conference on Statistical Physics 2011*, held in Larnaca, Cyprus on 2011 July 11-15.
http://www.sigmaphi2011.org/

5. Poster presentation: *'Effect of a fluctuating electric field on electron spin dephasing in III-V semiconductors* at *24th Marian Smoluchowski Symposium on*

Statistical Physics, S. Spezia, D. Persano Adorno, N. Pizzolato, B. Spagnolo, held in Zakopane, Poland on 2011 September 17-22.
http://th-www.if.uj.edu.pl/zfs/smoluchowski/2011/

A.3 Scientific school

From 2009 August 2 to 2009 August 9, *Quantum Monte Carlo and the CASINO program IV* (International summer school) at *The Towler Institute*, Vallico Sotto, Tuscany, Italy, organized by Mike Towler, physicist at the University of Cambridge (Cavendish Laboratory, TCM Group) and member of the Royal Society. http://www.vallico.net/tti/tti.html

A.4 Grants

1. High Performance Computing (HPC) Grant from February 2010 to December 2010 with research entitled *Noise induced effect in semiconductor devices* approved at the *CASPUR Consortium (Interuniversity Consortium for Supercomputing Applications for Universities and Research).*

2. From 2011 February 8 to 2011 March 17, visiting student at *Hefei National Laboratory for Physical Sciences at Microscale* and the *Department of Physics* of the *University of Science and Technology of China*, Hefei, Anhui 230026, China. Host: Prof. Dr. Ming-Wei Wu.

3. *HPC-Europa2* (2012) Transnational Access programme Grant to visit the supercomputing centre *SARA* (The Netherlands) for 13 weeks in the *Department of Applied Physics*, *Zernike Institute for Advanced Materials at University of Gröningen.* Host: Prof. Dr. H. A. De Raedt.